Master Thesis, Department of Geosciences

Depositional history of Late Ordovician – earliest Silurian storm dominated shelf, incised valley and open marine settings, inner Oslofjorden islands (Oslo Region)

Martin Madshus Sandbakken

UiO : Natural History Museum

UNIVERSITY OF OSLO

FACULTY OF MATHEMATICS AND NATURAL SCIENCES

Front page: Langøyene Formation sandstones and conglomerate,
46-47 meter above base of formation at locality Rambergøya.

Depositional history of Late Ordovician – earliest Silurian storm dominated shelf, incised valley and open marine settings, inner Oslofjorden islands (Oslo Region)

Martin Madshus Sandbakken

Master Thesis in Geosciences

Discipline: Sedimentology

Department of Geosciences

Faculty of Mathematics and Natural Sciences

University of Oslo

December 19th, 2014

Tutor (s): **Professor Hans Arne Nakrem (Natural History Museum, University of Oslo), Professor emeritus Johan Petter Nystuen (University of Oslo) and Dr. Philos. J. Fredrik Bockelie (Exploration Advisor Ithaca Petroleum Norge AS).**

This work is published digitally through DUO – Digitale Utgivelser ved UiO

http://www.duo.uio.no

It is also catalogued in BIBSYS (http://www.bibsys.no/english)

”If I have seen further it is by standing on ye shoulders of giants.”

- Sir Isaac Newton

Abstract

The uppermost Ordovician (Hirnantian) of the Oslo Region has been studied at three selected outcrops in the Husbergøya, Langøyene and Solvik formations on the islands Hovedøya, Rambergøya and Langøyene in the inner Oslofjord.

The outcrops have been logged in detail, from the uppermost part of the Husbergøya Formation, trough Langøyene Formation up to the first meters of the Silurian Solvik Formation. Representative samples have been collected from all three sections, and various laboratory and microscope techniques have been performed. The uppermost very fine-grained sandstone beds with brown colour in weathered outcrops in the Husbergøya Formation are capped by clean sand layers at the base of the Langøyene Formation. The Langøyene Formation is subdivided in a lower and upper part along a major unconformity. The lower part consists of mudstone and thin limestone layers interbedded with sand layers, forming a generally upwards coarsening succession. The erosional unconformity that cuts the lower succession reveals a relief of at least 35 m and is draped by a matrix-supported conglomerate with intrabasinal clasts up to boulder size. Imbricated clasts indicate a transport direction to the southeast. The infill succession above the lower erosional boundary contains two additional erosional unconformities with associated infill successions. Sedimentary structures and lithologies indicate a shallow, high energy, marine epicontinental sea during deposition of the lower part of the Langøyene Formation, terminated by the first major erosional surface as a subaerial, fluvial unconformity. The upper part of the Langøyene Formation is interpreted as deposited in three superimposed incised valleys, each defined by a lower subaerial unconformity and overlying sand-rich fluvial to estuarine marine high-energy infill succession. The uppermost unconformity and infill succession is interpreted laterally equivalent to a karstic surface on top of an oolithic Langøyene arenaceous limestone capped by a flooding surface beneath brown mudstone, and shale and nodular limestone of the Silurian Solvik Formation. The study favours that three events of fall in sea level took place during the Hirnantian; these are most likely connected to eustacy as a result of the glaciation of the Gondwana continent.

Acknowledgements

I direct a special thanks to my two supervisors, Professor Hans Arne Nakrem and Professor emeritus Johan Petter Nystuen, for help, guidance and support through this project, and also for all the sunny days we spent together out in field. I would also thank my external supervisor, Dr. Philos. J. Fredrik Bockelie, for sharing his overwhelming knowledge of the geology in the Oslo Region, and for taking us on his guided boat trip in the Oslo fjord, showing us exceptional geological localities.

Special thanks are also directed to Martin Kjærsgaard for the teamwork during fieldwork and good discussions. I will never forget how good that Tacos and beer(s) tasted during our stay at Langøyene.

I would also like to thank Ivar Midtkandal for having the patience and time to educating me in the Adobe Illustrator software. Oslo Harbor Police for taking the time to transport us to Langøyene during the off-season, the County Governor of Oslo and Akershus for permission to collect samples, Salahalldin Akhavan for making exceptional thin-sections, Maarten Aerts for analyzing my XRD-bulk samples and Professor David L. Bruton for helping me identifying the trilobite.

Finally, I would like to thank Tera E. Lyons for moral support and academic discussions during this last year, and also for helping me with my XRD-analyses. My brother Pål T. Sandbakken for inspiration and guidance through my education. And last but not least, thank you mom and dad for always believing in me and supporting my choices.

Oslo, December 19th 2014

Martin M. Sandbakken

Contents

1 Introduction

During the Late Ordovician the continent Baltica (the continent where present Norway was located) was set at around 30° south of palaeo-equator (Li et al. 2008). Erosion had formed a low relief peneplain that was drowned by the sea during the Cambrian-Ordovician rise in relative sea level and the resulting transgression, which also included the Oslo Region. This sea is believed to have been a shallow-marine epicontinental sea (e.g. Worsley and Nakrem 2008; Bruton et al. 2010). The Cambrian-Ordovician transgressive trend was replaced by a regressive trend during deposition of the Husbergøya Formation (Brenchley and Newall 1975; Kjærsgaard 2014). The Late Ordovician (Hirnantian stage) culminated in the uppermost Langøyene Formation with the deposition of a more low energy bioturbated silt/sandstone.

During deposition of the Langøyene Formation the input and deposition of clean sand increased in frequency and thickness upwards in the stratigraphy. Erosional surfaces in the upper part of the Langøyene Formation indicate a shallow, high-energy marine environment, according to Brenchley and Newall (1975).

The emphasis of this study is to enlighten the mechanisms causing the transition from the brown-coloured sandstone in the uppermost of the Husbergøya Formation, which Nielsen (2004) has described as the "Husbergøya flooding event", and over the boundary to the Langøyene Formation, which clearly is subjected to more siliciclastic input and higher energy. The origin of the distinctive brown weathered surface on the uppermost units in the Husbergøya Formation is also studied in order to supply previous petrographic and palaeontological data on the depositional environment before the onset of the deposition of the Langøyene Formation. Nielsen (2004) presented a sea level curve, which shows a decrease in sea level during the deposition of the Langøyene Formation. Brenchley and Newall (1980) and Brenchley and Cocks (1982) linked this to a eustatic sea level lowering caused by the glaciation of the continent Gondwana.

One main issue related to the deposition of the Langøyene Formation has been the mechanisms behind the erosional surfaces, floored with a conglomerate. Spjeldnæs (1957) suggested the erosional surfaces were formed due to erosion of anticlinal areas of Caledonian folding of the sedimentary strata, with concomitant deposition of the eroded sediments in as boulder conglomerates in the synclines. Brenchley and Newall (1980) suggested the channels

to be tidal, cutting through offshore bars. Brathwaite et al. (1995) proposed a more complex setting regarding the deposition of the Langøyene Formation with glacio eustacy combined with tectonic influence where faulted blocks had created a graben system.

The object of the present study is to supply data on the Langøyene Formation and the uppermost part of the underlying Husbergøya Formation on sedimentary facies, petrography, type of fossil content, and stratigraphic boundaries and their origin. The data, together with previously published information on this interval of the Cambrian-Silurian succession of the Oslo Region, will be applied in an analysis of the overall depositional environment of the Latest Ordovician in this part of the Oslo Region. Particular emphasis is given to the origin of erosional unconformities and subsequent sediment infill in the upper part of the Langøyene Formation during the Hirnantian stage.

With this scope of the study, field work has been located on the islands of Hovedøya, Rambergøya and Langøyene in the part of Oslofjorden, where this stratigraphic interval is well exposed. Representative rock samples have been studied by various methods in order to increase details of the total data volume.

2 Previous work

The geology in the Oslo Region is widely known for its variety, not only between geologists, but also within the population in general. The geology of the region includes a stratigraphy record from the Precambrian with its crystalline basement rocks, through a lower Paleozoic sedimentary succession, and sedimentary, volcanic and igneous rocks within the Permo-Carboniferous Oslo Rift. The geology in the area has been widely described, and according to Brenchley and Newall (1975) detailed studies date back more than 150 years. Theodor Kjerulf (1825-1888), "the father" of modern geology in Norway studied both the Lower Paleozoic sedimentary succession and the Permian igneous rocks, and was the first to publish relevant work of the geology of Oslo Region (Larsen and Olaussen 2005). Kjerulf also contributed to the establishment of the Norwegian Geological Survey in 1858 (Worsley 1982).

For the sedimentary rocks in the Oslo Region Kjerulf established a stratigraphic system, called "Etagen", which was used until recently. He was also known to be an inspiring and motivating lecturer, and had both Waldemar C. Brøgger (1851-1940) and Johan Kiær (1869-1931) as students; both contributed by a series of scientific papers to the understanding of the geology in the Oslo Region (Larsen and Olaussen 2005).

W. C. Brøgger performed studies in 1) Paleontology, stratigraphy and tectonics of the Lower Paleozoic sediments, 2) Mineralogy of the rare minerals of the Oslo Igneous province, and 3) Petrography and geology of the igneous rocks of the Oslo region (Larsen and Olaussen 2005).

Kiær had his main emphasis on the uppermost Ordovician and Silurian succession in the Oslo Region, and in his Dr. Thesis he described the unconformity between the Etagen (stages) 5 and 6, which today is known as the unconformity within the Langøyene Formation. In 1908 he described the whole Silurian stratigraphy and paleontology, and divided the stages 6 to 9 into subunits, which he later disregarded and made a more simplified version in 1922 (Larsen and Olaussen 2005). As a result of his dedicational work on the uppermost Ordovician and Silurian succession, there was not done any work before David Worsley and his research group started their work to modernize Kiær´s earlier work in the 1970´s (Worsley et al. 1983).

Brenchley and Newall (1975) described the stratigraphy of stage 5, and three new names for the formations were proposed; the Husbergøya Shales, the Langøyene Sandstones and the

Langåra Limestone-Shale Formation, which is the western equivalent of the Langøyene Sandstone (Brenchley and Cocks 1982). These formation names, in modified forms, are still used today (Owen et al. 1990). The British research group continued their study of the Langøyene Formation (Brenchley et al. 1979; Brenchley and Newall 1980). Owen et al. (1990) compiled all work done on the Ordovician of the Oslo Region, including recent Ph.D. and Master Theses, and presented a revised proposal of the Ordovician of the Oslo Region, with redefined units with lithostratigraphic names based on the old stratigraphic stages and previous as well as new defined type localities.

Brenchley and Cocks (1982) described the late Ordovician ecological associations, and related them both to vertical and lateral environmental changes and coupled this up to the glacio-eustatic sea level changes. Hansen et al. (2009) also presented new views on the sea level changes in the upper Ordovician and included in their study variations in the oxygen content of the bottom waters and the faunal changes in late Sandbian to early Katian.

Some attention has been given around the formation of nodular limestone in the Lower Paleozoic of the Oslo Region. It started with Brøgger (1882) where he stated that the nodules should not be regarded as concretions, as they have the same compositions as the continuous limestone beds. After Brøggers description, Bjørlykke (1973) published a paper of his interpretation of the formation of the carbonate nodules, focusing on the theory of partly dissolution of continuous limestone beds exposed on the seafloor. Henningsmoen (1974) commented on Bjørlykke (1973), with a hypothesis of that carbonate cementation had originated from saturated water from the sediments below the water-sediments interface. Möller and Kvingan (1988) stated that the nodular limestone was formed by early diagenetic concretionary carbonate cementation, centimetres to decimeters below the sediment-water interface. The most recent work was done by Kjærsgaard (2014), who stated that the limestone nodules was formed by dissolution of originally continuous micritic beds or early lithified limestone beds, as a result of variations in pH of the seawater, controlled by climatic changes. This relates to Brøgger (1882) hypothesis, that the nodules would not include quartz and differ more in lithology from the continuous limestone beds.

Some work was done on the uppermost Ordovician and Ordovician-Silurian boundary by different authors. Spjeldnæs (1957) presented a model regarding the angular unconformity found in the Upper Ordovician, just below the Ordovician/Silurian boarder. He linked this

unconformity to folding of the upper Ordovician, as a result of the compressional forces from the Caledonian orogeny. He explained the unconformity as erosion of the anticlines and deposition in the synclines as conglomerate. Braithwaite et al. (1995) had a reinterpretation of the sedimentological changes across the Upper Ordovician/Silurian boundary in Hadeland, and linked their observations to sedimentation in the Oslo Region.

3 Depositional setting

In this subchapter, main features and controlling factors of depositional environments that are supposed to be relevant for the discussion of formation of the Langøyene Formation are described.

3.1 Shallow seas

Shallow seas occur as rims surrounding continents, or as inundated parts within continental plates. They include processes related to shoreline dynamics to slope and more bathyal environments where deeper water dynamics are dominated. The features that define a shallow sea are as follows: (i) depths within the limiting factor of 200 meter, (ii) low dipping gradient (1-0.1°), (iii) normal marine salinities; and (iiii) wide range of physical processes (tidal currents, waves, storm-generated currents and oceanic currents) (Johnson and Baldwin 1996).

The shallow seas are divided into two different morphological types:

- Pericontinental seas are located on continental margins, and are characterized by the classic shoreline-shelf-slope profile with deposits shown as clinoforms on aggrading continental margins (see Figure 3-1). Modern examples of pericontinental seas are Bering Sea, Gulf of Mexico and The North Sea (Johnson and Baldwin 1996).
- Epicontinental or epeiric seas can be defined as a water mass in direct contact with the ocean covering a large area of land partially enclosed within a continent, with shallow depth and often displaying a uniformly dipping ramp profile, see Figure 3.1 (Johnson and Baldwin 1996). The Hudson Bay, Arafura Sea, Gulf of Carpentaria and the Barents Sea fulfill these criteria and can be studied as modern examples of epicontinental seas.

  As a result of their shallow depths, the basin floor of epicontinental seas is highly sensitive to eustastatic changes; just small changes in the relative sea level can expose large areas of the earlier seafloor (Midtkandal and Nystuen 2009; Glørstad-Clark et al. 2011).

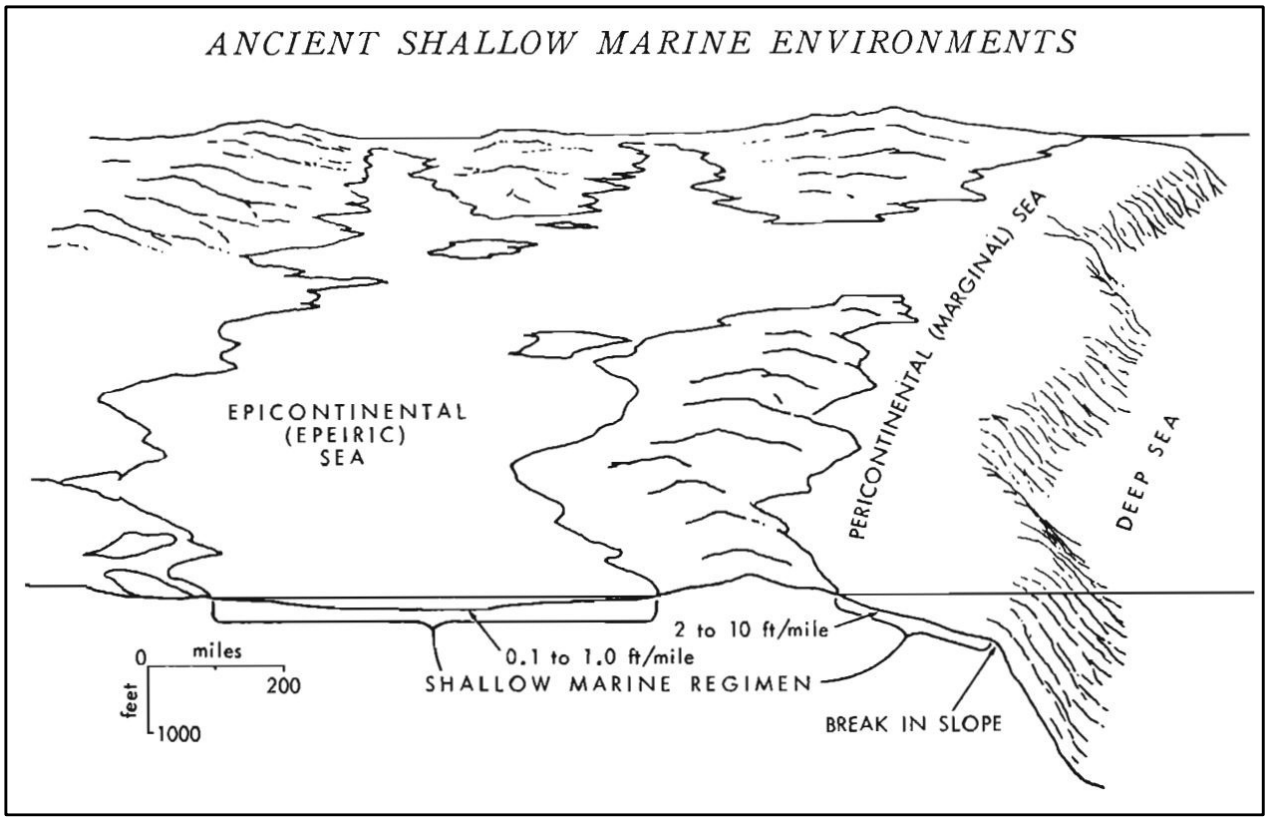

Figure 3.1: Illustration showing typical Epicontinental and Pericontinental Sea. Modified from Heckel (1972).

3.1.1 Sedimentation control and architecture

"All dynamic systems attempt to attain equilibrium, and as such the fluvial system is always seeking to become more efficient, aggrading or degrading to attain the hypothetical status of its equilibrium profile" (Dalrymple 1998).

The above quotation from Dalrymple (1998) describes how a dynamic system is always trying to find its own equilibrium stage, which is controlled by allogenic and autogenic factors. These factors will influence the depositional architecture of the basin, as also an epicontinental sea. Allogenic variables include physical factors and processes such as climate, tectonics, eustacy, orbital forcing, inherent topography and sediment source area (Midtkandal and Nystuen 2009, and references therein). The allogenic variables influence sediment influx rates, bottom morphology and slope, and position of drainage systems, and location of sedimentation; thus more or less influence the overall depositional architecture of the basin (Ethridge 1998). The autogenic controlling factors are constricted to a more local change in the depositional architecture and include i.e. avulsion of a river channel on delta, sediment build up on delta slopes that may cause slumping when sediment load exceeds the strength of the sediment, influence on bottom currents due to deposition of sandbars, sandridges

carbonate mounds, etc. Although these changes eventually will happen, they are usually caused by unusual events such as floods, storms or seismic shocks (Johnson and Baldwin 1996; Dalrymple 1998).

The equilibrium profile as mentioned earlier is defined as the longitudinal profile of a stream with a gradient sufficient enough to enable the stream to transport sediments made available to it, flattening towards the mouth and steepening towards the source (Gary et al. 1973). The principle of equilibrium profile can also be applied for marine sedimentary system in control and creation and destruction of accommodation space; most aggradation (sedimentation) and degradation (erosion) occur when the system is no longer in its equilibrium stage (Dalrymple 1998).

3.1.2 The epicontinental shelf

The different depositional features on clastic coasts can generally be distinguished from either a regressive or a transgressive shoreline and the amount of energy influenced from wave and tidal energy on the shelf (Boyd et al. 1992). When the rate of sediment supply exceeds the rate of relative sea level rise or when the relative sea level falls and sediments accumulate, the shoreline is regressional. Regressive shorelines formed by sediment progradation along the coast include the development of tidal flats, deltas or strand planes that over time move in basinward direction. On the contrary, when the relative sea level rise exceeds the rate of sediment supply, the shoreline is transgressive, and the development of tidal flats, estuaries, lagoons or strand plains takes place with a landward displacement through time (Boyd et al. 1992)

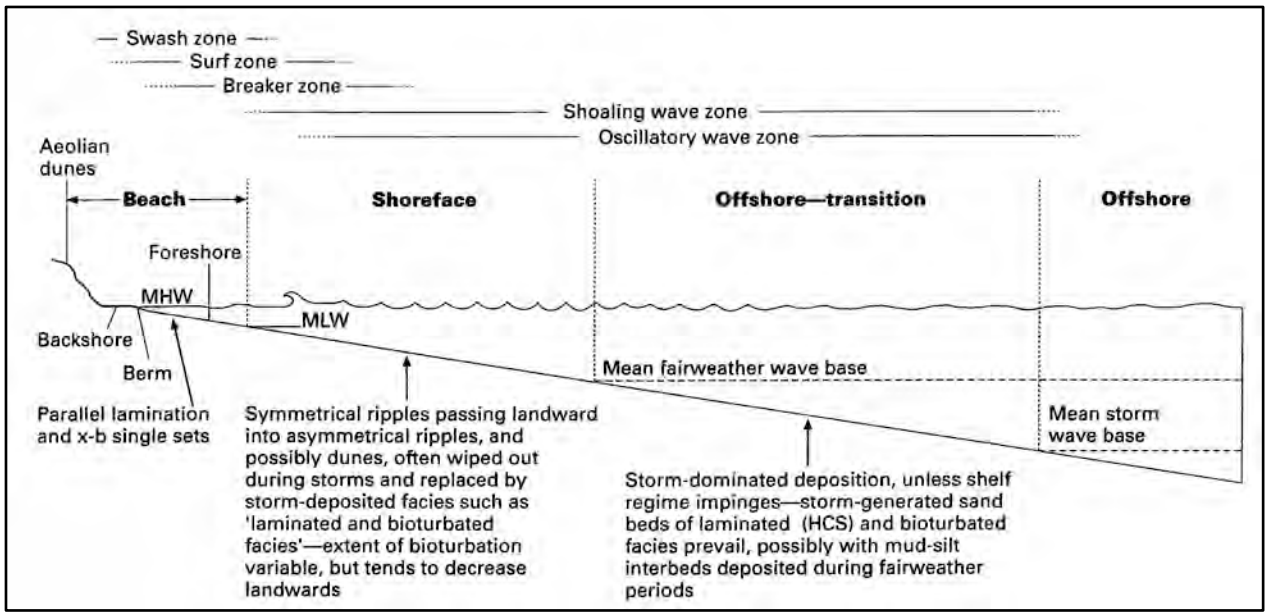

Figure 3.2: Schematically presented shelf profile from the beach out to the offshore setting (Reading and Collinson 1996)

The shelf profile can be divided into different zones, where each zone represents its own facies, morphology and characteristic physical processes that define them. In Figure 3.2, the different zones are represented schematically by (Reading and Collinson 1996) and explained beneath.

- The offshore transition zone is restricted between mean storm wave base and mean fair weather wave base. The sediments therefore has an alteration of high- and low-energy characteristics of fine grained sediments settled from suspension during fair weather with bioturbated sediments, and during storms the sediments are reworked by oscillatory and shoaling waves. Coarser sediments can during extreme storms be transported from the shoreface and be deposited as tempestites in deeper waters.
- The shoreface is subjected to oscillatory and shoaling wave processes in the deeper part, and breaker/surf zone processes operate in the upper shoreface. During storm events the shoreface is subjected to erosion from shoaling waves, storm currents and enhanced rip currents. The sediments are suspended and carried landward on to the beach, or are carried in suspension and deposited as tempestites in the lower shoreface zone or offshore.
- The intertidal foreshore is dominated by tidal processes and the daily swash and backwash of waves. It has a relatively steep profile termed the beach face, which is subjected to breaker, surf and swash zone processes.

- The supratidal backshore has a relatively flat profile and usually no vegetation. It is only affected by rare very high tides and storm events, which will carry sediments landward and be reworked. Landward it passes into an aeolian dune field formed from exposed sand on the beach (Reading and Collinson 1996).

3.2 Incised valleys

As a result of fall in relative sea level, the exposed sea floor will be subjected to erosion from rivers creating *incised valleys.* They are typically filled with tidal and fluvial sediments, and will often laterally pass into abandonment facies (Posamentier et al. 1988a, b; Reading and Collinson 1996).

Incised valleys are defined as fluvial eroded, elongate topographic lows, which are larger than single channel forms, and characterized by a sea-ward shift of depositional facies. An incised valley is recognized across a regionally extended sequence boundary formed as a subaerial unconformity (SU). First when the next base-level rise initiate, the infill of the incised valleys begin and a combined marine flooding surface (FS) and transgressive surface (TS) is formed across the subaerial unconformity (Zaitlin et al. 1994).

Even though an incised valley system can vary in a large extent, some fundamental characteristics have been given to such a system in Zaitlin et al. (1994) and references therein. These are as follows:

"(i) The valley is a negative (i.e. erosional) paleotopographic feature, the base of which truncates on underlying strata including any regional markers that may be present. (ii) The base and walls of the incised valley system represent a sequence boundary that may be correlated to an erosional (or hiatal) surface outside the valley (i.e. on the interfluve areas). This erosional surface may be modified by later transgression, forming an E/T surface, or a combined flooding surface and sequence boundary. The sequence boundary may be mantled by a pebble lag, and/or burrows belonging to the Glossifungites ichnofacies. On the interfluves, the exposed surface may be characterized by a soil or rooted horizon. (iii) the base of the incised valley fill exhibits an erosional juxtaposition of more proximal (landward) facies over more distal deposits. Finally, (iv) depositional markers within the deposits of the incised fill will onlap the valley walls."

3.2.1 Sedimentation control

Because of the large variety of incised valley fill successions, Dalrymple et al. (1994) has generalized a simplified model concerning the incised valley from highstand to lowstand to highstand, this is illustrated in Figure 3.3.

As the fall in relative sea level initiates, the exposed region undergoes erosion, creating an incision, which will propagate headward with time. If the lowstand is relatively short lived, the incision will be concentrated near the coast and will landward pass into a non-incised fluvial system not influenced by the base level fall. As the base level begins to rise, the creation of accommodation space exceeds the rate of fluvial sediment supply, which results in a drowned-valley estuary at the end of the incised valley close to the marine realm. As the shoreline merges landward, the estuary setting follows throughout the transgression, and will stabilize when the rate of rise in relative sea level equals zero (next highstand). The highstand deposits will fill any remaining negative impression from the incised valley. The typical facies during a highstand will be deltaic or coastal plain, which will progradate. By a very fast rise in relative sea level, the incised valley fill can be abruptly overlain by deep shelf or open-marine mud (e.g. Midtkandal and Nystuen 2009; Ahokas et al. 2014a, 2014b).

Four key points from this generalized evolution of an incised valley are identified by Dalrymple et al. (1994) along the length of an incised valley system.

- The first is the boundary between the incised valley and the sea, and corresponds to the landward limit of the lowstand wedge.
- The second is the limit between the incised valley and the sea during the time at maximum transgression, and corresponds to the position of the shoreline during the start of highstand.
- The third is the boundary of how far landward the marine influence reached during maximum transgression.
- The fourth is the boundary of how far landward the incision took place during maximum lowstand.

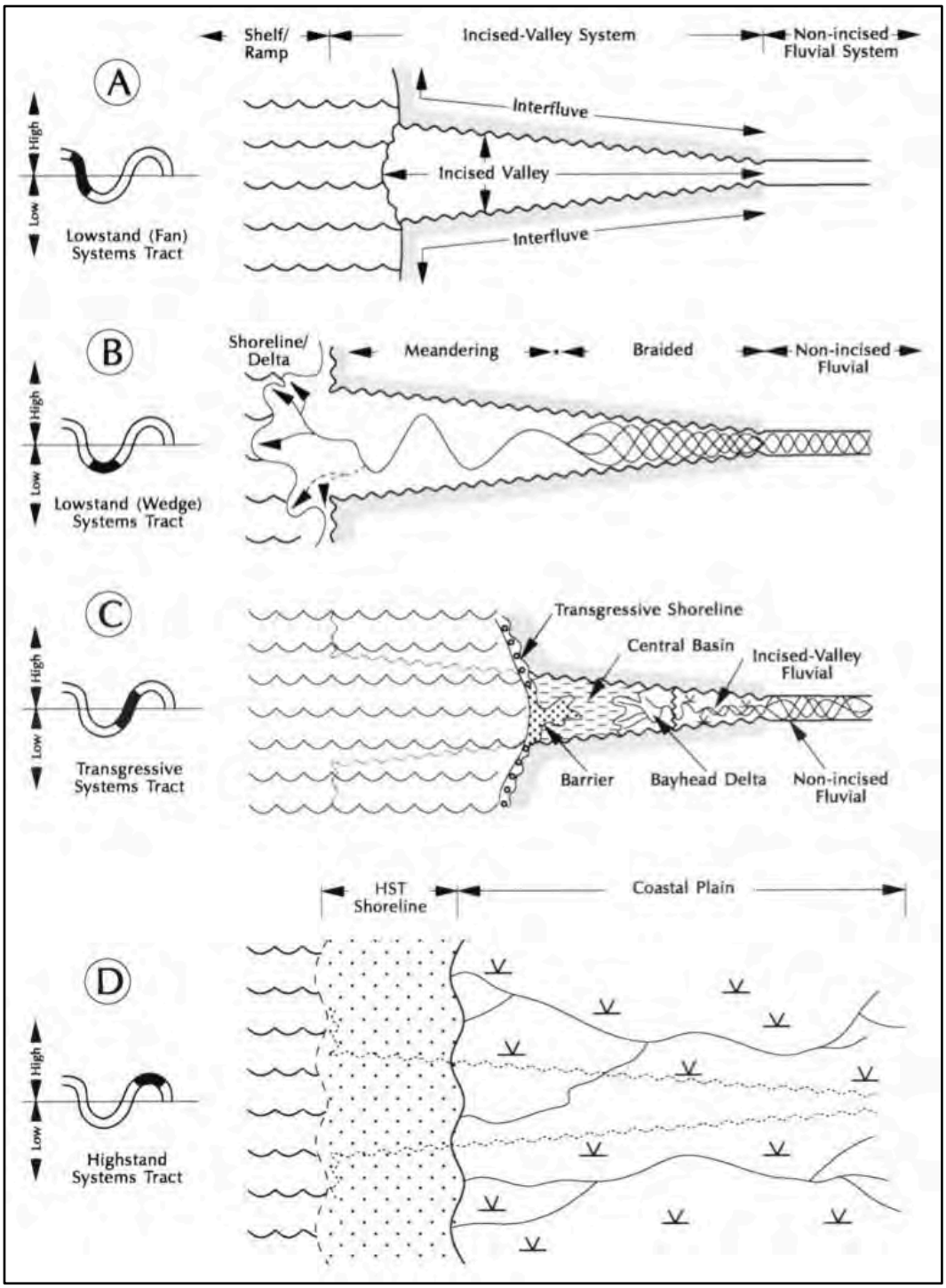

Figure 3.3: Illustration shoving the evolution of an incised valley system from lowstand to highstand. From Zaitlin et al. (1994).

In order to identify an incised valley it thus will be important to document criteria of a subaerially formed unconformity (SU), the concave shape of the erosional feature defined by the SU and the fluvial-deltaic to marine character of the succession filling in the erosional low.

3.3 Foreland Basin

DeCelles and Giles (1996) defined a foreland basin as: ”(a) an elongate region of potential sediment accommodation that forms on continental crust between a contractional orogenic belt and the adjacent craton, mainly in response to geodynamic processes related to subduction and the peripheral or retroarc fold-thrust belt; (b) it consists of four descrete depozones, referred to as the wedge-top, foredeep, forebulge and backbulge depozones – which of these depozones a sediment particle occupies depends on its location at the time of deposition, rather than its ultimate geometric relationship with the thrust belt; (c) the longitudinal dimension of the foreland basin system is roughly equal to the length of the fold-thrust belt, and does not include sediment that spills into remnant ocean basins or continental rifts.”

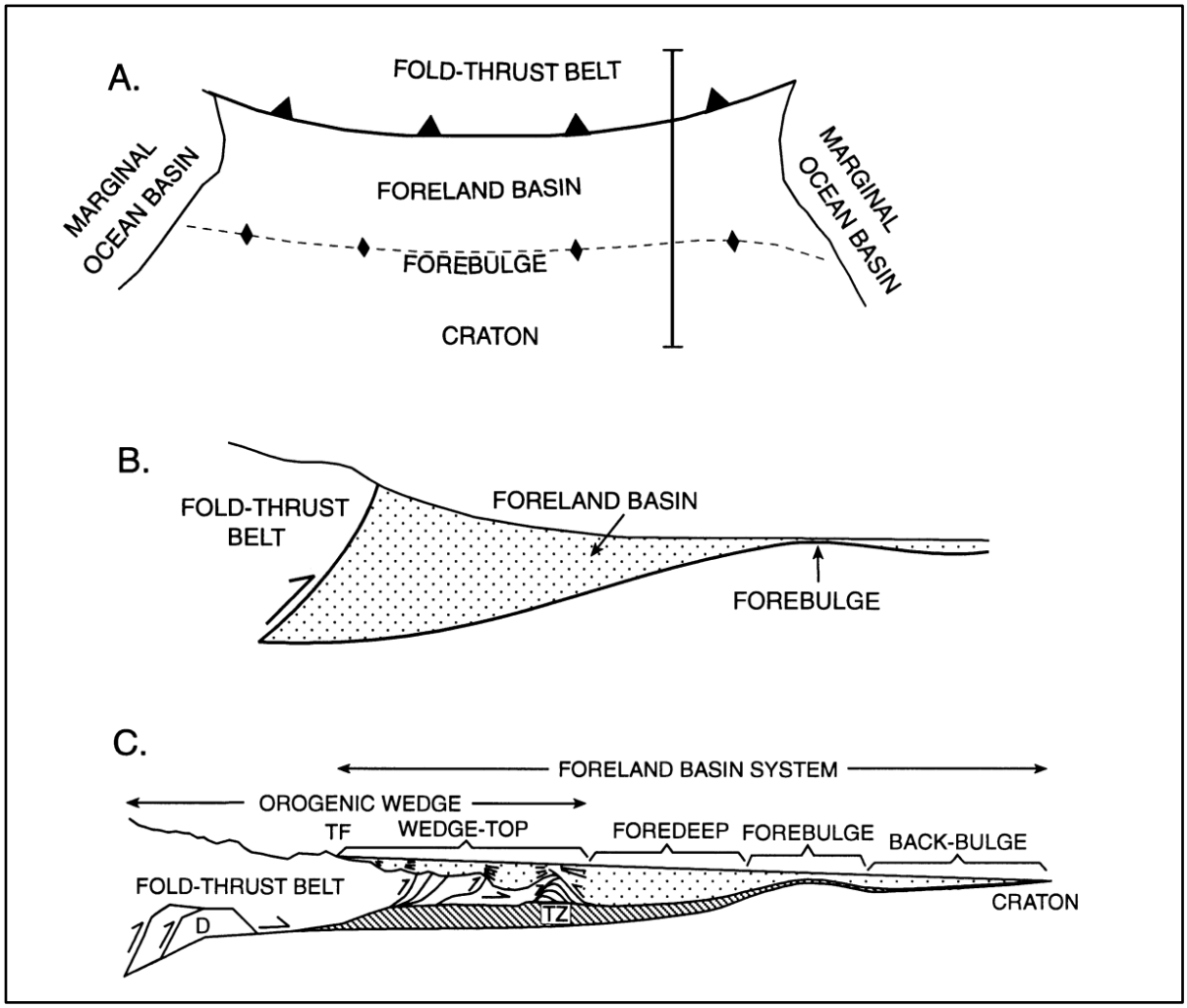

Figure 3.4: A: birds eye view of a foreland basin system. The line viewed on the right side of the figure is shown as cross sections in A and B; B: simplified cross section of a foreland basin system, showing the fold-thrust belt, foreland basin and forebulge; C: division of the different depozones between the fold-thrust belt and the craton in a cross section. Modified from DeCelles and Giles (1996).

The wedge-top depozone is the package of sediments accumulated on top of the frontal part of the orogenic wedge, piggyback and thrust top basin is included in package. The characteristics are extreme coarseness and a high amount of unconformities caused by tectonic forces. The foredeep depozone is located between the front of the thrust belt and the proximal flank of the forebulge. The sediments have a characteristic of thick units close to the thrust belt, which is thinning out towards the forebulge. The forebulge depozone is the broad flexural uplifted part of the crust, as a result of the heavy loading from the fold and thrust belt. It is located between the foredeep and back-bulge depozone. The back-bulge depozone is caused by flexural subsidence cratonward from the forebulge, creating a broad, shallow zone for sediments to accumulate in (DeCelles and Giles 1996).

4 Regional setting

The Oslo Region as a geological term covering an area of approximately 10000 km^2, which extends about 115 km both to the north and south from the City of Oslo (Bruton et al. 2010). To the north the region is bordered by the Caledonian nappe region, and to the east and west by the Precambrian basement. See Figure 4.2.

The Oslo Region contains an approximately 2500 m thick lower Paleozoic succession, spanning from the Early Cambrian to the latest Silurian. The succession was during the Caledonian orogeny folded, faulted and thrusted, as well as cut by numerous normal faults during the Late Paleozoic rifting phase. Thermal metamorphism is also apparent due to the local magmatic activity linked to the Permian rifting (Bruton et al. 2010).

4.1 From an epicontinental sea to a foreland basin

During Neoproterozoic from about 720 Ma to Early Cambrian for about 530 Ma ago, continent Baltica (the continent where present Norway was located) moved from a position at around 50-60° south of paleo equator to about 30° south of paleo equator (Li et al. 2008), see Figure 4.1. During this time period, Baltica was exposed to erosion after the Sveconorwegian orogeny (ca. 1000 Ma) and turned into the low-relief Sub-Cambrian peneplain (Gabrielsen et al. 2014). The peneplain was flooded by the sea during the Cambrian-Ordovician transgression. Most of Baltica, including the Oslo Region, was drowned and covered by a shallow-marine epicontinental sea (Worsley and Nakrem 2008; Bruton et al. 2010). During the Cambrian there was a divergence between the two continents of Baltica and Laurentia, and by seafloor spreading the Iapetus Ocean was created. Later on this divergence was reversed and turned into convergence and closing of the Iapetus Ocean and creation of the Caledonian mountain chain in Silurian-Caledonian time began (Fossen et al. 2008). As the Caledonian thrust and fold belt migrated from the west to the east during the Caledonian Orogeny, the epicontinental sea turned into a foreland basin, changing the lithology of the sediments throughout Silurian and Early Devonian (Bruton et al. 2010). It is well documented that during Cambrian there was an explosion of life in the ocean with a high diversity of species. Because of the sea level rise, large areas of the low relief Baltica continent was flooded creating an epicontinental basin where the fossils of the early life can be recognized (Worsley and Nakrem 2008).

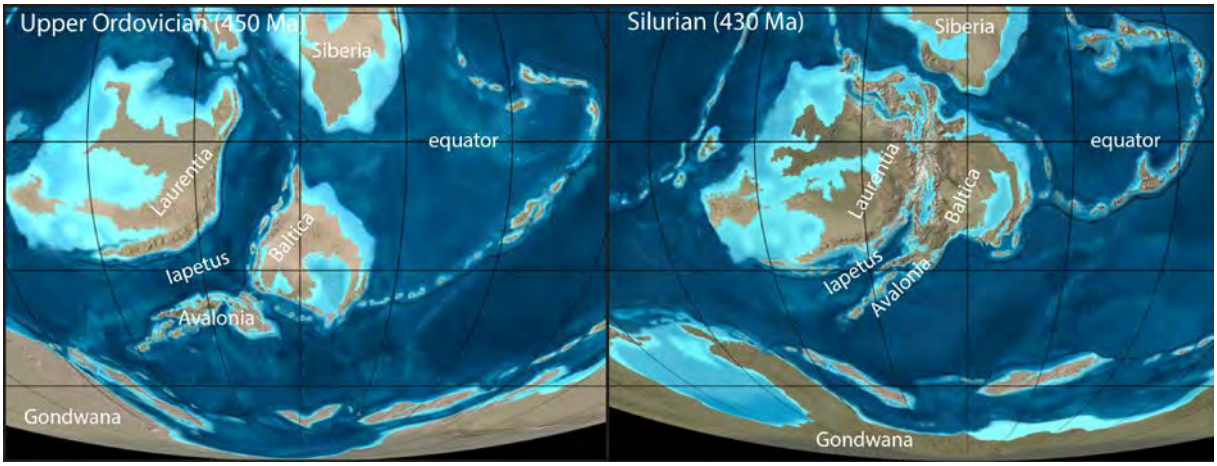

Figure 4.1: Upper Ordovician and Silurian paleogeography showing the merging of the two continents Laurentia and Baltica and closing of the Iapetus Ocean. The paleogeographic maps have been modified from the file available at the website of Ron Blakey (http://www2.nau.edu/rcb7/) and information found in Calner et al. 2013.

In the northernmost part of the Oslo Region, the Early Cambrian onlap strata onto the Precambrian basement, is quartzarenite sandstone and greenish-grey siltstone and shale (Skjeseth 1963; Vidal and Nystuen 1990; Nielsen and Schovsbro 2011). The organic-rich black Alum shale characterizes the succession from the Middle Cambrian to Early Ordovician (Bjørlykke 1974; Bockelie and Nystuen 1985), followed by the carbonate- and mudstone dominated Lower to Middle Ordovician succession (Bjørlykke 1974; Owen et al. 1990). The Upper Ordovician is characterized by coarser siliciclastic material, but still the mud and carbonate sedimentation was dominating the succession (Bjørlykke 1974). The Silurian succession turned transitionally into the Caledonian foreland basin succession of increasing supply of siliciclastic sediments, culminating with the continental fluvial sandstones of the late Silurian Ringerike Group (Bruton et al. 2010).

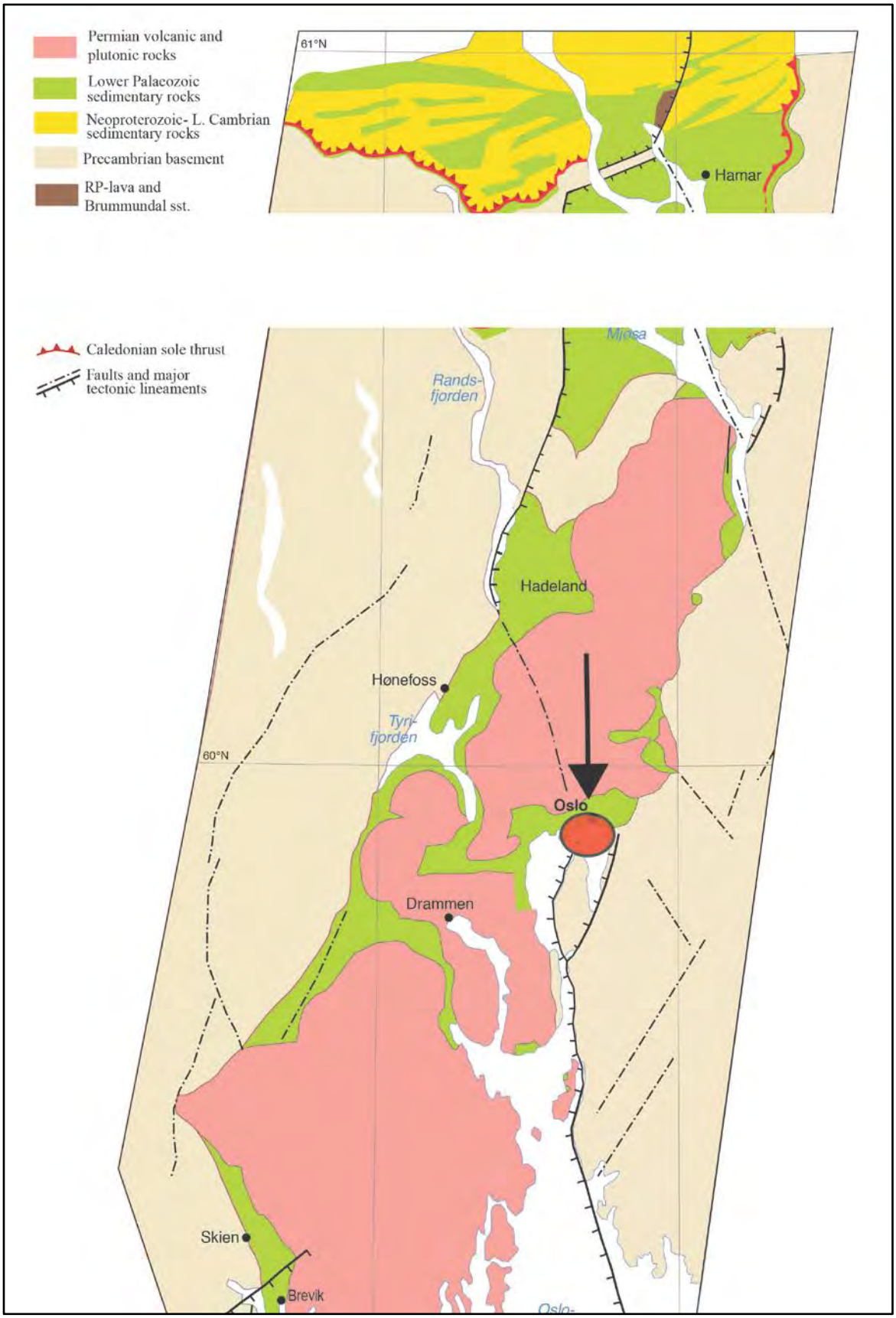

Figure 4.2: Simplified map showing the geology of the Oslo Region and the distribution of Lower Palaezoic sedimentary rocks, Permo-Carboniferous magmatic rocks and the surrounding Precambrian and Caledonian terrain. Highlighted area shows the study area. Modified from Worsley and Nakrem (2008) with information from Nystuen (1987).

4.2 Climate

In the late Ordovician, the Oslo Region was situated at sub-tropic to tropic latitudes and was out of reach in respect to direct glacial influence. As earlier mentioned during this time the Iapetus Ocean was closing due to the collision of the Baltic and the Laurentian plates (Brenchley and Newall 1980). Epicontinental seas were widespread, probably more than during any other period, and land areas were mostly restricted to archipelagos rather as wide continents. These cratonic land areas had a low relief with rivers with low gradient and low energy. The low supply of terrigenous siliciclastic debris into the epicontinental sea, resulted in widespread deposition of carbonate sediments (Jaanusson 1984).

According to Spjeldnæs (1961) the climate was most likely not stable throughout the whole Ordovician. From migration of warm water faunas, towards the poles and back again in a relatively short period of time, the increase and subsequent drop in temperature is well documented. This sharp climatic zoning was, like today, most likely due to ice caps in the polar regions. Because of the presence of ice caps the ocean currents were considerably different of what they would have been if the ice caps were absent. The Earth's climate would have been more uniform with no sharp zoning.

4.3 Eustacy in the Ordovician

The *eustacy* is measured between the sea surface and a fixed datum. Factors that affect the eustacy are change of the ocean-basin volume or/and variation in ocean-water volume. The water volume in the ocean gets reduced by accumulation of water on continental icecaps during periods of glaciation and increases again during deglaciation. A eustatic sealevel change can easily be mixed with the concept of change in relative sea level, which is measured between the sea-surface and a local moving datum, such as a sedimentary package deposited in a basin, making the water depth shallower, or tectonic subsidence or uplift of a basement (Myers and Milton 1996).

The sea level during the Ordovician is believed to be relatively high (Nielsen 2004). Even though there was limited supply of clastic input into the ocean, and no extensive tectonic activity until the Silurian, the record shows a fluctuation of the sea level. Some of these sea level changes seem to have been rapid according to Nielsen (2004). As shown in Figure 4.3,

the sea level has been inferred to have been low during the deposition of Husbergøya Formation, with a small shallowing event in the middle. From Husbergøya Formation up to the Langøyene Formation, there was a rapid upward shallowing according to this sea level reconstruction, with a small increase of sea level in the middle of the deposition of Langøyene Formation. In the upper part of Langøyene there was a rapid regression, which was followed by a new sea level rise, marine flooding and transgression with the deposition of the dark grey to black shales of the Solvik Formation.

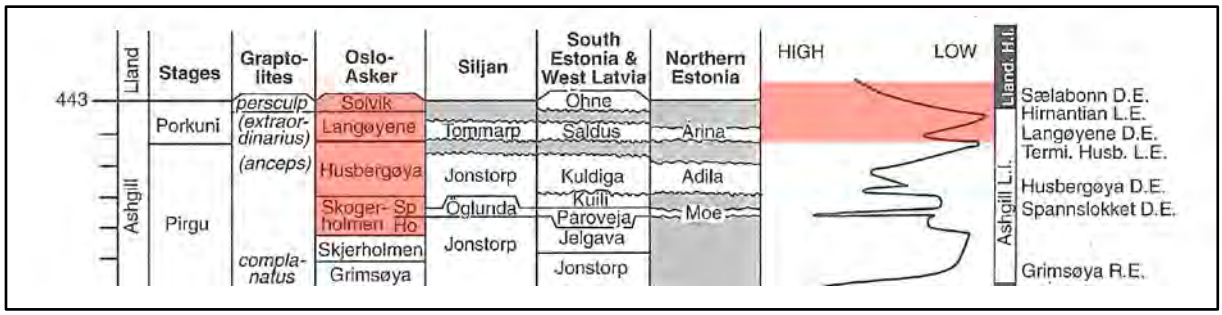

Figure 4.3: Showing the late Ordovician eustacy, the section of the curve outlined in red represent the sea level during deposition of Langøyene and Solvik Formation. Modified from Nielsen (2004).

4.4 The uppermost Ordovician succession

During the late Ordovician and early Silurian period the previously mentioned epicontinental sea covered the Baltic Shield. The typical facies of an epicontinental sea, like shale, nodular-limestone and limestone can be observed in the Husbergøya Formation, capped by the regressional succession of the Langøyene Formation, consisting of conglomerate and sandstones, which is the uppermost formation in the Ordovician in the Oslo area. The next stage in the succession is the transgressional Solvik Formation, which is exposed on the islands in the inner part of Oslofjorden (Owen et al. 1990; Worsley et al. 1983).

400 m of fossiliferous, alternating limestone and shale units of the total 2500 m of lower Paleozoic succession belong to the Ordovician strata in the Oslo, Asker and Ringerike districts (Bockelie 1982).

Period	Epoch	Ringerike	Asker District	Oslo District	Stages
Silurian	Llandovery	Sælabonn Fm.	Solvik Fm.	Solvik Fm.	6a
Ordovician	Late	Langøyene Fm.	Langøyene Fm.	Langøyene Fm.	5b
		Husbergøya Fm.	Husbergøya Fm.	Husbergøya Fm.	5a
		Skogerholmen Fm.	Skogerholmen Fm.	Skogerholmen Fm.	4d

Figure 4.3: The stratigraphic and lateral extend of the Husbergøya, Langøyene, Sælabonn and Solvik Formation in the Ringerike, Asker and Oslo district. Based on information in Brenchley and Newall (1975) and Owen et al. (1990).

4.4.1 The Skogerholmen Formation

The Skogerholmen Formation consists of alternating siltstone, limestone and shale beds. The limestone is developed as a nodular limestone in the uppermost part. The occurrence of fossils is rather sparse, but some shelly fossils such as trilobites, brachiopods and cephalopods have been identified, mostly in the upper part (Owen et al. 1990) and references therein.
The formation consists of two members, the Spannslokket and Hovedøya members.
The Hovedøya Member is developed as layers of limestone, siltstone and shale. The difference in contrast to the alternating layers from the underling formation is that the

thickness of the limestone and siltstone beds exceeds the thickness of the shale beds. The base is defined as the first appearance of a continuous limestone bed.
The Spannslokket Member starts with dark shale in the lower part, which gradually turns into a more greenish, gray and silty shale. This shale is what distinguishes the Spannslokket Member from the Hovedøya Member. In the upper part of the Spannslokket Member the appearance of alternating succession of limestone, siltstones and shale is prominent. The limestone appears as continuous beds in the lower part, but become nodular in the uppermost part, and siltstone is more absent (Owen et al. 1990).

4.4.2 The Husbergøya Formation

The sediments of the Husbergøya Formation were deposited in a relatively calm shelf environment forming a fairly uniform succession. Evidence like appearance of nodular limestone and an increase of faunal diversity upwards in the stratigraphy indicates periods of fall in relative sea level (Brenchley and Newall 1980).
According to Brenchley and Newall (1975) the Husbergøya Formation shows an upward shallowing succession, with shale and silt as alternating layers, and thin sandstones interbedded throughout the sequence, with a more frequent appearance of the siliciclastic input in the uppermost part.

The base is defined as a sharp contact between a 2 - 2,5 m thick succession with shale overlying nodular limestone, which belongs to the underlying Skogerholmen Formation. The shale is interbedded with laminated sandstone beds (1-4 cm thick), which also shows some small-scale ripple drift lamination (Brenchley and Newall 1975). Brenchley et al. (1979) suggested that these sands were formed during intense storms with 10000-15000 year periodicity, most likely transported by hurricane driven ebb currents. Paleocurrent measurements show that currents moved sand from the west, most likely the shoals of a continent to the south-west (Brenchley and Newall 1980).
The thickness of the unit is relatively constant between 17-25 m, but can be as thin as only 10 m in Asker, and thickens to about 35 m farther north at Sandvika. In the Oslo-Asker district it varies from 23.5 m at Skjærholmen and Skogerholmen to 18 m at Husbergøya, Høyerholmen and Torbjørnsøya (Brenchley and Newall 1975).

4.4.3 The Langøyene Formation

At the time when the sediments of the Langøyene Formation were deposited, there had been some changes in the paleogeography of Baltica. The slightly inclined palaeoslope was directed south-eastward in the Oslo region according to Brenchley et al. (1979). These changes result in a more energy-rich depositional environment compared to the one found in the Husbergøya Formation, suggesting a regressive event (Brenchley and Newall 1980). The base of the formation is defined in Brenchley and Newall (1975) above the brown weathered bioturbated sandstone (approx. 2 m thick), belonging to the top Husbergøya Formation. Overlying the brown weathered bioturbated sandstone is shale with laminated sandstone and thin limestone, which represents the base of the Langøyene Formation, is developed.

In the first few meters of the Langøyene Formation the beds are characterized with its soft-sediment deformation and oolitic limestone beds with well rounded, sub-spherical quartz grains (Brenchley and Newall 1975). The formation shows, according to Brenchley and Newall (1977), an upward increase in sandstone bodies, a change in bedforms indicating an increase of current strength, and a change of fossils and ichnofauna, even though this happens mainly in the uppermost part of the formation (Brenchley and Newall 1980). The thickness of the formation varies from 1 m at Sandvika to 53 m in the more southerly sections. In the thickest sections, the formation consists of thick successions of sandstone beds cut by channels and filled in with limestone conglomerates and/or millet seed sandstones. The more northerly outcrops, found for instance at Gressholmen, Hovedøya and Bleikøya, the formation is still mainly dominated by sandstone but has also partitions of interbedded shale (Brenchley and Newall 1975).

Oolitic limestone facies is described in Brenchley and Newall (1975) as a 3 to 8 meters thick unit of oolitic limestone, intermixed with spherical “millet seed” quartz grains. The oolites are through cross-stratified with a bed thickness of approximately 50 cm or less. This facies is located at Gressholmen, Bunnefjorden and most sections of the Langøyene Formation exposed in Asker.

4.4.4 Ordovician – Silurian boundary

The Ordovician- Silurian boundary in the Oslo district has been described and placed at different levels by Scandinavian stratigraphers. Kiær started the work in his first papers (1897, 1902), and went back and forth on where to put the border. In the end he decided to place the border below the bed termed 5b and above the stage 5a, as most of the other Scandinavian stratigraphers did. This boundary is based on the hiatus between the Dalmanitina-beds and the Tretaspis beds, which is present in Sweden, but the hiatus found between 5b (corresponds to the Dalmanitina-beds in Sweden) and 6a in the Oslo Region are of greater interest (Spjeldnæs 1957).

At the end of the Ordovician a mass extinction affected the living fauna and created a discontinuity in the sediments between the Ordovician and Silurian faunas (Brenchley and Cocks 1982). This is now documented in the fossil record across this transition (Hansen et al. 2009).

4.4.5 The Solvik Formation

This formation corresponds to the stage 6 of Kiær (1908) in the Oslo, Asker and Holmestrand districts. The characteristics of the Solvik Formation are dominant dark grey shales with interbedded thin siltstones and limestones (Worsley et al. 1983). The extensive thrusting in the area makes the determination of the thickness of the unit difficult, but the interpreted thickness is approximately 190 meter in its type area (Worsley et al. 1983). The base is defined by a sharp contact between the underlying sandstone of the Langøyene Formation and the dark-grey silty shales with minor siltstones of the Solvik Formation. The nodular limestone with a thickness of approximately 60 cm is defined as a basal development of the Solvik Formation.

The 190 m thick formation in the study area is divided into two members, Myren and Padda members. The Myren Member is approximately 160 m thick, and has the same lithology as mentioned earlier. The Padda Member has more or less the same lithology; the only difference is the occurrence of nodular limestone together with thin lenses and interbeds of calcareous siltstone and limestone (Worsley et al. 1983). The diverse benthic fauna and sedimentary structures indicate deposition in a distal environment below storm wave base (Worsley et al. 1983).

The shale-dominated succession of the Solvik Formation reflects the rapid increase in relative sea level in the Oslo area during the Early Silurian and with the creation of a sublittoral depositional environment. The siltstone beds in the Myren Member were storm generated and deposited in a calm muddy environment below normal wave base. The sediments of the Padda Member, with its shale and limestone facies, are interpreted as deposited in a shallower environment both by its sedimentary structures and fauna (Worsley et al. 1983).

5 Methods

5.1 Field work and study object

The fieldwork was carried out during the summer/autumn of 2013 and spring/summer 2014 on three different localities; Hovedøya, Rambergøya and Langøyene shown in Figure 5.1.

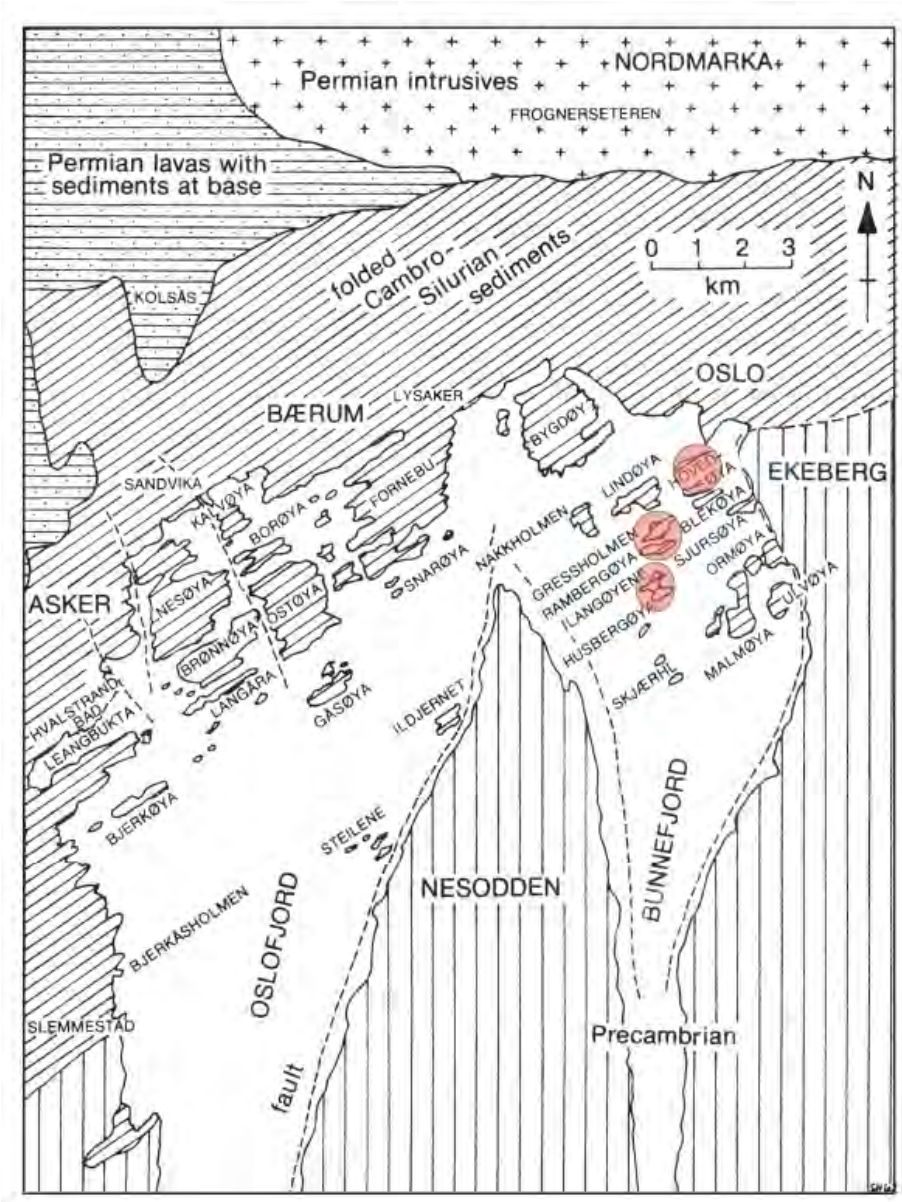

Figure 5.1: Simplified geological map of the Oslo District. Study areas are outlined in red circles. Modified from Bockelie (1982).

The summer of 2013 was mainly used to explore the different localities in the inner Oslo fiord to get an overview of the area, and to decide which localities that were best suitable for further study. The exploration of the area was done by peer student Martin Kjærsgaard and

the author, with supervision by Professor Hans Arne Nakrem (Natural History Museum, University of Oslo), Professor emeritus Johan Petter Nystuen (University of Oslo) and Dr. Philos. J. Fredrik Bockelie (Exploration Advisor Ithaca Petroleum Norge AS). Other equivalent localities were visited in the Asker district by boat supervised by J. Fredrik Bockelie, with the company of peer student Martin Kjærsgaard, Hans Arne Nakrem and Johan Petter Nystuen. These localities were not studied further due to the limitation of time and amount of work this would implicate. The fieldwork on the three localities mentioned above was completed during a timeframe of approximately eight weeks during the autumn of 2013. During the first few days of field work Hans Arne Nakrem and Johan Petter Nystuen supervised and followed up. The rest of the fieldwork was done in collaboration with peer student Martin Kjærsgaard on all localities with the exception of Hovedøya. The collaboration resulted in many good discussions on observations, as well as all decisions were given a second opinion.

The nature environment authorities gave permission to collect material in protected areas (nature reserves) (Oslo Municipality).

The original plan was that both Martin Kjærsgaard and the author were supposed to focus on the same formation (Husbergøya Formation), with different angles. However, after a meeting with all people involved in the project in February 2014, there was an agreement that the author should have the overlying unit (Langøyene Formation) as his main focus. The agreement was for the author to continue logging up to the Ordovician/Silurian boundary, which fortunately was well exposed on the selected localities. The fieldwork of 2014 was completed during a timeframe of approximately 6 weeks, and was entirely done by the author alone. Regards to field safety, the author has good experience with mountaineering and hiking so deliberate precautions were taken.

5.1.1 Logging

The profiles on the three localities Hovedøya, Rambergøya and Langøyene were chosen because of its visibility, continuity without vegetation, accessibility, and minimum disturbance from tectonic events.

During the fieldwork in 2013 a point zero (datum) was placed at the boundary between the nodular limestone of the Skogerholmen Formation and the shale of the overlying Husbergøya Formation. To document the boundary between the formations, the logging started four meters down in the Skogerholmen Formation and was completed four to five meters up in the Langøyene Formation. The same was executed at all localities. Because of the thin beds of sandstone throughout the Husbergøya Formation, the scale was set at 1:10, and measured in meters from point zero. The whole profile was measured up with thickness correlation, and each meter was marked on the outcrop before the logging started. The logs obtained during the fieldwork of 2013 are not studied any further during the project (see Kjærsgaard 2014 for details).

The same reference point as zero was used during the logging of the Langøyene Formation spring/summer 2014, with the exception of the logging on Hovedøya where point zero was set approximately 3.5 meters down in the Husbergøya Formation. True thickness correction of the stratigraphic section was also executed in the same way by measuring the dip on the bedding. Because of the thicker beds of the Langøyene Formation, the logging continued in the scale of 1:25. Because of the new scale, the logging was redone from the base of the brown bioturbated sandstone in the uppermost part of the Husbergøya Formation, and ended within the first few meters of the Solvik Formation, just above the Ordovician/Silurian boundary. The amount of bioturbation is classified by three different grades; extensive, medium and little, displayed by three different symbols in the log, see legend in Appendix: A. The reason for using only 3 grades instead of the usual 6 grades is because in field the amount of bioturbation was more easily to record by using 3 grades.

Three different sections were logged during the fieldwork in 2014, one on Rambergøya (Figure 5.2), one on Langøyene (Figure 5.3), and one on Hovedøya (Figure 5.4). However, the section on Hovedøya had to be divided into two parts (HS1 and HS2), as the uppermost logged section is not located directly stratigraphic on top of the lowermost, but correlated laterally so the Ordovician/Silurian boundary was included in the log. All sections are logged

in 1:25 scale using a log-sheet provided by Ivar Midtkandal. The log-sheet used is viewed in Appendix: D.

Rambergøya

The section is located on the southwestern shore on the island, see Figure 5.2. The bedding of the layers has a dip of approximately 71°, and is well exposed up to the Ordovician/Silurian boundary. This section is the roughest as regard topography and relief, and great precautions were taken during the fieldwork. The accessibility of the section is easy. A minimum of tectonic influence is observed. The Rambergøya Profile 1 is abbreviated to "RS1".

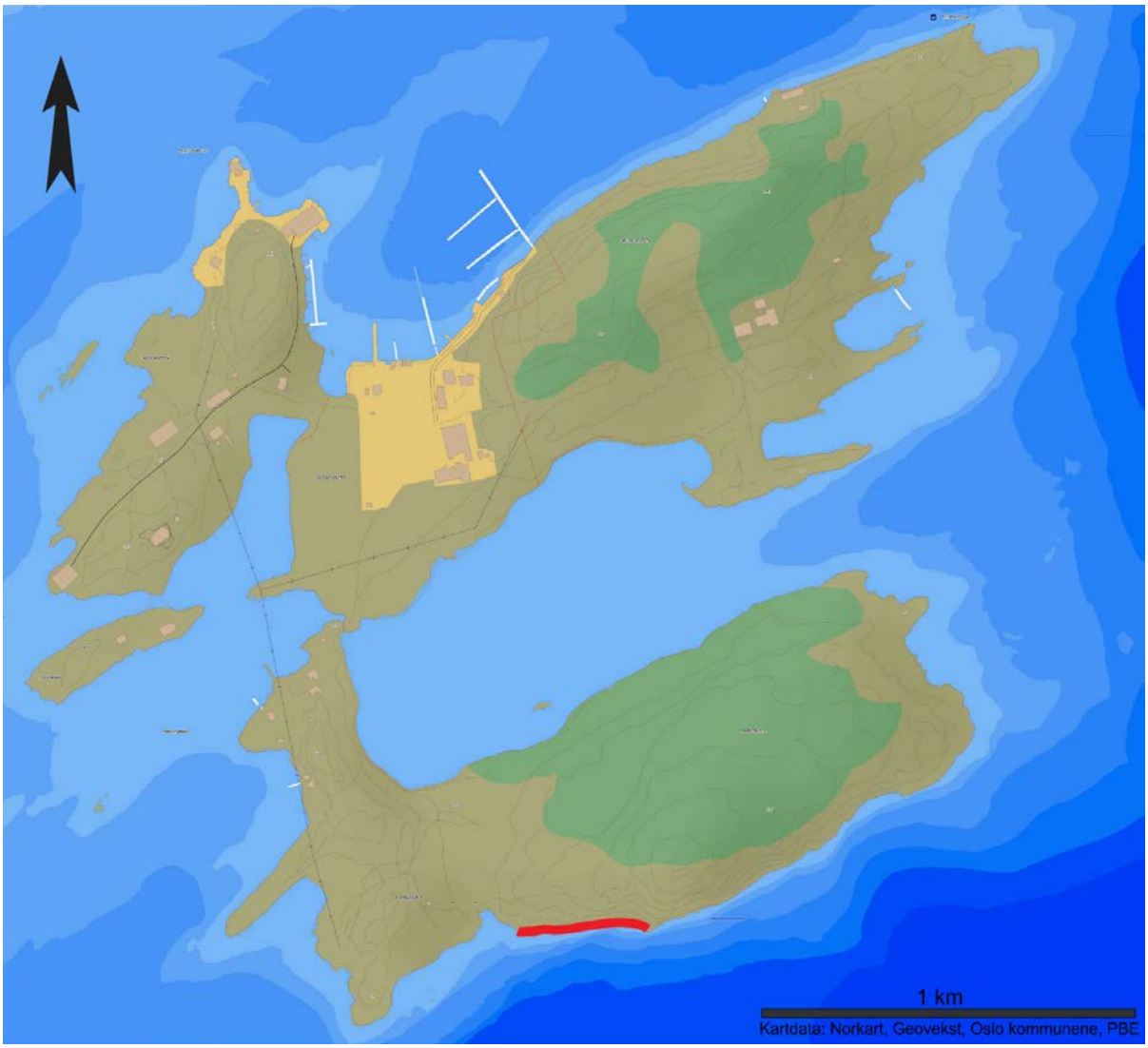

Figure 5.2: Close-up map of the Gressholmen to the north and Rambergøya to the south. The logged section is marked with a red line. Map acquired from http://kart.finn.no/

Langøyene

The section is located on the southeastern tip of the island, see Figure 5.3. The bedding has a dip of approximately 76°, and the strata are well exposed up to the Ordovician/ Silurian boundary. Although some parts of the section are exposed in relatively rough terrain, the section is easily accessible and has well-exposed outcrops. Some tectonic influence is observed, including a faulted gliding plane of a couple of meters (noted in the log). The Langøyene Section 1 is abbreviated to "LØS1".

Figure 5.3: Close-up map of Langøyene. The logged profile is marked in a red line on the southwestern part of the island. Map acquired from http://kart.finn.no/

Hovedøya

The section is located on the southwestern tip of the island, see Figure 5.4. The bedding has a dip of approximately 76° in the start of the section, whilst in the end of the section the bedding reflects an overturned fold with a higher dipping angle. The section is well exposed up to the Ordovician/Silurian boundary and is easily accessible, some tectonic influence is observed. The Hovedøya Section 1 and 2 is abbreviated to "HS1" and "HS2".

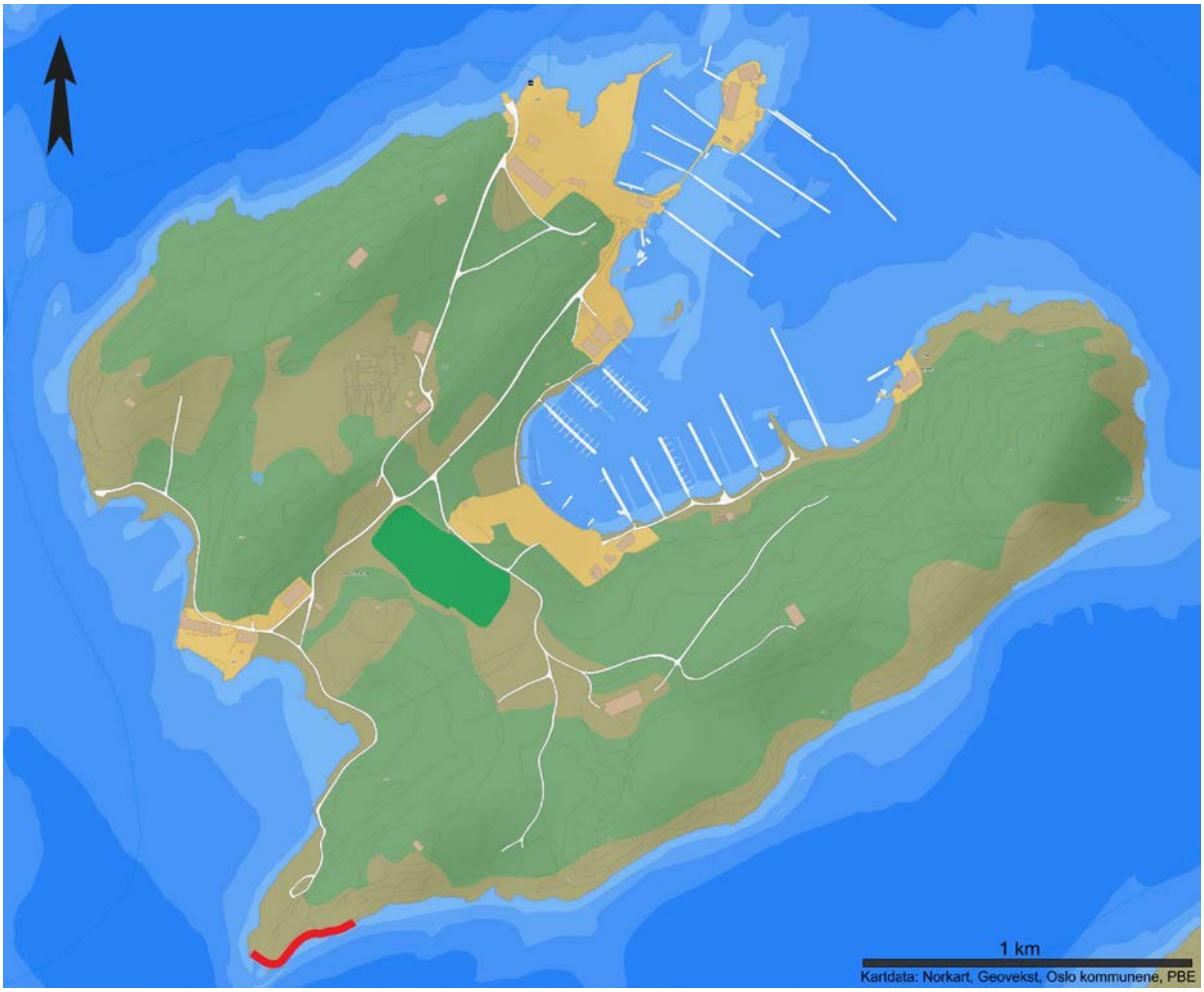

Figure 5.4: Close-up map of Hovedøya. The logged section is marked in a red line on the southwestern part of the island. Map acquired from http://kart.finn.no/

5.1.2 Sampling

The samples were collected simultaneously with the logging of the different sections. The author collected a total of 40 representative samples from the three sections; 13 from HS1, 14 from RS1 and 13 from LØS1 (see Figures 5.2, 5.3, 5.4). Each sample was given an identification number, reflecting the locality of which the sample was collected and their level (in meters) in the profile. The same identification number was also noted in the logs at the level from were it was collected. All the samples were marked with an arrow pointing stratigraphic up. In Appendix: E, all collected samples are presented in a table showing their sample-number, the level it was collected from (m), which facies association it belongs to, a short description, PMO-number for those sent to thin-section preparation, and which methods were used.

Sample preparation and methods, in which the samples were used in, are described later in this chapter. All pictures of the samples are presented stratigraphic right way up, if nothing else is noted.

5.1.3 Paleocurrent and imbrication measurement

Palaeocurrent measurements were executed at RS1. Measurement of pebble imbrication was done on the third conglomerate in LØS1, where the clasts had best imbricational features. The results are noted in the right column of the digitalized logs, and presented in Table 6.4 and 6.5. As the imbricational measurements were done on an outcrop showing the clasts only in 2D, the longest axis might not have been exposed and must be considered as uncertainties. To measure the palaeocurrent and imbrication a Silva Expedition S compass was used.

5.1.4 Photo documentation

Photos documenting observed fossils, structures and so on were taken with a Casio Exilim and a Canon Eos 1200D. Two pictures of each observed feature were taken, one with a folding rule as a scale and a post-it note, on which the location, arrow pointing in stratigraphic right way up and level were noted. The second picture was taken at the same distance as the first, including only the observed feature. The photos were later edited and scaled using Adobe Photoshop CS6.

5.2 Laboratory work

5.2.1 Digitalization of the logs

The drawing software Adobe Illustrator CS6 was used in digitalizing the logs. The hand-drawn raw-logs were scanned and opened in Illustrator as separate "layers", different tools were used in the software to draw the logs and best to illustrate structures and fossil content. The digitalized raw-logs are found in Appendix: C, and the legend for the logs in Appendix: A. Collected samples are registered in the right column in the log.

5.2.2 Sample preparation, sample scan and sample scan editing

All samples were cut in approximately 1 cm thick slabs at the Natural History Museum at Tøyen in Oslo. Because of the robustness of the samples no further preparation was necessary. The slabs were then polished on the side of interest using a rock-polishing machine until the surface was smooth. The polished side was flat-bed scanned by adding some water on the glass on the scanner, which enhanced the contrast of the structures in the rock. The scanner was a "Canon CanoScan 9000F Mark II". To obtain the best quality, boiled water (to avoid air bubbles) was used and the samples were laid on the glass in a way that removed all air bubbles. Photoshop CS6 was used to remove unwanted background and to adjust the brightness and contrast to get the best possible result of the scan, see example in Figure 5.5.

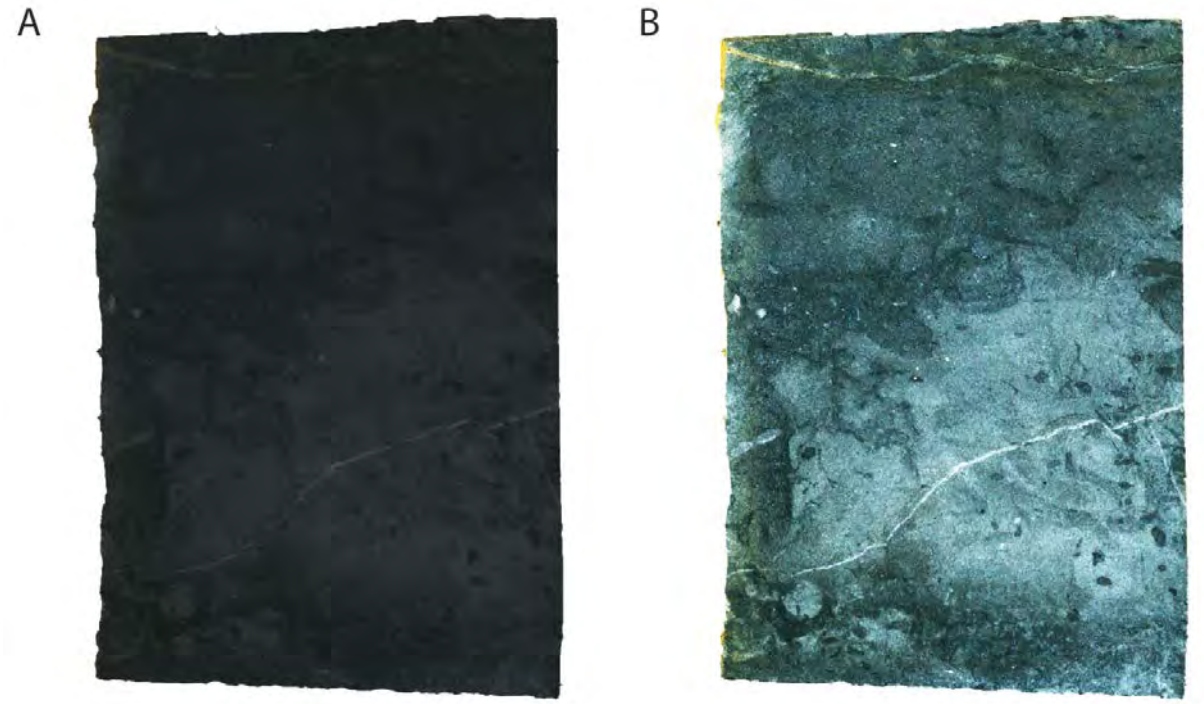

Figure 5.5: A: scanned polished slab before editing, from RS1 (18,75m). B: the same scanned polished slab as viewed in A, after editing in Photoshop CS6.

The scanned polished slabs are presented in Appendix: B, where they are presented next to the digitalized logs, and can easily be studied and correlated to their level of where they were collected from.

5.2.3 Thin-section preparation

When all the samples were scanned, a section of interest was outlined on the polished surface and cut out using the rock saw once again. Each piece was given a unique PMO (Paleontological Museum Oslo) number representing the location and level according to the logged section. The PMO number is shown in an Excel sheet, with an overview to which slab the thin-section is derived from. The cut out pieces were also marked with an arrow, pointing stratigraphic up, before it was delivered to Salahalldin Akhavan at the Department of Geoscience (University of Oslo) for preparation. A total of 43 thin-sections were prepared and used in this thesis.

5.2.4 XRD – analysis

The reason for making the XRD-analyses is to identify the mineral(s) that gave rise to the brown weathered silt/sandstone in the Husbergøya Formation. In Appendix: E an overview of all the samples with methods is presented.

An X-ray diffractometer (XRD) uses x-rays fired to a crushed sample. The different minerals present in the sample will diffract the radiation at different angles by the crystal lattice. A pattern of intensity of the angles of the diffracted x-rays is recorded and related to certain minerals, which then can be identified (Nichols 2009).

Three different samples from the brown weathered silt/sandstone at the top of the Husbergøya Formation in LØS1 were selected for XRD-bulk analysis. The three samples were located at different levels in the silt/sandstone succession, one sample from the base (LØS1 – 19 m), one from the middle (LØS1 – 20.4 m) and one from the top (LØS1 – 22 m).
After selecting the samples they were crushed first using a hammer into smaller pieces, then put into a rock crusher, in order to crush the samples into even smaller pieces. The samples were gathered in each small plastic container marked with the sample, date and the author's name.
About 3 grams of the sample were measured on a scale and crushed for the third time in a mortar by hand. To exclude possibly contamination from previously preparation, a small part of the measured sample was added in the container together with some ethanol, which on beforehand was thoroughly cleaned, and run in the micronizing machine for about 30 seconds. The container, which contained small cylinders made of agate, stacked on top of each other, was emptied before the remaining sample was added together with 8 ml of ethanol and run in the micronizing machine for 12 minutes. The micronizing machine used was a "Glen Creston, McCrone Micronizing Mill".

The micronized sample was cleaned out from the container, using ethanol, into a new small plastic container, also marked with sample, date and the author´s name. It was then put in a heating-cabinet, which would expedite the evaporation of the ethanol, leaving only the micronized sample in the container. Between the crushing and micronizing of the different samples, the equipment was thoroughly cleaned, to avoid any contamination. The preparation and XRD – analyses were done at Department of Geosciences, University of Oslo.

The software “Diffrac Suite EVA V 2.0” was used to conduct the qualitative analyses from the XRD results. The different mineral peaks in the diffractogram were manually identified by the use of d-spacing values and intensities, from the PDF-2 database. When all the mineral peaks were identified a different software (Diffrac Suite Topas) was used to quantify the different minerals into percentages and later imported into Excel.

Uncertainties related to the XRD-bulk analyses include that the peak intensity and shape of the different mineral phases are influenced by the crystal size, orientation and crystallinity of the samples. The detection limit of the Lynxeye detector is usually around 1-2% in multi-component samples, but this detection limit is affected by the overlapping of certain minerals.

5.2.5 Point counting

A quantitative analysis was performed on each thin-section used in the point counting analysis, in order to get an overview over the components represented. The minerals counted are as follows; quartz, feldspar, pyrite, opaque minerals, calcite, mica, metarhyolite and matrix. 400 counts were taken from each thin-section. The quartz was separated into three separate groups; mono-crystalline, poly-crystalline and metamorph.

In the samples where the quartz has a grain-size of silt to very fine sand, they are all counted as monocrystalline quartz. As the fossils mostly are crushed into pieces beyond recognizing, and are rather sparsely in some samples, they are counted either as calcite or matrix. This is due to the limitations of time because the delayed preparation of the thin-sections. The calcite also includes calcite cement. A “Nikon Labophot-pol” microscope and a “Swift model F” point counting device was used in the analysis.

5.2.6 Maximum particle size and roundness/sphericity analysis

The apparent maximum particle size (MPS)analysis was done on all thin-sections from all three profiles. A microscope connected to a camera feeding live images to a computer was used in this analysis. In each sample, 30 of the largest quartz grains were measured on its longest axis in the computer software "ScopeView 3.0", and when the counting was done, the results were exported to Excel. The Wentworth (1922) grain-size classification, shown in Table 5.1, was used in the grain size analysis. Because the grains are only viewed in two dimensions, the longest axis might not be represented and could be a source of error. Due to the few numbers counted, no statistical calculations on the deviation from the true longest axis have been performed. However, the mean value of the 30 apparent longest particle axis is supposed to reflect the real MPS and stratigraphic variation in the apparent MPS a trend reflecting variation in true grain size.

Table 5.1: Grain size classification with corresponding Phi-units and correct terminology. Modified from Wentworth (1922).

Size range (mm)	Phi-units	Wentworth size class
256 - ∞	∞ - -8	Boulder
64 - 256	-6 - -8	Cobble
4 - 64	-2 - -6	Pebble
2 -- 4	-1 - -2	Granule
1 -- 2	0 - -2	Very coarse sand
0,5 – 1	1 - 0	Coarse sand
0,25 – 0,5	2 – 1	Medium sand
0,125 – 0,25	3 – 2	Fine sand
0,0625 – 0,125	4 – 3	Very fine sand
0,0039 – 0,0625	5 – 4	Silt
∞ - 0,0039	1/∞ - 8	Clay

After an overview of the particle size was obtained, the roundness/sphericity could be estimated simply by dividing the quartz grains into two groups by its grain size. Quartz grains larger than 0.3 mm are well rounded with a high sphericity, and quartz-grains smaller than 0.3 mm are angular to sub-angular with low sphericity. The roundness table from Powers (1953), shown in Figure 5.6 was used to classify the grains. Here again the sphericity of the grains could be misleading, as the grains are only represented in two dimensions.

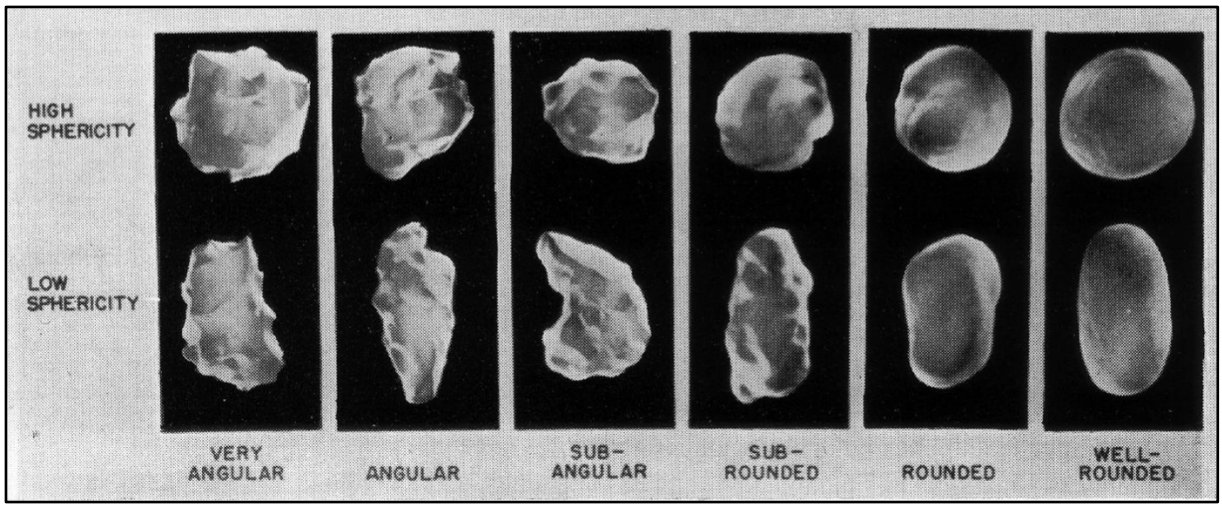

Figure 5.6: Roundness scale used to determine roundness of the grains represented in the thin-sections. Acquired from Powers (1953).

6 Results

During this chapter the Hovedøya Section 1 and 2 will be referred to as HS1 and HS2, the Langøyene Section 1 as LØS1 and the Rambergøya Section 1 as RS1. If not specified, all pictures in this chapter are presented stratigraphic right way up.

6.1 Facies and facies associations

The term facies is used for correlating and determining different depositional environment. It has been used since the pioneers in geology and mining engineering found it as a useful tool for locating valuable minerals, coal and oil.
Rock-facies can be a single layer, or multiple layers put together with certain characteristics, which reflects a depositional feature or event. The different facies can be put together, which is called a facies-association (Reading and Lewell 1996).

The different facies observed during the fieldwork will first be defined and described, then the facies will be put together in different facies-associations. The facies-associations will reflect different depositional settings.

6.1.1 Facies

Shale, siltstone, fine-grained sandstone and limestone

Table 6.1: Schematically overview of the observed low-energy facies.

Facies	Description	Physical structures	Interpretation
F1	Brown weathered sand/silt-stone	No structures Bioturbation Index: 6	Pause in sedimentation, brown reddish colour as a result of weathering, oxic conditions
F2	Shale with high grade of bioturbation	No structures Bioturbation Index: 6	Deposited in open marine environments below storm wave base, low sedimentation rate, oxic conditions.
F3	Nodular limestone	Beds of nodular limestone	Deposited as continuous beds, nodules formed during diagenesis
F4	Structureless calcareous siltstone	Structureless beds	High amount of carbonate due to a low rate of siliciclastic input, the discontinued beds can be a diagenetic feature
F5	Soft sediment deformed sandstone	Folded primary lamination, and chaotic oriented clasts	Semi-consolidated layers with high water saturation slumped due to sediment instability

F1: Brown weathered sand-/silt-stone

Description: Silt to clay grain size dominate this facies that can be characterized as a sandy siltstone with 30% sand with the largest sand grains around 50 micrometer (Figure 6.24 A and C). It appears with a protruding brown-reddish weathered colour in field (Figure 6.1 A). It occurs in the top of the Husbergøya Formation, with a thickness of approximately 2-3 meters, but the facies is also recurring up through the Langøyene Formation. Included in this facies are massive beds with alternating lighter and darker colour, varying in thickness in the range of 5-40 cm. It is heavily bioturbated, with no preserved lamination, with a value set to 6. This facies is represented on all localities.

Interpretation: The substantial high grade of bioturbation interpret to indicate a very low rate in sedimentation, giving the benthic organisms time to rework the sediments, destroying all primary lamination. As fresh broken surfaces of the facies are greyish in colour, the brown-reddish colour is most likely due to weathering of certain minerals containing iron.

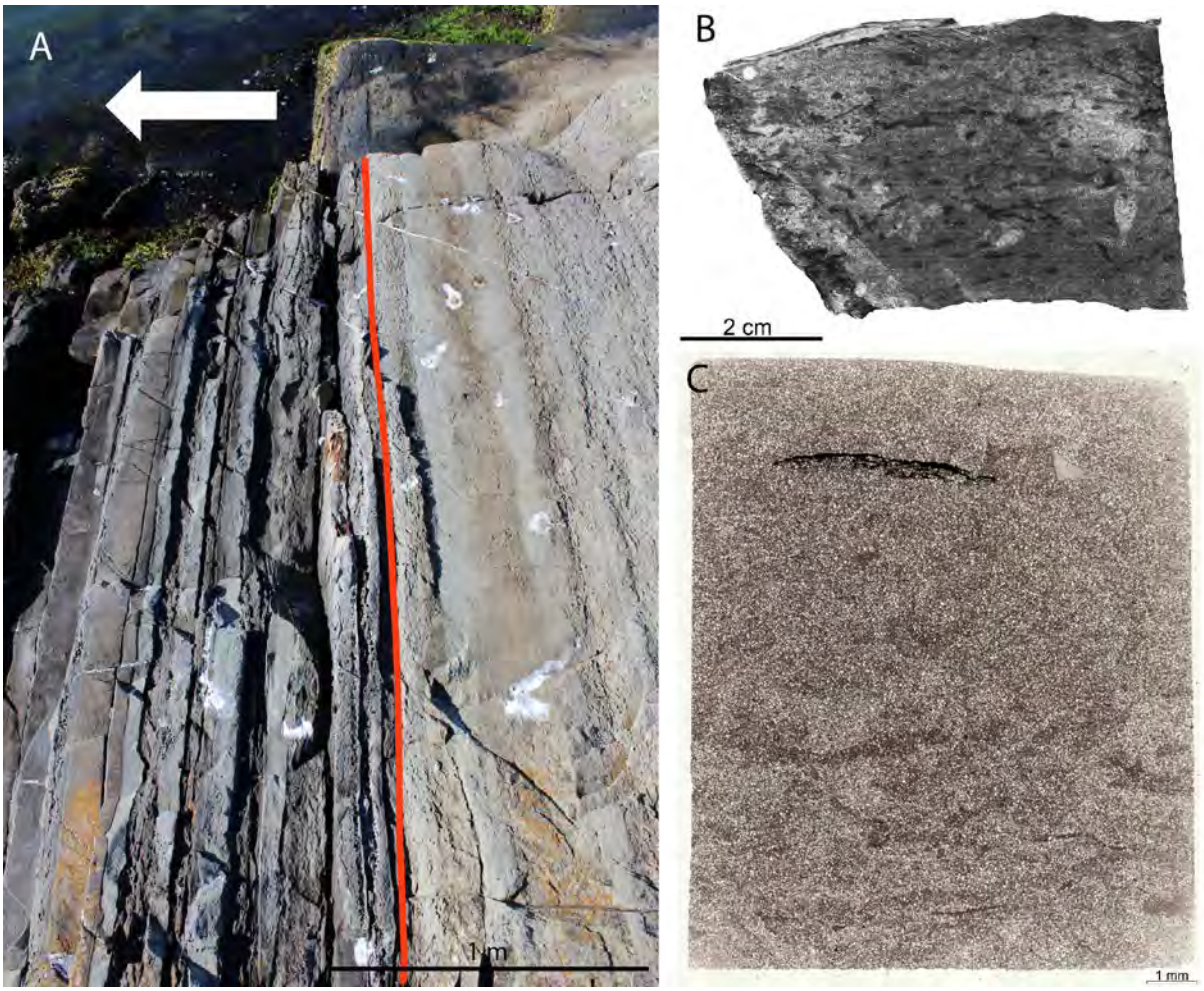

Figure 6.1: A: Field photo from LØS1(22-23m). The red line represents the boundary between the brown weathered silt/sandstone of the Husbergøya Formation (to the right) and the first storm-deposits of the Langøyene Formation, arrow pointing stratigraphic up. B: Scanned polished slab from facies F1 from LØS1 (22m), showing the high grade of bioturbation and absence of any lamination. C: Scanned thin-section of facies F1 from RS1 (17m), showing the bioturbated sediments.

F2: Shale

Description: Clay-sized grains dominate the sediments of this facies. A high grade of bioturbation is observed, set to Bioturbation Index 6. The shale has a dark grey to black colour, and is mainly represented in the Solvik Formation (Figure 6.2); however, some places it can be found interbedded in facies F1 in the Langøyene Formation.

Interpretation: Fine particles, such as clay-sized grains, are carried in suspension by water. When the currents with the suspended material enter quiet water, the suspended material will be deposited. This happens in open marine environment beneath fair weather and storm wave base. The rate of sedimentation has generally been very low, the benthic organisms therefore had time to rework the sediments and destroy all primary lamination. The high grade of bioturbation also indicates oxic bottom conditions.

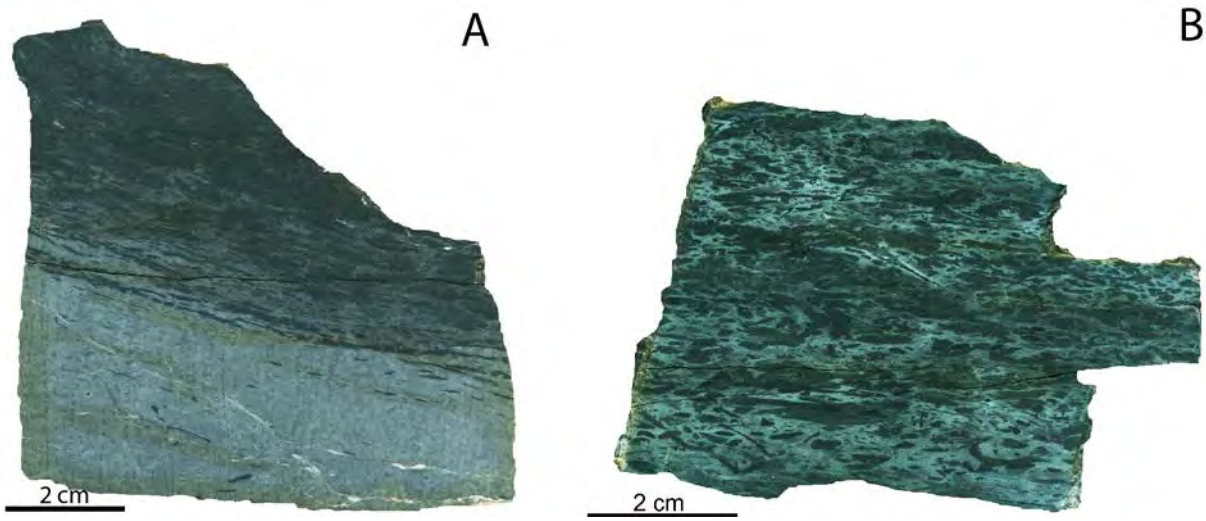

Figure 6.2: Scanned polished slabs of facies F2 from the shale of the Solvik Formation. A: Cleanlier calcareous layer overlain by the bioturbated shale from HS1 (49.7m). B: Highly bioturbated shale of facies F2 from RS1 (71.25m).

F3: Nodular limestone

Description: This facies is easily recognized by its sub-rounded nodules, which form layers, or occur along definite stratigraphic levels. The facies seems to have gradually transition from continuous massive layers of calcareous siltstone (F4) into more discontinuous layers to nodules in the top. It is interbedded in F1, and the unit consisting of nodules range from 50-70 cm in the three profiles (Figure 6.10). Brenchley and Newall (1975) included the nodular limestone be a part of the Solvik Formation.

Interpretation: The formation of the nodular limestone has been discussed by Bjørlykke (1973) and Henningsmoen (1974). However, Möller and Kvingan (1988) concluded that the formation of the nodules is connected to the palaeogeographic setting, where carbonate sediments are deposited below fairweather wave base and the nodules are formed during diagenesis below the sediment/sea-water interface.

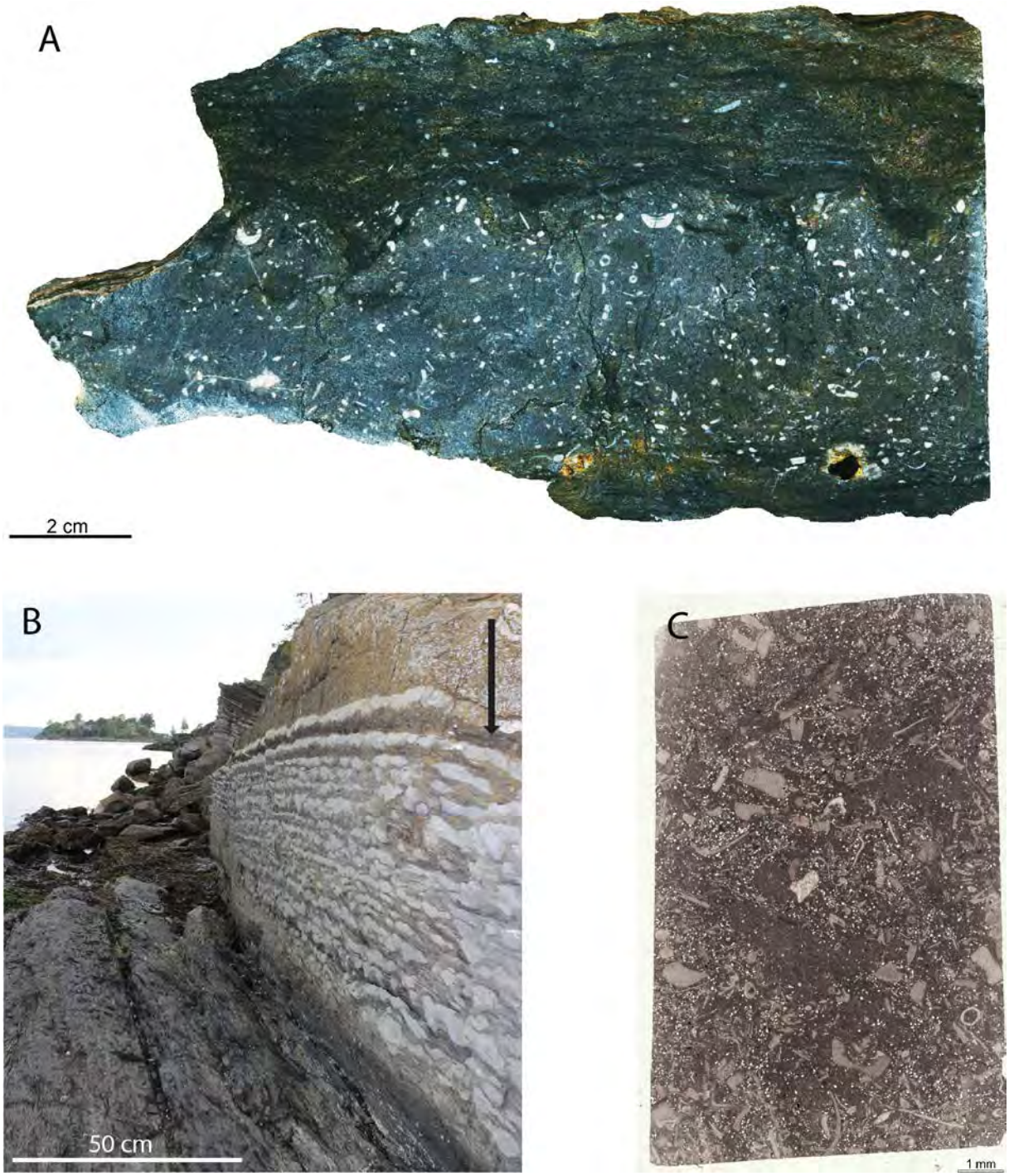

Figure 6.3: Nodular limestone in different appearance. A: Scanned polished slab of a nodule viewed as the lighter section, with more fossiliferous particles, overlain by the interbedded brown weathered silt/sandstone. From RS1 (69.9m) B: Field photo from HS1 (47.5 - 49m), showing the brown weathered silt/sandstone, nodular limestone and shale in the Solvik Formation. Arrow showing stratigraphic up. C: Scanned thin-section of a nodule, showing the high amount of fossil fragments in a mud matrix, from RS1 (PMO: 221.876).

F4: Structureless calcareous siltstone

Description: This facies is similar in colour to the nodular limestone, but differs from the nodular limestone by its massive continuous beds, without any sign of lamination (Figure 6.4). In some localities the facies contains a large quantity of fossil fragments. The continuous layers end in some places abrupt, with rounded edges and continued by divided sections at the same level. It is represented on all three localities.

Interpretation: The high amount of carbonate is most likely related to a very low supply of siliciclastic particles the basin. The discontinuous layers with rounded edges, can be a diagenetic feature, such as described in the formation of nodular limestone.

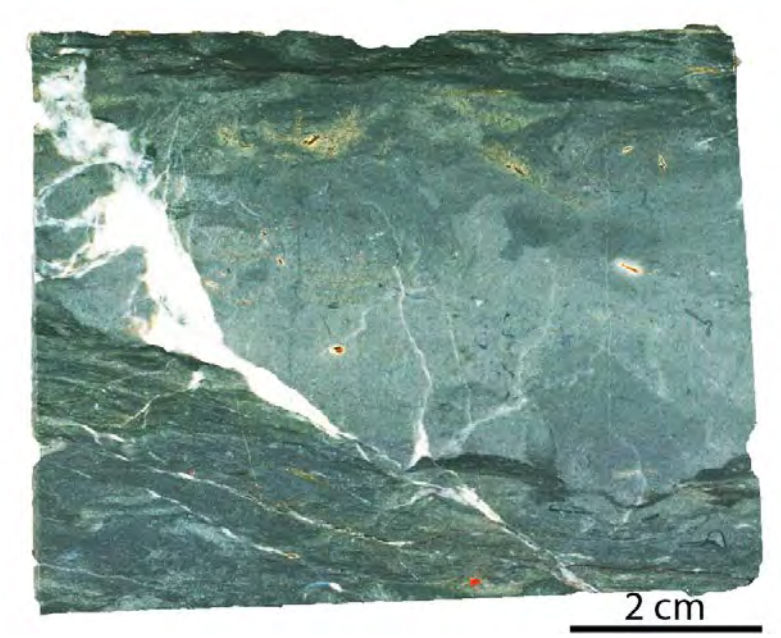

Figure 6.4: Scanned polished slab of facies F4 from HS1 (48m).

F5: Soft sediment deformed sandstone

Description: This facies is recognized as large slumped layers of sandstone, where the primary lamination is disturbed and folded. Some layers seem to have collapsed into the underlying layer, see Figure 6.5. The soft sediment deformation structures are often found together with water escape structures. It is located in all logged sections, and the ones found on LØS1 are recorded to be several meters thick.

Interpretation: Soft sediment deformation with some primary lamination preserved as folded lamination can indicate that the sediments were semi-consolidated. The appearance of water-escape structures together with this facies means that the sediments were highly water saturated. Where the sediments seem to have collapsed into the underlying layer can be related to the rate of deposition onto the layer into which it collapsed. If finer sediments are deposited with high porosity and water saturation, and if i.e. a storm deposited layer of coarser, denser sediments are deposited in a short period of time, this will collapse into the underlying layer (Nichols 2009).

Stability of sands is reduced by three principles:

1. When a sand bed is enclosed between two impermeable layers, the pore-pressure increases as a result of the increasing vertical stress. This can lead to a point where the pore pressure equals the hydrostatic pressure, and a small horizontal stress can cause movement in the over-pressured layer (Hubbert and Rubey 1959).
2. Fluidization – upward moving water causes a fluid drag, which in fact can equal the downward force from the particles.
3. Liquefaction – this happens when particles are shaken loose from one another by sudden events, such as earthquakes (Allen and Banks 1972).

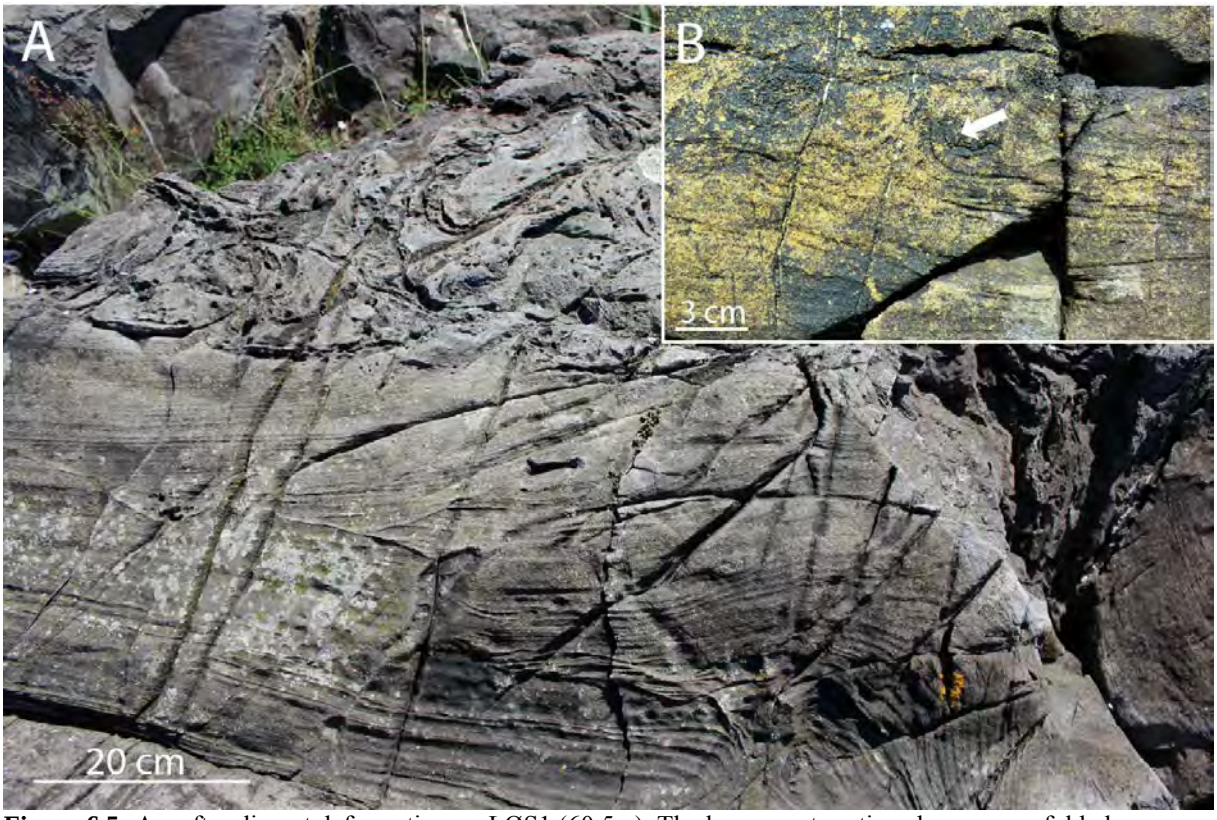

Figure 6.5: A: soft sediment deformation on LØS1 (60.5m). The lowermost section shows some folded lamination, whilst the uppermost part is too deformed to show any primary lamination. B: water escape structures found beneath a soft sediment deformed layer on RS1 (38,6m).

Sandstone and conglomerate

Table 6.2: Schematically overview of the observed high-energy facies.

Facies	Description	Physical structures	Interpretation
F6	Laminated sandstone	Parallel laminated, asymmetrical and symmetrical ripples, hummocky cross stratification, structureless sandstone.	High rate of deposition, interpreted as storm deposited layers (tempestites).
F7	Tabular cross-stratified sandstone	Set of tabular cross-bedded sandstone, with parallel laminated sandstone beneath and a thin pebble conglomerate on top.	Developed from migration of unidirectional straight crested dunes in a lower flow regime.
F8	Low angle cross-stratified sandstone	Low angled cross –stratification which downlaps on parallel laminated sandstone.	Top of channel infill, medium- to fine-grained sand grains. Belongs to the upper flow regime.
F9	Coquina bed	No observed structure	Mechanically sorted and abraded fossil fragments, deposited within 4-20 meters.
F10	Pebble conglomerate	Imbricated clasts, large scale cross bedding of well rounded quartz grains and calcareous silt/sand/bioclasts.	Imbrication of the clasts indicates a unidirectional current. Lithological similarity between the clasts and the tempestites indicates the pebbles are derived by erosion from underlying sea-floor.
F11	Boulder conglomerate	No structure, but the boulders have large scale cross-bedding as primary stratification.	Size and angularity, suggests that the boulders have fallen from margins of channels cut into underlying beds.

F6: Laminated sandstone

Description: This facies consists of very fine to fine grained sand, which is relatively homogenous with a matrix of unknown content. Some bioclastic material can be present. F6 includes the following physical structures; parallel lamination, asymmetrical ripples, symmetrical ripples, hummocky cross stratification (HCS) and structureless sandstone. These structures can all be observed in the same layer, but also separated in different beds. The base is observed both as erosive and non-erosive with load casts. Water escape structures are also recognized in some of these layers. The beds are laterally continuous for several meters, but can also be discontinuous (lenticular). Bioturbation, both vertical and horizontal is present, especially where the layers have small amounts of the primary lamination left, which is referred to here as structureless sandstone. The thickness ranges from 3-50 cm and is present at all three localities, see examples in Figure 6.6.

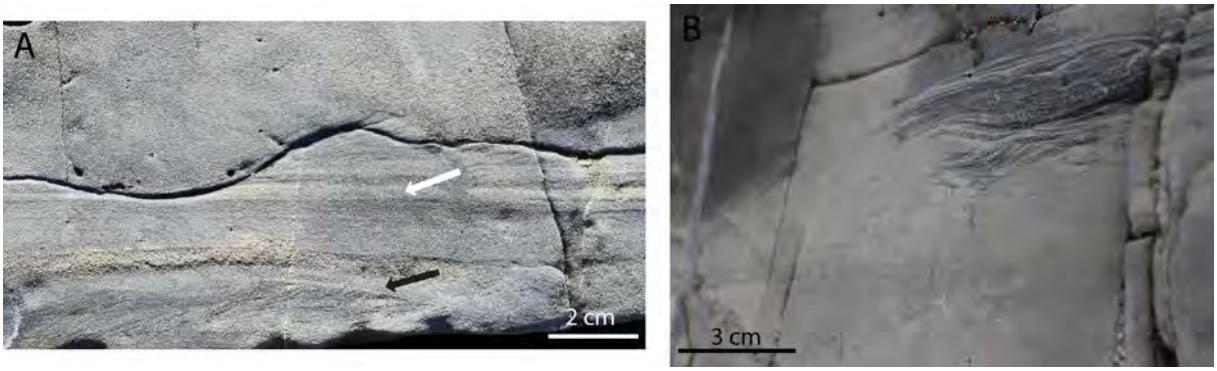

Figure 6.6: Two examples of facies F6. A: Black arrow viewing some asymmetrical ripples, overlain by parallel laminated sandstone (white arrow). Uppermost in the picture a structureless sandstone with an erosive base is also represented, all together called an amalgated bed. From LØP1 (22.72m). B: Small-scale Hummocky Cross Stratification represented on HP1 (19m).

Interpretation: The abrupt change from underlying silty mudstone to homogenous, very fine to fine sandstone, together with the erosive base and loading structures, indicates a rapid rate of deposition. Parallel laminated sandstone is deposited during powerful wave oscillations followed by weaker ones (Myrow and Southard 1996). Hummocky cross stratification is created during an unidirectional flow, most likely by geostrophic currents and wave oscillation (Myrow and Southard 1996). The symmetrical ripples are developed during the waning stages of storms by oscillatory wave flow. The beds of massive structureless sandstone have been deposited too fast to show any structure, or destroyed by bioturbation. It is probably a mix of both the mentioned reasons.

The loading structures are created post-depositional, and are formed due to porosity and density differences between the sediments and indicates a rapid deposition of sand.

These physical structures put together are characterized as storm deposited layers, known as tempestites (Myrow and Southard 1996). An idealized storm succession is divided into different levels, reflecting energy and stage of the storm during which it was deposited. A generalized storm succession has been described in Dott and Bourgeois (1982), and has been named the "Dott-Bourgeois sequence", see Figure 6.7.

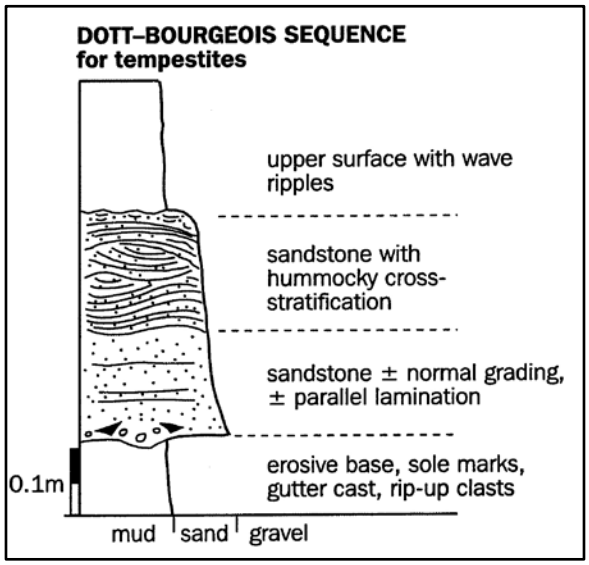

Figure 6.7: An idealized storm sequence, named the "Dott-Bourgeois sequence". From Stow 2005.

F7: Tabular cross-stratified sandstone

Description: Facies F7 are composed of fine to medium sand in a bed of approximately 30-40 centimetres in thickness. The bed is overlain by a 10-centimeter thick layer of conglomerate, and is observed only in the uppermost part of the Langøyene Formation in RS1. The base of the bed seems to be erosive and has a honeycomb coral facing downwards in the basal part. The first ten centimetres consists of parallel laminated sandstone, before the prominent through cross stratification appears, see Figure 6.8.

Interpretation: The tabular cross-bedded sandstone is developed from migration of unidirectional straight crested dunes. These forms are deposited in the lower flow regime. The unit where it is observed is composed of a layer of structureless sandstone, then the through cross stratification, which is capped by a ten-centimeter thick pebble conglomerate. This may reflect a periodicity in water flow, i.e. monsoon seasons, which will show a variety in structure and sediments.

Figure 6.8: Facies F7; tabular cross-stratified sandstone (red outlined area) overlain by a thin conglomerate and parallel laminated sandstone, from RS1 (66 – 67m). The conglomerate is interpreted to represent the base of channel-shaped down-cut structure.

F8: Low angle cross-stratified sandstone

Description: This facies is in all observations related to the infill of sediments above the conglomerates and consists of a homogeneous fine to medium sand grains. The low angled cross stratification downlaps on parallel laminated sandstone. The thickness of the beds of facies F8 varies from 5 to 20 centimeters. It is represented in all three logged sections, related to the conglomerates, see example in Figure 6.9 (A).

Interpretation: As the facies F8 is mostly represented in the upper part of the channel it is interpreted to be the last deposit of a channel infill succession before it gets inflicted by the marine environments. In (Collinson 1996), it is also described to be more common in the top of a channel infill belonging to the upper flow regime.

F9: Coquina bed

Description: One observation is done of facies F9, it is located in the uppermost part of the Langøyene Formation on HS1. The coquina bed consists of crushed bioclastic material from cornulites, trilobites, crinoids, bryozoans and corals in a calcareous matrix. Laterally the F9 facies passes gradually into a homogeneous sandstone bed.

Interpretation: The coquina beds are deposited in depressions in the seafloor after being mechanically sorted and abraded by wave currents. They are deposited within a depth of 4-20 meters (Talbot and Allen 1996).

F10: Pebble Conglomerate

Description: Facies F10 is composed of pebble-sized bioclasts from corals, well-rounded clasts with interlaminated sandstone and structureless siltstone. The bioclasts appear to have an imbrication, see Figure 6.9 C. The matrix is mostly calcareous, but extremely well rounded, coarse quartz grains, referred to as "millet-seeds" in Brenchley and Newall (1975), are also present in various amounts. This facies is recognized on LØS1 and RS1, and is repeated three times in each profile.

Interpretation: The imbrication of the clasts indicates deposition in a unidirectional current, and because of the well-rounded clasts, a considerable distance of transportation must have taken place. The clasts, which resembles the storm deposited layers (tempestites) described in F6 and brown weathered sand/siltstone described in F1, are probably derived from erosion of the old sea floor.

F11: Boulder Conglomerate

Description: Facies F11 is composed of angular boulder-sized clasts with internal cross bedding. The boulders are composed of well-rounded coarse quartz grains and medium- to coarse-grained calcareous sand. The orientation of the boulders is chaotic and shows no common lineation, as indicated in Figure 6.9 D.

Interpretation: The angularity and size of the boulders suggests a short distance of transportation, and the similarity between the lithology of the boulders and the uppermost beds of the overlying part of the Langøyene Formation found further north and east on Hovedøya, outside the logged section (see Figure 6.10 D), indicates that the boulders have fallen into the base of the channel from the channel margins.

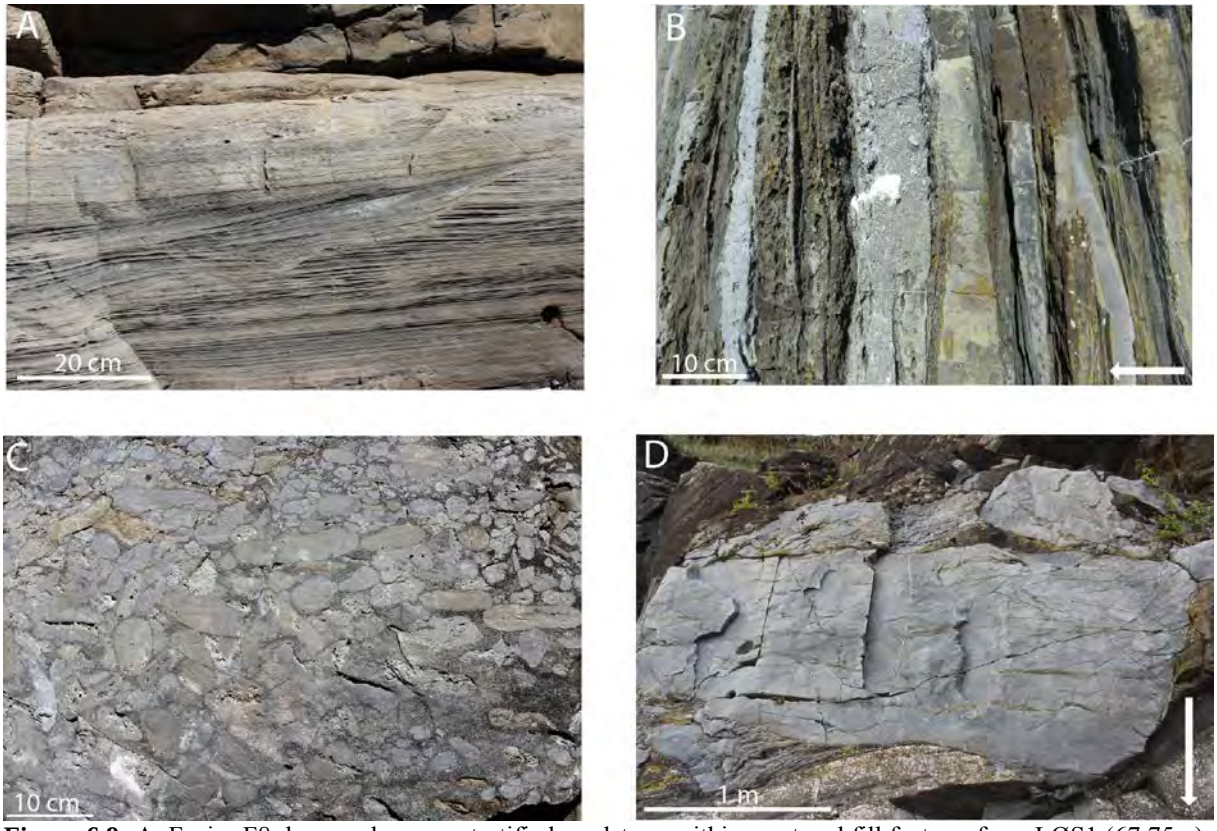

Figure 6.9: A: Facies F8; low angle cross-stratified sandstone within a cut and fill feature, from LØS1 (67.75m). B: Facies F9; Coquina bed which laterally turns over to a coarse sandstone bed (white arrow pointing stratigraphic up), from HS1 (46m). C: Facies F10; pebble conglomerate with imbricated clasts on LØS1 (76.32m). D: Facies F11; a large boulder in the base of the conglomerate on HS1 (base of channel).

6.1.2 Facies associations

Table 6.3: Schematically overview of the different facies associations with including facies and location.

Facies Associations	Including facies nr.	Located in stratigraphic unit
FA-Ia	F1	Husbergøya and Langøyene Fm.
FA-Ib	F1, F3, F4	Langøyene and Solvik Fm.
FA-II	F1, F2, F4 → F9	Langøyene Fm.
FA-IIIa	F5, F6, F7, F8, F10	Langøyene Fm.
FA-IIIb	F5, F6, F8, F9, F11	Langøyene Fm.
FA-IV	F6, F7, F8	Langøyene Fm.
FA-V	F2	Solvik Fm.

FA – Ia

Description

This facies association includes only one facies and is recognized in field by its brown weathered colour, has a siltstone/very fine sandstone fraction and is heavily bioturbated. It is first recognized in all three profiles as an approximately 3 meter thick unit, representing the top of the Husbergøya Formation. On HS1 the brown weathered colour is not as prominent as it appears to be in LØS1 and RS1. The first occurrence of a sandstone layer marks the end of this facies association, see Figure 6.1 A.

Fossils such as cystoids, trilobites, brachiopods, bryozoans and cornulites are observed in the logged section on Rambergøya and Langøyene.

Interpretation

The extensive bioturbation of the silt/very fine sandstone can indicate a calm marine environment with very low sedimentation rate, which allowed the organisms to rework the sediments and obscure all signs of lamination. The bottom conditions were most likely not anoxic, again because of the evidence of living organisms feeding in the seafloor. This coincides with Brenchley and Newall (1975) who suggested that the extensive bioturbation of the silt/very fine sandstone indicates a hiatus in the sedimentation. In Appendix B, the scanned polished slabs of FA-Ia from each logged section can be observed, and correlated to their level in the logs.

FA – Ib

Description

This facies association resembles the FA – Ia in colour and the extensive bioturbation, but includes in addition to facies F1, both facies F3 (nodular limestone) and F4 (structureless calcareous siltstone). FA-Ib is dominated by facies F1 in the lower part and interbedded with facies F4, before it becomes more nodular (F3) in the uppermost part. It is located in the uppermost part of the Langøyene Formation and continues through the Ordovician/Silurian boundary. The bioturbated shale of the Solvik Formation succeeds beds of this facies association.

The facies association is recognized at all three localities with some differences from each other. The FA – Ib in LØS1 is the one who distinguish itself mostly from RS1 and HS1. The interbedded nodular unit is not as prominent, but appears more like continuous layers (Figure 6.10). In addition, the dominant brown weathered silt/sandstone in the lowermost part of the facies association has a smaller thickness at LØS1. On the other hand, both the thickness and appearance of nodules is rather comparable in HS1 and RS1. The bed starts with massive brown weathered silt/very fine sandstone, which gets interbedded with structureless calcareous siltstone, after two or more continuous layers the siltstone gets more nodular. The size of the nodules decreases before the Solvik Formation caps it, see Figure 6.10.

Interpretation

The F1 facies is most likely deposited during the same conditions as described in FA – Ia. The deposition of facies F4 (structureless calcareous siltstone) is most likely deposited during a relatively short time period. The formation of the nodular limestone has been described in facies F3.

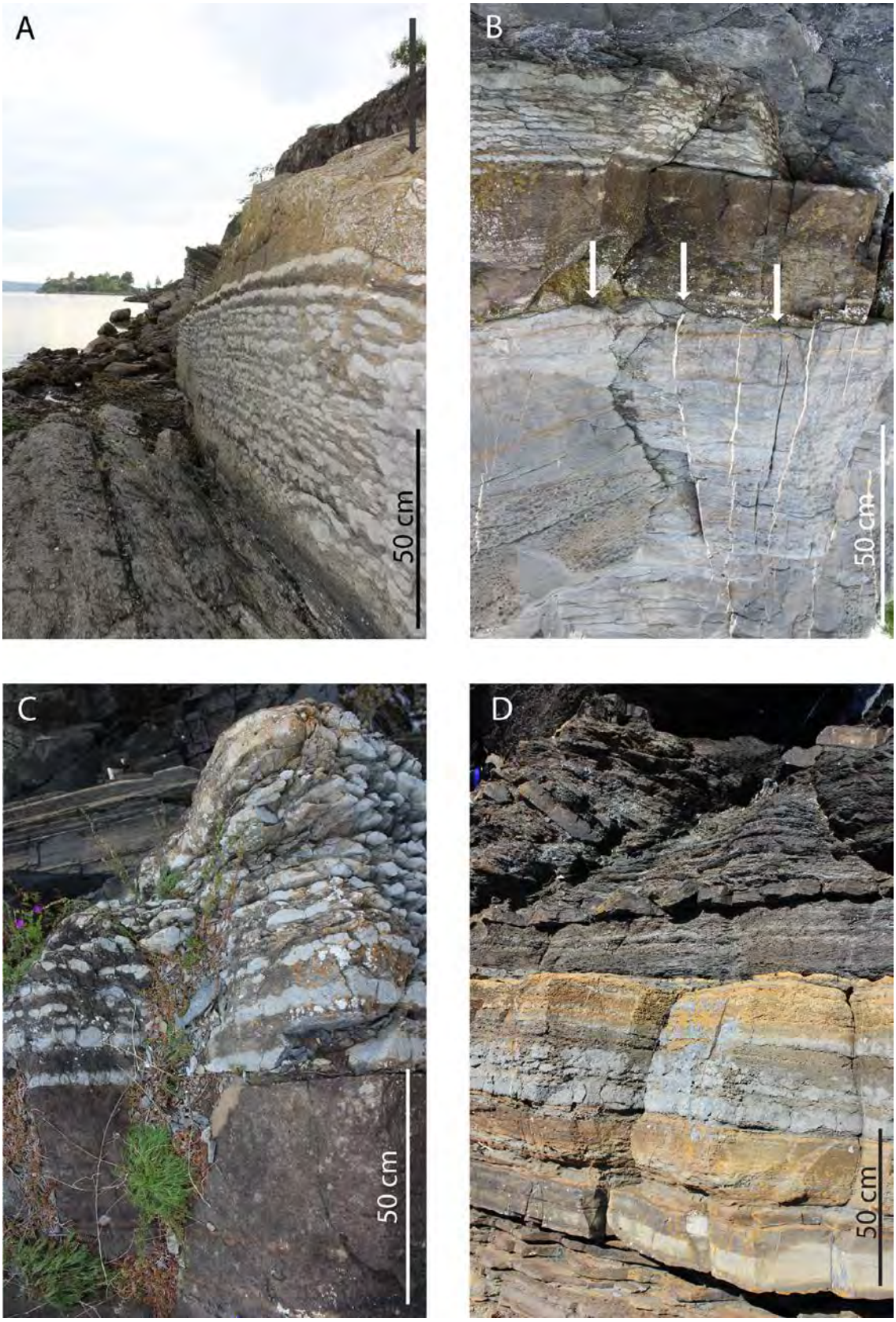

Figure 6.10: Field photos of nodular limestone and shale in the Solvik Formation, and boundary between the Langøyene and the Solvik Formation. A: FA-Ib and FA-V on HS1 from the logged section, arrow pointing stratigraphic up. B: FA-Ib and FA-V further north outside HS1, the underlying unit resembles the boulders found in the base of the channel in HS1, note the karstic surface viewed by arrows. C: FA-Ib on RS1. D: FA-Ib and FA-V on LØS1.

FA – II

Description

This facies association occurs first just above FA – Ia and marks the boundary between the Husbergøya Formation and the Langøyene Formation with the first occurrence of a bed with sand. It is repeated two times in the stratigraphy in all logged sections. The FA – II is made up with alternating layers of heavily bioturbated silt/very fine sandstone with no apparent structure, and layers with coarser sand including structures such as erosive base/loadcasts, parallel lamination, asymmetrical ripples and hummocky cross stratification. Soft sediment deformation is also present in all three profiles, with a difference in frequency and thickness.

The FA – II is relatively alike in all three sections, but RS1 and LØS1 resembles more, compared to HS1. The slumping is more frequent and the coarser sandstone layers are relatively thicker with more structures in RS1 and LØS1. The thickness and frequency of the soft sediment deformed layers found in LØS1 exceeds what is found both in HS1 and RS1. The first occurring unit of FA-II is represented in Figure 6.11 A as a section from the log.

Interpretation

The silt/very fine sandstone is most likely deposited during a period of low sedimentation rate, whilst the coarser layers of sandstone could be related to storm deposition. The erosive base, parallel lamination, hummocky cross stratification and asymmetrical ripples correspond well to the definition of a tempestite. The appearance of load casts and lack of bioturbation suggests that the layer was deposited in a short period of time.

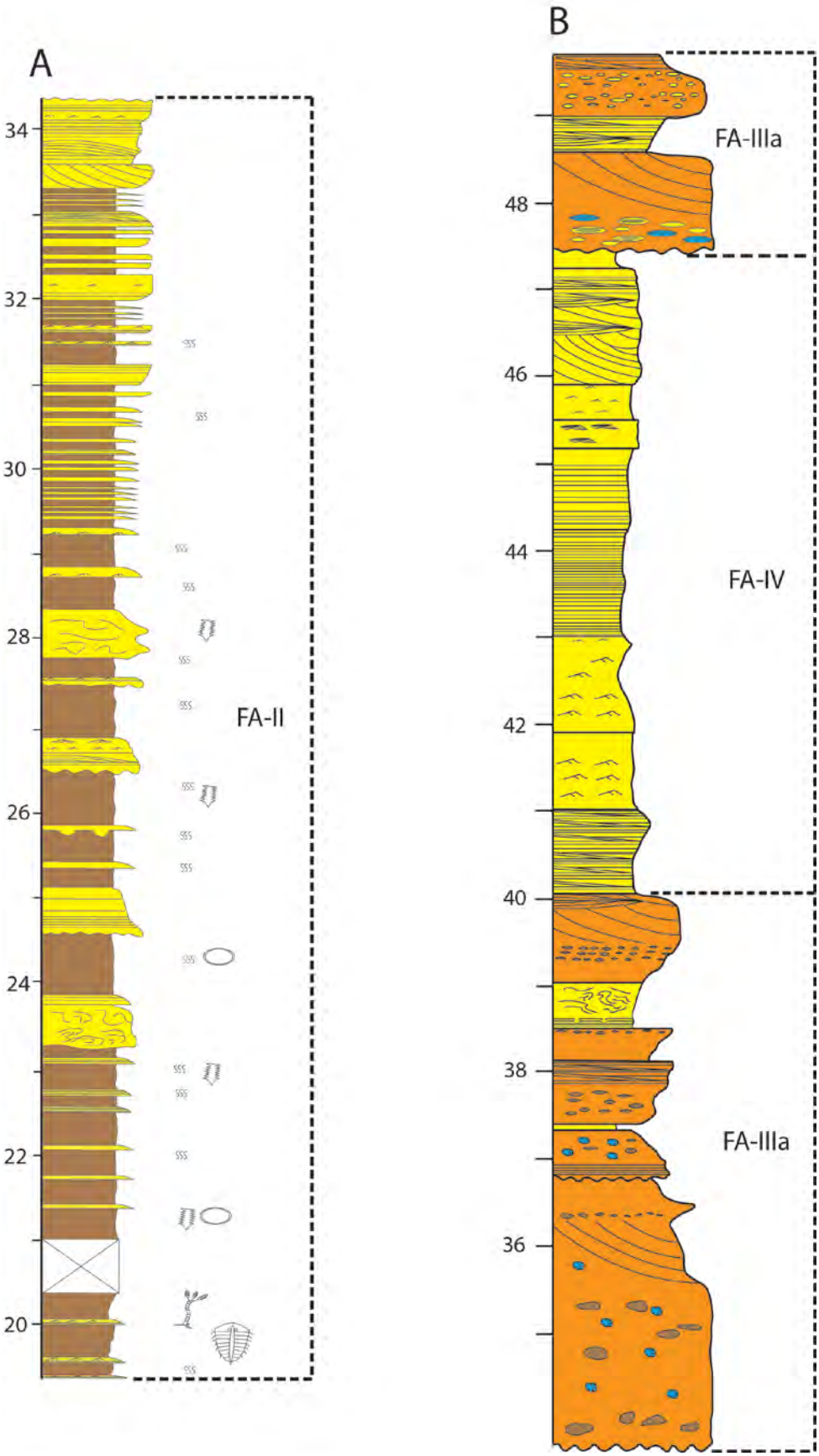

Figure 6.11: From the logged section on RS1. A: FA-II, with the first input of a clean sand bed in bottom. B: FA-IIIa with the first conglomerate in the lower part, and second conglomerate at the top of the log. FA-IV is represented between the conglomerates.

FA – IIIa

Description

This facies association marks the end of FA – II, with the erosive base of a conglomerate. This pebble-conglomerate is located in RS1 and LØS1 but not on HS1. The FA – IIIa is repeated three times in both sections.

The first conglomerates in both sections have more or less the same lithology (Figure 6.12 A), with brown weathered laminated clasts just above the erosional surface, coral fragments and large-scale cross bedding. The sand grains are coarse and well rounded, and the conglomerates appear to have a carbonate matrix. There are several erosional surfaces located within the first conglomerate.

The second conglomerate in RS1 (Figure 6.12 B) has a different lithology than the second one in LØS1. It has larger clasts of laminated sandstone, while the one in LØS1 has mainly sand in large scale cross bedding with occasional clasts and corals. Another difference is the facies association FA – IV between the first and second conglomerate in RS1, this is not present in LØS1. The second conglomerate is separated from the first one only by 1.5 meter of parallel laminated sandstone with some bioturbation.

The composition of the third conglomerate in LØS1 resembles the first conglomerate in RS1 with imbricated laminated clasts, but the thickness is almost three times in LØS1. Between the conglomerate units two and three in LØS1, there is a unit of facies association FA – II, including layers of slumping, several meters thick. However, the third conglomerate unit in RS1 is only 2.5 meters thick, and starts with a cross bedded sandstone with an erosive base. A thin layer with conglomerate, approximately 10 cm thick, which has the same type of clasts as in conglomerate 1 in RS1 and conglomerate 2 in LØS1. Coral fossils are also observed. Large-scale tabular cross bedding, turning into parallel laminated sandstone, which is partially deformed, succeeds the thin layer of conglomerate. In Figure 6.11 B conglomerate one and two, from RS1, is illustrated from a section of the log.

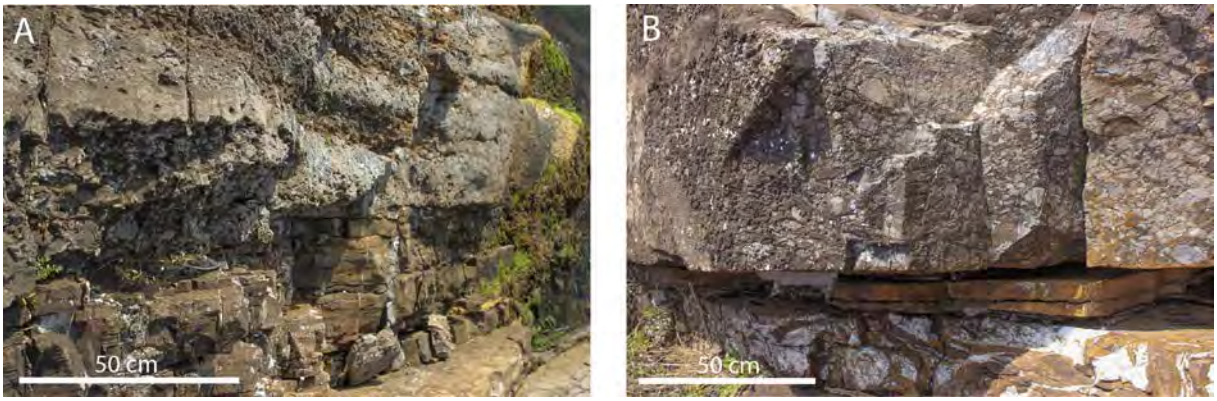

Figure 6.12: Pebble conglomerate in RP1. A: Conglomerate one. B: Conglomerate two.

Interpretation

Brown weathered laminated clasts located at the base of conglomerate 1 resemble the underlying unit, and are most likely clasts derived by erosion of underlying strata. The carbonate matrix is probably crushed corals and other shelly organisms. All fossils found in the conglomerates are most likely allochthonous, hence their demolished structure.

The well-rounded coarse siliciclastic sand-grains must have had a terrigenous source, and because of the roundness, the grains must have been transported far from the source, or been reworked for a long time. As for the laminated clasts of sandstone found in conglomerate 1 and 3 in RS1 and conglomerate 3 in LØS1, they resemble the lithology found in what was interpreted as tempestites in facies association FA – II. Because of their roundness, transport must have taken place and the layers it was derived from must have been relatively consolidated. The tabular cross-bedded sandstone in top of conglomerate 3 in RS1 probably represents a 2D dune.

FA – IIIb

Description

This facies association is observed only in HS1. It has an erosive base to the underlying facies association FA – II and starts with big boulders of cross-bedded sandstone just above the erosive base. Low angular cross-bedded sandstones and cut and fill structures are observed before it is succeeded of facies association FA – II.

Interpretation

The angularity of the boulders indicates that the transport distance has been rather moderate. If observed from a distance, the boulders make up a base of the infill succession of a channel-like structure. Further north on Hovedøya, outside the logged section there are observed the same lithology of what the boulders are made up of, located just below the facies association FA – Ib. See Figure 6.9 D for the boulders and 6.10 B for the similar lithology found further north.

FA – IV

Description

This facies association is located on top of FA – IIIa and FA – IIIb. It is observed in HS1 and RS1, but is not recognized on LØS1. In the two sections FA-IV is present, it only occurs at one stratigraphic level. No fossils, nor bioturbation has been recorded, and the observed facies are parallel laminated sandstone, structureless silt/sandstone, symmetrical ripples, asymmetrical ripples, cut and fill structures and cross bedding.
The FA – IV observed in RS1 is composed of more facies than the one in HS1, it has also a greater thickness.

Interpretation

The facies association FA-IV, together with its location on top of a conglomerate, has been interpreted to represent a channel infill succession. The lack of bioturbation and fossil can indicate a restricted degree of marine influence. The high-energy facies observed in FA – IV in RS1 indicates a difference in energy relative to HS1.

FA – V

Description

This facies association is the uppermost logged in the studied stratigraphic section, and is represented in all three localities. It is located on top of FA – Ib, and belongs to the Solvik Formation. It is dark-grey shale, which is intensely bioturbated with no observed differences between the profiles.

Interpretation

Because of the shale fraction it must have been deposited in a relatively calm marine environment, and the bioturbation favours oxic conditions.

6.2 Palaeocurrent and imbrication measurement

The measurements done on the asymmetrical ripples are presented in Table 6.4. The measurements were obtained by measuring the ripple crests in three-dimensional exposed surfaces.

Table 6.4: Results from palaeocurrent measurements on asymmetrical ripples from section RS1.

Asymmetrical	
Level in profile (m)	**Direction of transport**
29.25	48°
32.25	48°
41.25	58°
42.50	58°
58.00	56°
58.25	56°

The imbrication measurements done on the third conglomerate in section LØS1 at approximately 74 meters are presented in table 6.6.

Table 6.6: Results from imbrication measurements from LØS1.

Imbrication measurements	
Measurement nr	**Direction of transport**
1	220° SE
2	232° SE
3	214° SE
4	228° SE

6.3 Fossils observed in field and in thin-sections

Algae

Some algae have been recognized in the thin-sections, and some are only tentatively identified as algae, even though they have not been found described in any textbooks. The dasycladacean and codiacean green-algae are the ones recognized, see Figure 6.13 A, C, E, F.

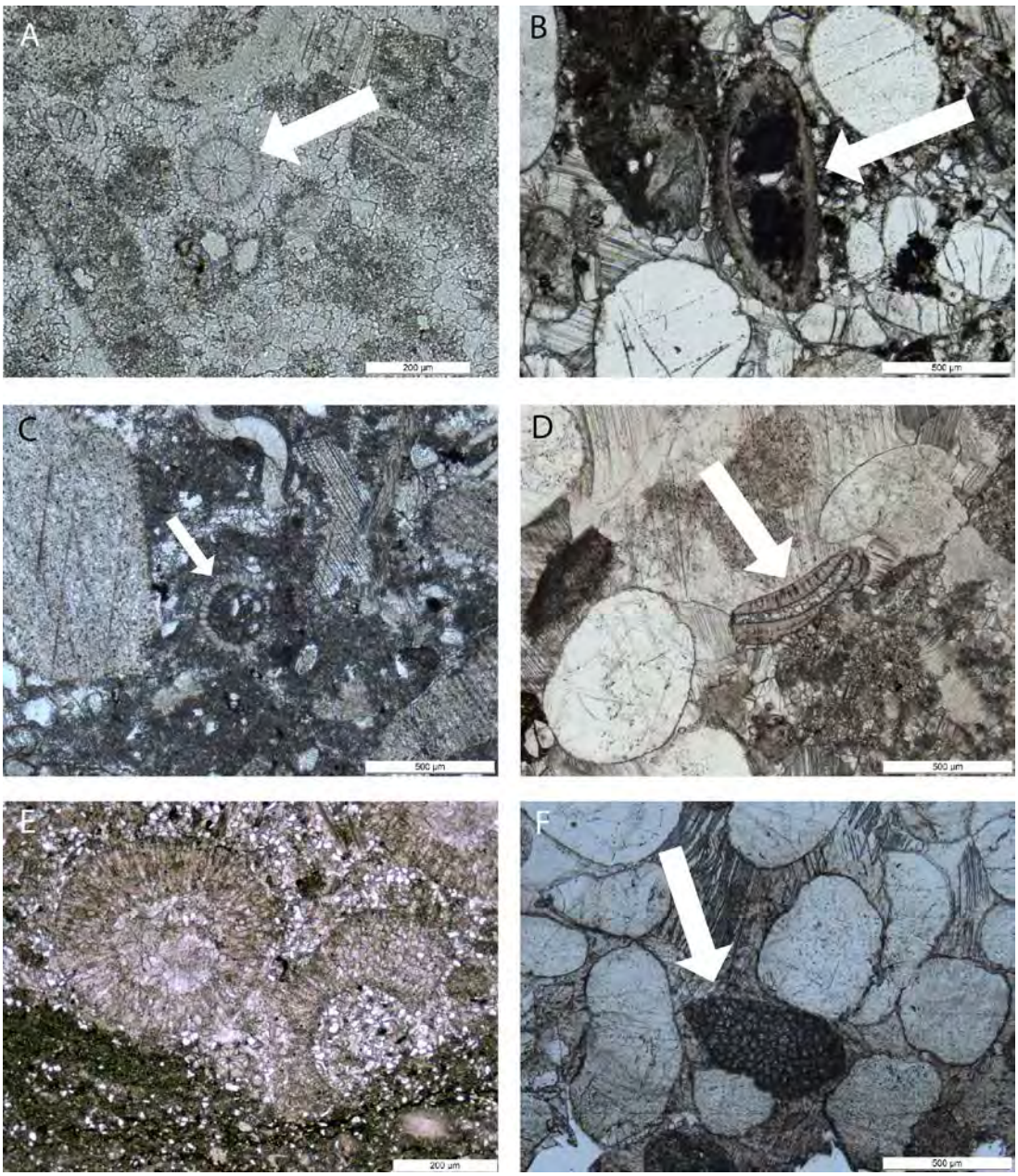

Figure 6.13: Algae from thin-sections. A: a possible green algae. B: Unknown. C: Dasycladacean green algae. D: Unknown. E: transverse cross section of Dasycladacean green algae. F: Codiacean green algae.

Corals (Middle Cambrian - Recent)

Rugose corals have a geological record from the middle Ordovician through the Permian, and were a well-developed fauna at the end of the Ordovician. The order declined during the Permian to only 10 families, which disappeared during the late Permian mass-extinction (Benton and Harper 2009).
They appear as both colonial and solitary, have a calcite skeletal material and a poor growth stability (Benton and Harper 2009). Example is shown in Figure 6.14 B.

Tabulate corals were common from early Ordovician, predating the rugose corals. At the late Permian only five families were left at the end of the period (Benton and Harper 2009). They are exclusively colonial with calcite skeletal material and have a poor stability (Benton and Harper 2009).
Two different genera of the tabulate corals were identified in the studied area, *Heliolites* (figure 6.14 A) and *Favosites* (Figure 6.14 C).

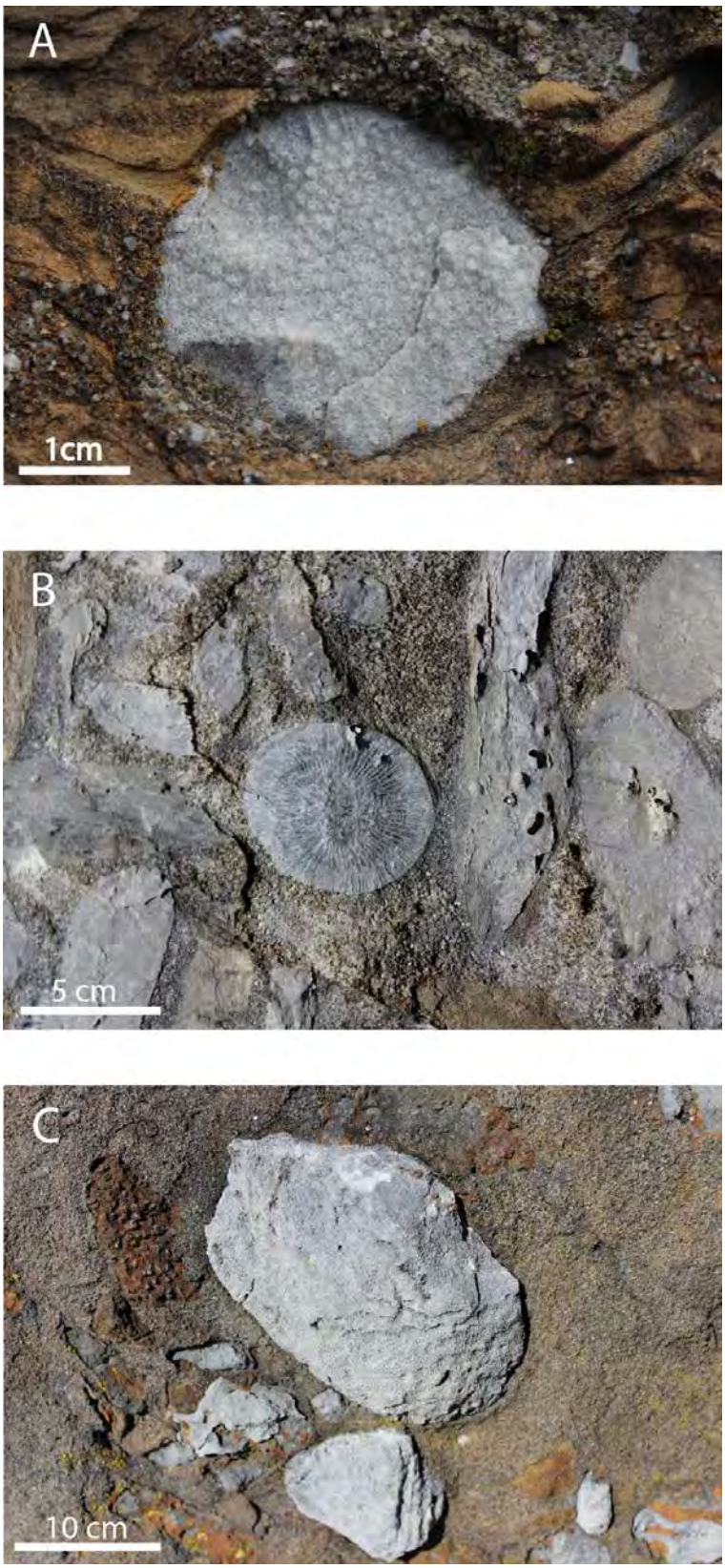

Figure 6.14: Field photos of observed corals. A: Tabulat coral of the genus *Heliolites* from LØS1 (46m). B: Rugose coral from LØS1. C: Tabulat coral of the genus *Favosites* (LØS1).

Shallow-water corals commonly grow within a depth of only 30 meters and not below 18°C, and within 30° north and south of the equator (Benton and Harper 2009).

Brachiopods (Early Cambrian – Recent)

The brachiopods are marine organisms and spans almost throughout all Phanerozoic. They are composed of two hinged shells, but are unrelated to the molluscs because of their feeding system, which is rather complex and hidden inside the shell. Because of their peak of species diversity during the Palaeozoic, dominating the shallow marine environments, they are widely used in palaeoenvironmental studies (Doyle 1996). The brachiopods are not limited by water temperature, are most common in oxygenated water, thrive in normal marine salinities and are most abundant in shallow depths with moderate to high turbulence where suspended food particles are abundant. As sessile organisms, they are associated with relatively firm substrates, where they can attach their pedicle (Doyle 1996). However, fossil brachiopods can be found in different substrates. Brachiopods observed in field are shown in Figure 6.15.

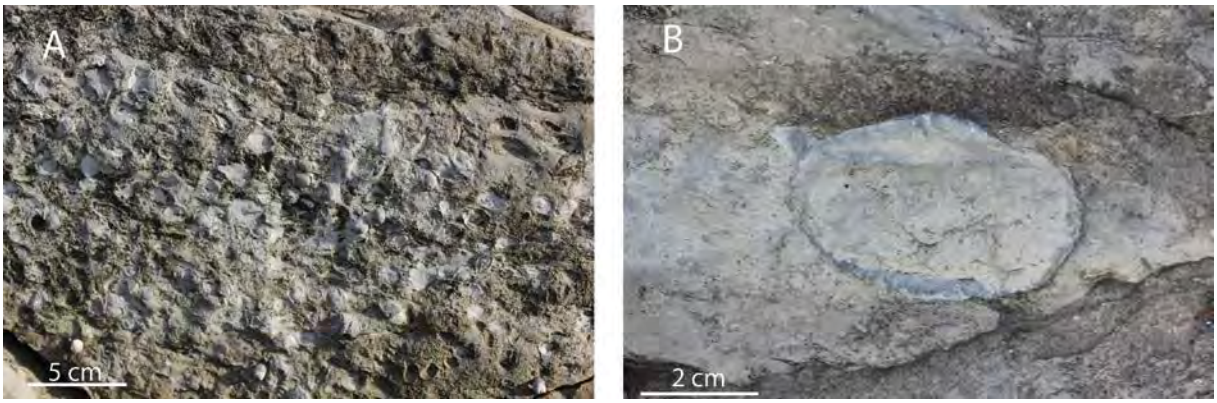

Figure 6.15: Field photos of brachiopods. A: Exposed surface of a coquina bed made up of brachiopods from HS1 (42,5m). B: Large brachiopod from LØS1.

Bryozoans (Early Ordovician – Recent)

The bryozoans span from early in the Ordovician to present in the geological record. During Ordovician they constituted a large part of the epifaunal assemblages as colonial benthic animals, getting their nutrition as filter feeders (Ross 1984). As well as all Ordovician bryozoans belong to the class of Stenolaemata, which includes the orders Cryptostomata, Trepostomata, Cystoporata and Cyclostomata (Ross 1984).

One of the bryozoans found in the study area can be identified as a Cryptostomata, which had bifoliate colonies with the zooecia opening only on two opposing sides, see Figure 6.16 F. Trepostomata is also recognized in field (Figure 6.16 B, D and E) as a Ramose-bryozoa

(branch-bryozoa). These are typical in more quiet water conditions, but this is dependent on their degree of calcification (Doyle 1996). The preserved spines in Figure 6.16 C, which is identified as a stick-like colony Trepostomata, indicate no transportation, and that the specimen most likely lived where it is found. Encrusting bryozoans (Figure 6.16 A) growing around *Cornulites*, were observed several times on RS1 and LØS1. These encrusting forms are the most robust, and are typical for shallow marine environments (Doyle 1996).

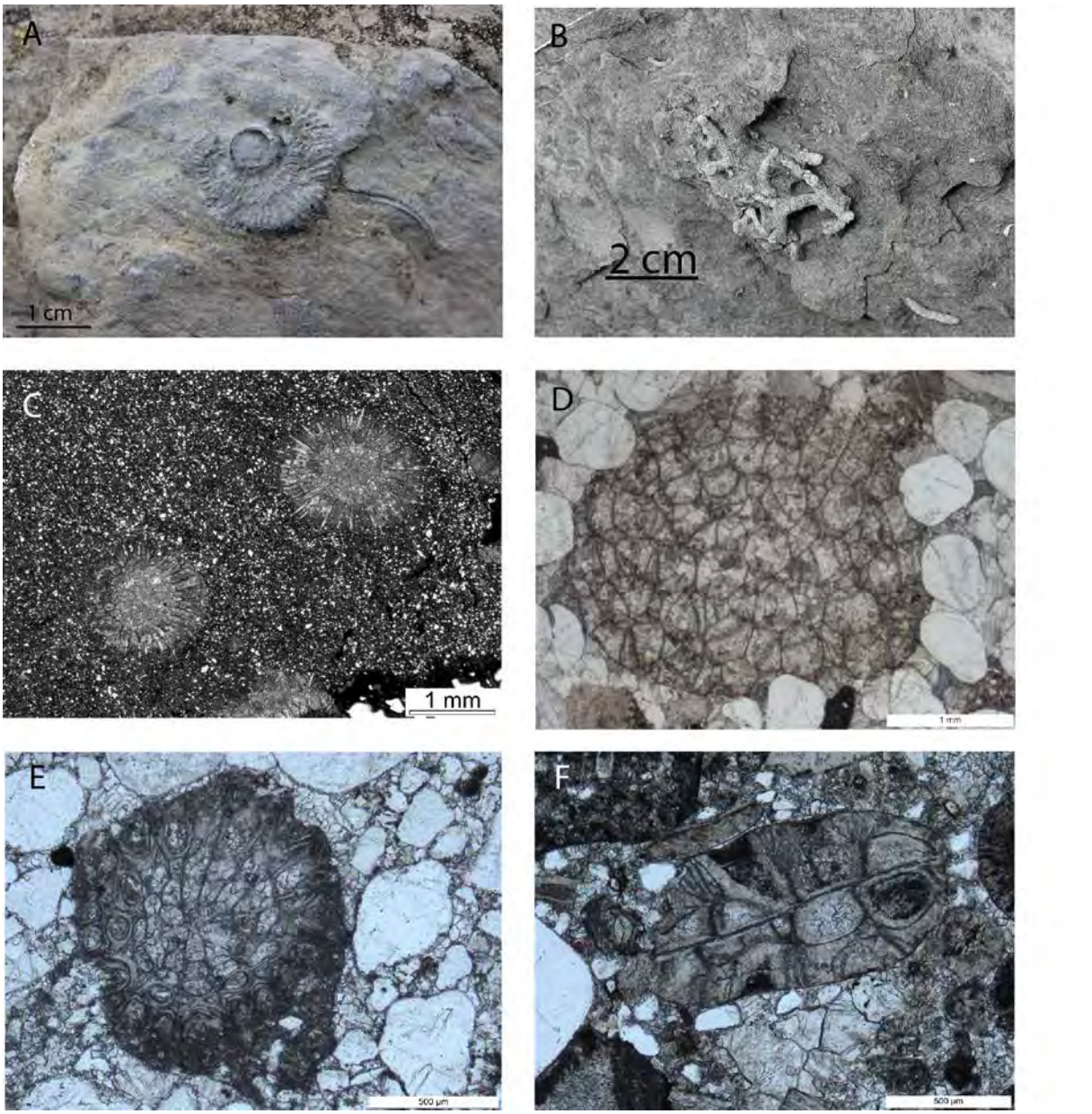

Figure 6.16: A: cross section of a cornulites with an encrusting bryozoan (LØS1).
B: Trepostomata, ramose-bryozoan (LØS1-23m). C: scanned acetate peel of a stick-like Trepostomata bryozoan, note the preserved spines. From the brown-weathered sandstone in RS1. Photo H.A.Nakrem. D: cross section of a branching colony of bryozoans LØS1 (74,7m). E: a transverse section of a branching colony of bryozoans from RP1 (47.6m). F: bifoliate Cryptostomata bryozoan from RP1 (35.5m).

Mollusks

Cornulitids range from Middle Ordovician to Lower Carboniferous (Fisher 1962; Richards 1974), and have morphological features as single tubes or as clusters of tubes cemented together, which together creates a fan-like structure (Vinn and Mutvei 2004). The four genera; *Cornulites*, *Conchicolites*, *Cornulitella* and *Kolihaia* were included in the family Cornulitidae by Fisher (1962), which is believed to be the family of the ones found in the study area. *Cornulites* fossils are abundant throughout the sections, except in FA-IV. The morphology of the ones observed in the studied areas are identical to the genus *Cornulites*, see Figure 6.17 A. Their ecological preferences are believed to be restricted to normal marine environments (Vinn 2013).

Gastropods are benthic organisms that have a single chamber coiled shell with no internal dividing walls. They are limited by water depth, substrate, salinity and oxygenation levels (Doyle 1996). There has not been found any good specimen to identify to family or genus level, only complex cross sections, see example in Figure 6.17 B and C.

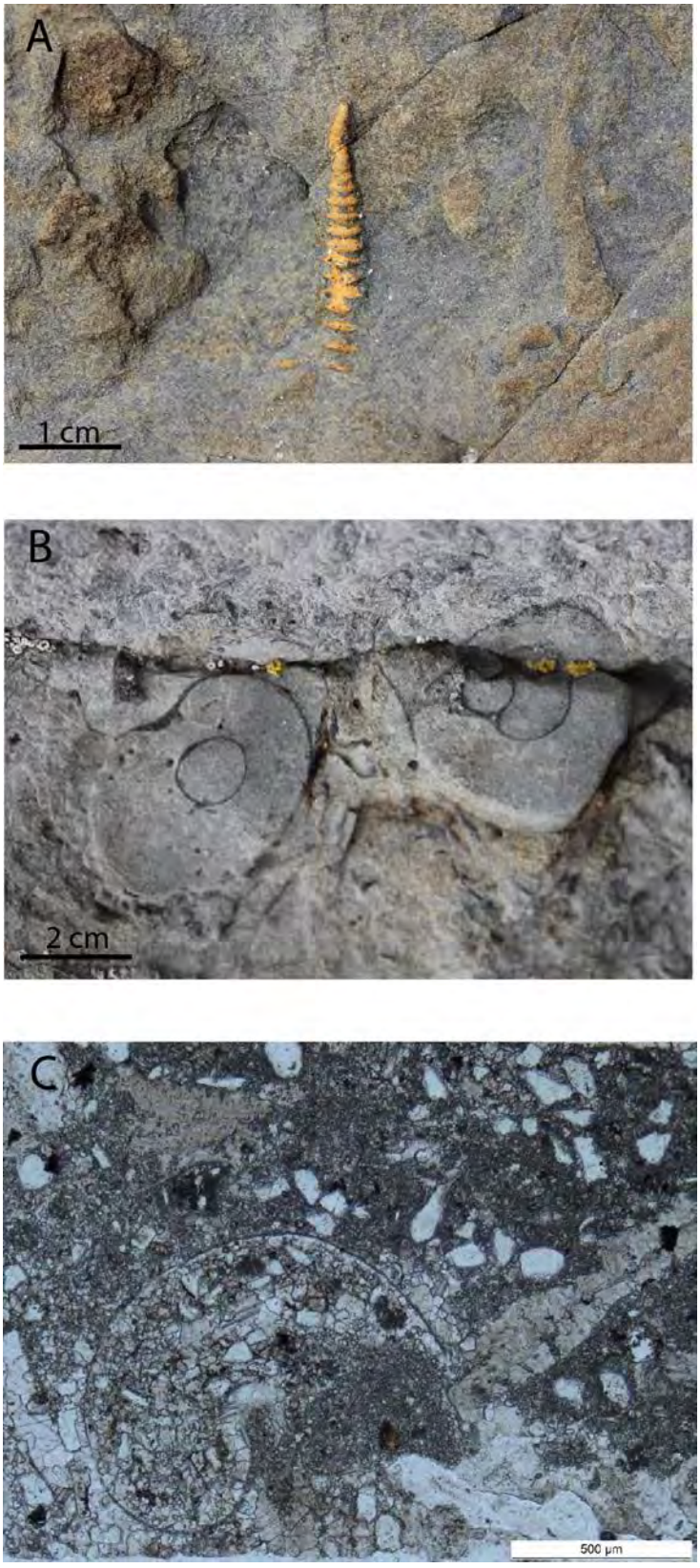

Figure 6.17: Molluscs. A: field photo on LØS1 (34,75m) of a *Cornulites*. B: field photo from LØS1 of a gastropod. C: thin section photo of a gastropod from LØP1 (79.9m).

Trilobites (Early Cambrian – Late Permian)

There have been observed many cross-sections and fragments of trilobites during the fieldwork, see example in Figure 6.18 B, but only one complete specimen was found (Figure 6.18 A). It has been identified as a Styginid of the trilobite family Styginidae with help from David L. Bruton.

Trilobites are most common in shallow marine environments, with greatest diversity in normal marine salinities. They are limited by salinity, substrate and oxygenation levels. As extinct organisms, trilobites are difficult to use in paleoenvironmental reconstructions. However, they are widely used in the reconstruction of the Iapetus Ocean in the early Palaeozoic (Doyle 1996).

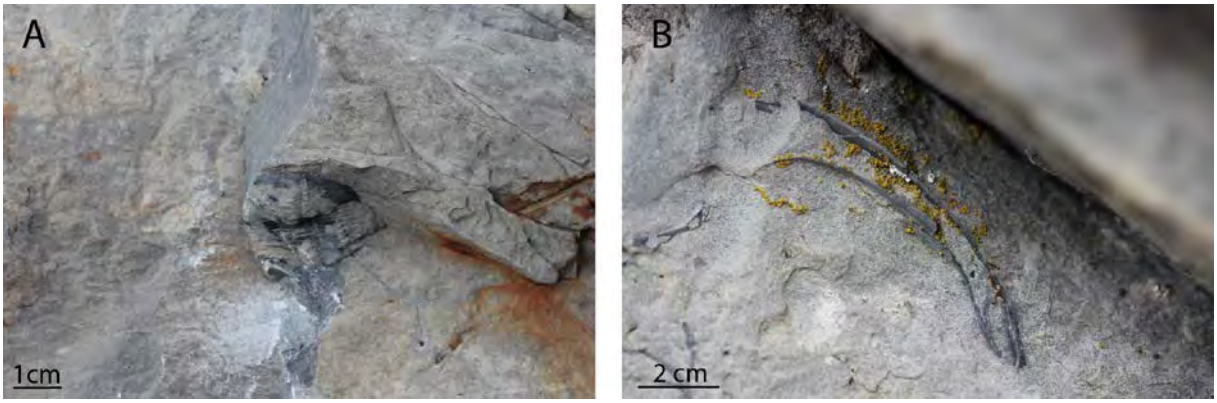

Figure 6.18: Field photo from LØS1. A: *Styginid* trilobite, from the family *Styginidae*. B: cross-section of a trilobite, unknown genus from LØS1.

Echinoderms (Early Cambrian – Recent)

Crinoids range from Cambrian to recent and are common in the fossil record. They are composed of three basic structural elements; stem, cup/calyx and arms. Some crinoids have a root-like feature at the base of the stem, which functions as a anchor in soft sediments or cement the crinoid to a hard substrate (Doyle 1996). As the crinoid dies the body is prone to disarticulation, this is because of their construction, which is a series of plates held together by the external skin. It is therefore extremely rare to find perfectly preserved, intact examples of crinoids (Doyle 1996), which is also the case in the three studied sections. The stem is the one seen most in field, but closer studies in thin-section reveal a large quantity of plates derived from dead crinoids, see Figure 6.19 A, B and C. The well preserved stem of a crinoid seen in Figure 6.19 B, is the best one found during the fieldwork. No family or genus is identified.

Cystoid is a collective term for some echinoderms found in the marine rocks of Ordovician, Silurian and Devonian age. In the Oslo Field they are restricted to the middle and upper Ordovician (Bockelie 1984). In the studied area they are most abundant in FA-I in the uppermost part of the Husbergøya Formation, but they occur also in facies F1 in FA-II in the lower part of the Langøyene Formation. Bockelie (1984) has identified these as the *Tetraucystis tetrabrachiolata*, see Figure 6.19 D.

The echinoderms are mainly limited by salinity, substrate and oxygenation. They are mainly fully marine organisms and can tolerate a wide temperature range, most common in fully oxygenated waters, although some species can be found in low oxygen levels. They are restricted to normal marine salinity levels (35‰), can be found down to abyssal depths, both soft and hard substrates and some have adapted to relatively turbulent conditions (Doyle 1996).

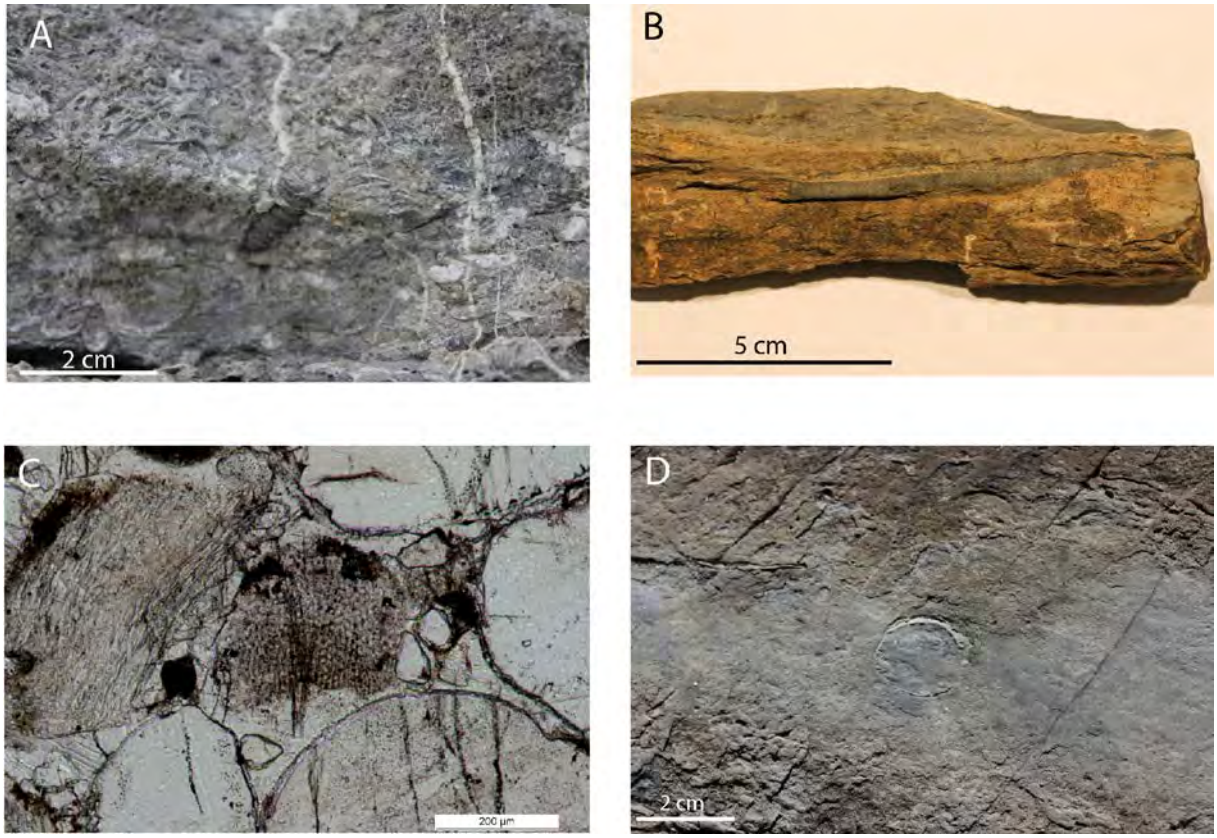

Figure 6.19: Echinoderms. A: field photo of a crinoid in a coquina layer from HS1 (46m). B: photo of a crinoid from the uppermost part of Husbergøya Formation in RS1. C: cross-section of the stem from a crinoid in LØS1 (77,9m). D: field photo of a cystoid in the uppermost part of Husbergøya Formation in RS1.

6.4 Ichnology

Because the exposure and preservation of the trace fossils is not always of the optimal quality for their identification, the classification and name setting is difficult. However, the author has selected the best photos from the fieldwork to show some of the trace fossils represented in the studied areas.

Trilobite feeding tracks are shown in Figure 6.21 A. It is located on LØS1 at 65 meters. As the trilobite is feeding on the nutrition in the mud, it pushes itself forward by the help of its limbs, leaving the jagged marks on the sides of the traces, see arrows in Figure 6.21 A.

Chondrites is classified as a feeding burrow and has a downward-branching appearance, see Figure 6.21 B. They are a component of the Cruziana ichnofacies, which represents mid and distal continental shelf, located below the normal wave-base, but is still affected by storm events (Benton and Harper 2009).

Large trace fossil presented in Figure 6.21 C, was recognized by Brenchely and Cocks (1982) as *Scalarituba*, an infaunal feeding trace from a soft-bodied animal. However, Seilacher and Meischner (1965) referred to some large trace fossils as *Trichophycus*, these are also observed in the studied area, but occur further down in the stratigraphy (Husbergøya Formation), see Kjærsgaard (2014) for details. They also observed *Scalarituba* in Langøyene Formation on Malmøya, and separate these from the *Trichophycus*. In Buckman (2001), a new ichnogenus is proposed, the *Parataenidium.* This relates closely to the ones located in the uppermost Ordovician/early Silurian beds. They are described as parallel to the bedding, occurring with straight curves and loosely meandering patterns, which is also the case in the studied area.

Figure 6.20: Polished slab of a vertical cross-section from the large trace fossil shown in figure 6.21 C. From LØS1 (79,5m).

The cross section of the large trace fossil (Figure 6.20) also fits closely to the detailed description of the *Parataenidium monoliformis*.

The *Parataenidium* is not restricted to any single facies, but *P. mullagmorensis* is found in muddy sandstones with bedding exceeding decimeter-scale. *P. monoliformis* is on the other hand most abundant in clean, thick-bedded sandstones related to channel deposits (Buckman 2001). In other words, *P. mullagmorensis* is positioned below fair-weather wave base, whilst *P. monoliformis* is positioned above fair-weather wave base.

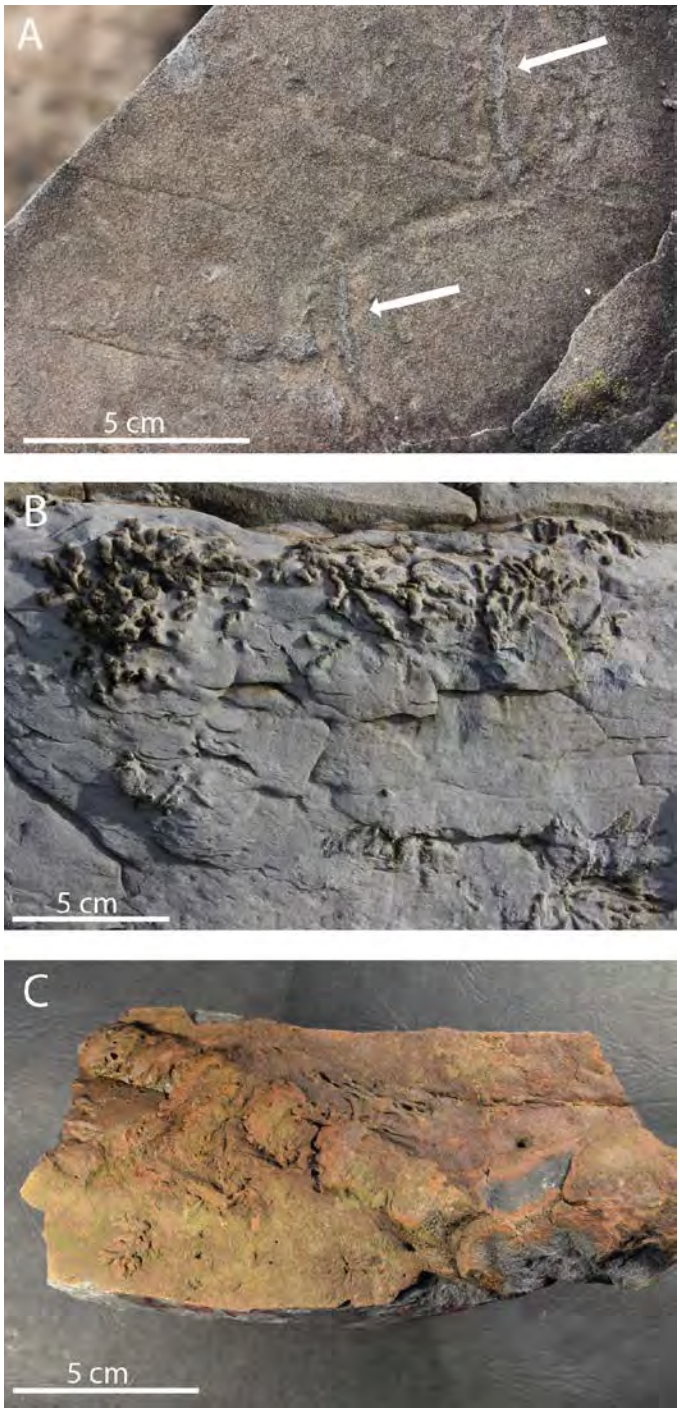

Figure 6.21: Trace fossils. A: Trilobite feeding tracks, arrows pointing at the jagged marks from the limbs of the trilobite. B: Chondrites burrows, from LØS1. C: Large trace fossil from LØS1 (79,5m).

6.5 Thin-section analysis

Eighteen thin-sections from RP1 were selected for point counting to acquire the distribution of the mineral content. Because of the similarity between the sections and because time is a limiting factor, this analysis was only performed on one locality, RS1 which is the stratigraphic section with the most complete representative thin-sections from each represented feature.

The grain size analysis was performed on all forty-three thin-sections, because the method was rather effective, and a small amount of extra time was required to perform the grain-size analysis on all the thin-sections.

6.5.1 Point counting

The main components from section RS1 are quartz and calcite, disregarding the matrix. Quartz ranges from 5,5% to 47,5% including the metarhyolites, the calcite ranges from 0,75% to 45%.

The feldspar constitutes from 0.25% to 2.75% of the total mineral content in the samples, and is present in all thin-sections, except from the Solvik Formation shale (PMO: 221.878). Pyrite (0.25% - 2.75%) is present in all samples except from three (PMO: 221.870, 221.876, 221.878), and appears either as crystals or as pyrite-veins in darker patches in the thin-section, see Figure 6.22. Clay minerals (0.25% - 0.50%) and opaque minerals (0,50% - 1,25%) are present in a few samples and are close to insignificant.

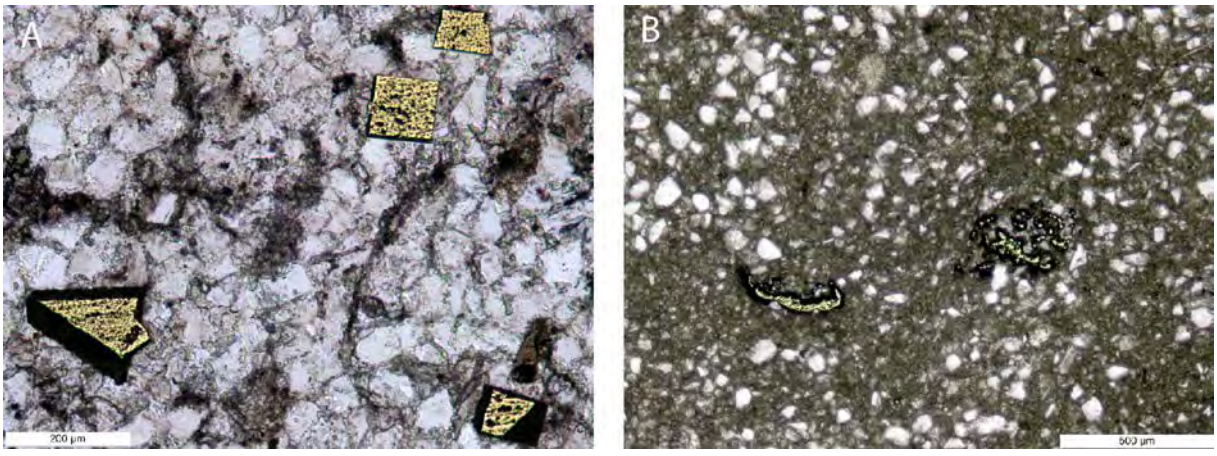

Figure 6.22: A: Pyrite crystals from thin-section RS1-8-221.871. B: Pyrite veins from thin-section RS1-3-221.862.

The rocks have a varying sedimentary composition, which can be related to the lithology and facies. In the finest siliciclastic marine facies, quartz-grains in silt-fraction are scattered in a mud-supported brownish matrix, as shown in Figure 6.22 B. However, the more coarse-grained sandstone rocks appear cleaner, and the pore space is filled with calcite cement between the various clastic grains, see Figure 6.23 B and C. The coarse-grained, well-rounded quartz grains, referred to as "millet seeds" by Brenchley and Newall (1975), often shows corroded surfaces, as seen in Figure 6.23 B.

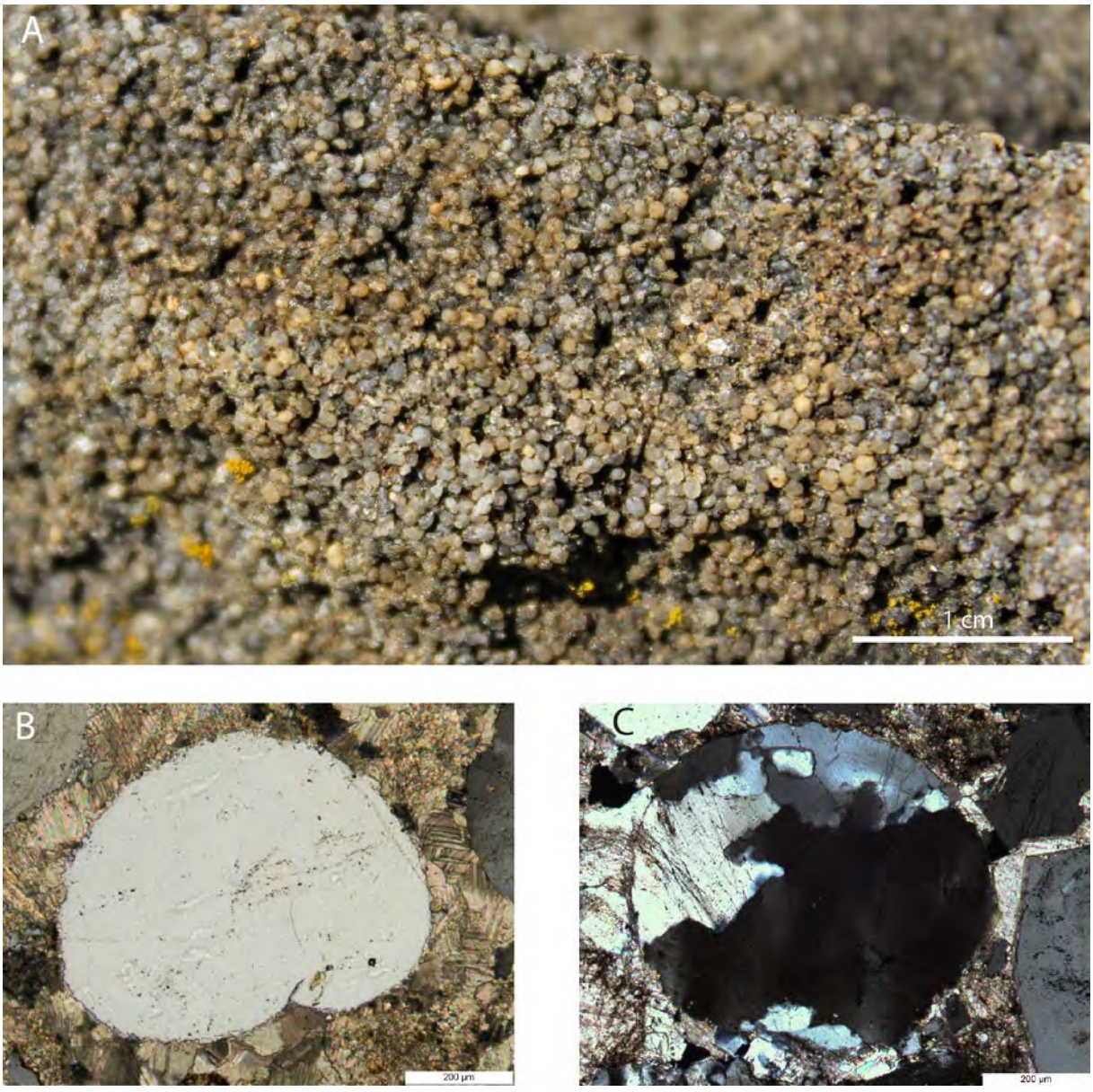

Figure 6.23: A: Well-rounded quartz grains in field, from the top of conglomerate 3 on LØS1. B: Mono-crystalline quartz-grain with corroded surface surrounded by calcite cement, from thin-section LØS1-5-221.848. Apparent dust-rim to the right is due to preparation. C: Poly-crystalline quartz-grain, surrounded by calcite cement, from thin-section LØS1-7-221.850.

The point-counted samples through section RS1, shown in Figure 6.24 A, are represented in correct stratigraphic order from lowermost in the section starting at 221.860, to uppermost 221.878. They are presented in the same way beneath, starting at the base of the section and related to their facies associations.

- The three first samples (221.860 to 221.862) are collected from FA-Ia, from base, middle and top of the facies association. The quartz content increases upward, with a peak in sample 221.861. The calcite content also increases upward in this facies association, from 0% in 221.860 to 6.25% in 221.862.

- Samples 221.863 to 221.869 are collected from the base, middle and top of the first conglomerate (FA-IIIa) in the section. They have the highest (44.5%) content of quartz at the base, decreasing in the middle, and then increasing again towards the top. The calcite content shows the same trend in the opposite way, with increasing toward the middle and decreasing towards the top of the conglomerate.

- The second conglomerate (FA-IIIa) is represented by the samples from 221.870 to 221.872, collected from the base and middle. They show an increase of both quartz and calcite, with the quartz content ranging from 32.5% in the base to 46.25% at the middle, and the calcite ranging from 12% to 20.25%.

- Sample 221.873 is collected from a layer with typical tempestite features (FA-II). Here, both the quartz and calcite contents are relatively high, quartz with a value of 40.75% and calcite with 34.50%.

- Samples 221.874 to 221.877 all represent FA-Ib, uppermost in the Langøyene Formation. 221.874 and 221.875 are collected from the base and middle of the brown weathered sandstone lowermost in FA-Ib. The two samples show an upward decrease of the content of both quartz (43.25% - 31.5%) and calcite (22% - 10.5%). Sample 221.876 represents a nodule from the beds of nodular limestone, and have a very low content of quartz (7.75%) and calcite (1.25%). Sample 221.877 is taken from the brown weathered sandstone interbedded with the nodular limestone, and has a content of quartz and calcite similar to the three lowermost samples in the section.

- Sample 221.878 represents facies FA-V, and is collected from the shale in the Solvik Formation. As shown in Figure 6.24 A, it has the lowest amounts of quartz in the section with only 5.5%. Calcite is only 0.75%.

The quartz/feldspar ratio shown in Figure 6.24 B, varies from 87% to 100%, with most of the samples over 90%. Overall the maturity of the rock seems to be increasing upward, with small breaks at the base of the two conglomerate beds, ending with 100% in the shale of the Solvik Formation.

As for the maximum particle analysis for RS1, which is shown in Figure 6.24 C, has a small increase up to the erosional surface of the first conglomerate (221.864). It is all classified as very fine sand, except from 221.863 and 221.864, which is fine sand. From the position of sample 221.865 the grain-size increases drastically, from medium sand up to coarse sand, with a small decrease in grain-size at the position of 221.868, which is the top of the first conglomerate. In the second conglomerate (221.870 – 221.872), the grain-size increases even more, before it returns into very-fine sand in layer (221.873) and the brown weathered sandstone (221.874 and 221.875). In the nodular limestone (221.876) the grain-size is still within the very-fine sand fraction, but in the inderbedded brown weathered sandstone (221.877) it increases to medium sand again. In the shale of the Solvik Formation the low amounts of quartz is within the very-fine grain fraction, even though many of the grains are only of silt-fraction.

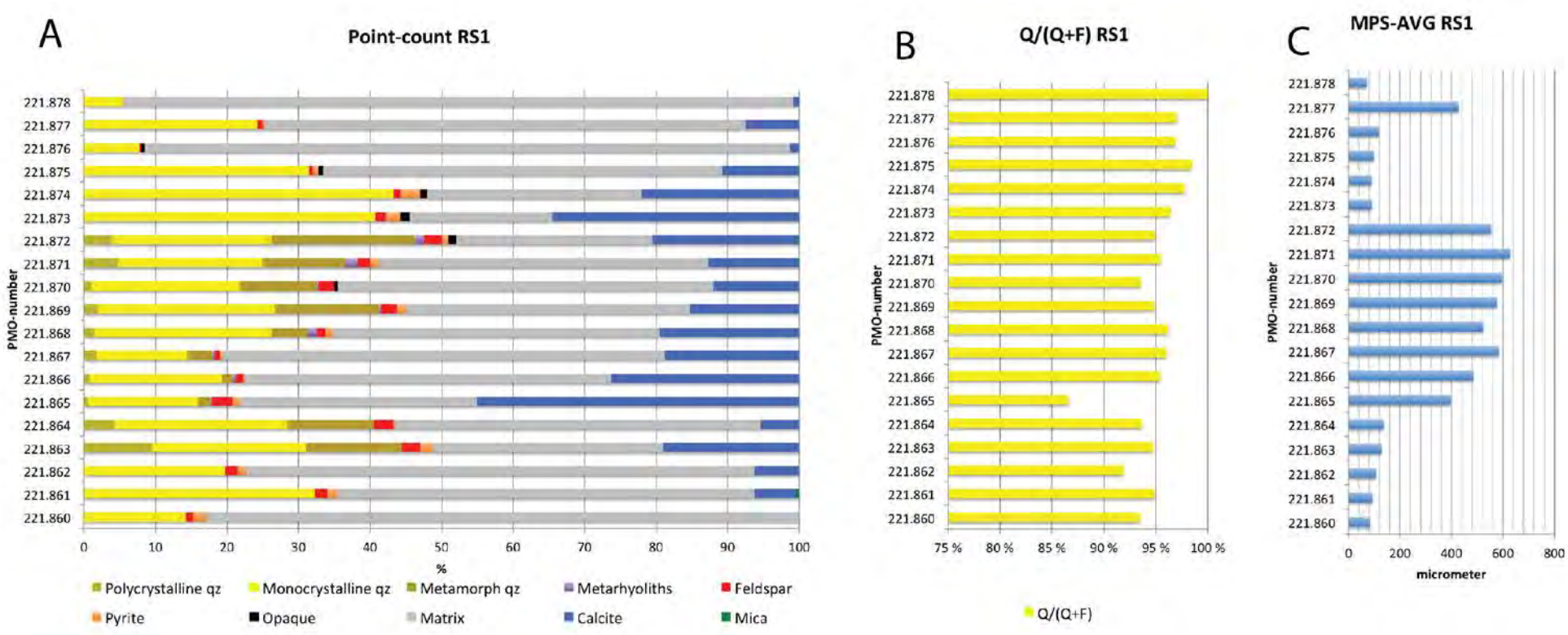

Figure 6.24: A: results from point counting. B: results from quartz/feldspar-ratio. C: average results from maximum particle size.

6.5.2 Maximum particle size analysis

Maximum particle size (MPS) analysis was executed on all of the thin-sections from all three sections, and is presented in Figure 6.25. As pointed out in the Method chapter, the MPS obtained from thin-section measurements are apparent MPS, but is here for simplicity called MPS. The grain sizes obtained from section HS1 are the lowest and most stable compared to the other two, starting with very fine sand in the three lowermost samples (221.879 – 221.881), collected from the brown weathered sandstone. There is a small increase in grain size from sample 221.882 to 221.883, up to fine sand, which is collected from parallel laminated sandstone. From sample 221.884 to 221.886 is similar, with very fine sand.

The grain size from RS1 and LØS1 is more similar compared to HS1. The grain size shows a small increase from 221.860 to 221.864, which is up to the erosional surface of the first conglomerate, but all within the fraction of very fine sandstone. From the position of sample 221.865 to that of 221.872 in RS1, which represent the two conglomerates, the succession reveals an increase in the MPS from medium up to coarse-grained sand, and show a small decrease at the top of the first conglomerate, see sample 221.868. From sample 221.873, and up to 221.876 very fine sandstone again dominate the MPS, but in sample 221.877, collected from the interbedded brown sandstone layer in the nodular limestone, the MPS is medium again. The uppermost sample (221.878) is collected from the shale from the Solvik Formation and has the lowest MPS grain-size of all the studied samples, with an average of 70.45 micrometre.

The results from LØS1 have the same trend as RS1, with virtually the same MPS as in the first three samples. From the base of the first conglomerate (221.846) there is an increase in grain-size from fine sand to coarse sand in the middle of the conglomerate (221.848). At the top of the first conglomerate (221.849), a decrease down to medium sand happens, before it increases again in the second conglomerate to a fraction of coarse sand (221.850 – 221.855). Samples 221.856 and 221.857 are collected from the brown weathered sandstone uppermost in the section and show a MPS in the very fine sand fraction. A small increase to fine sand occurs in samples 221.858 and 221.859, which are collected from the border between the nodular limestone and the interbedded brown weathered sandstone.

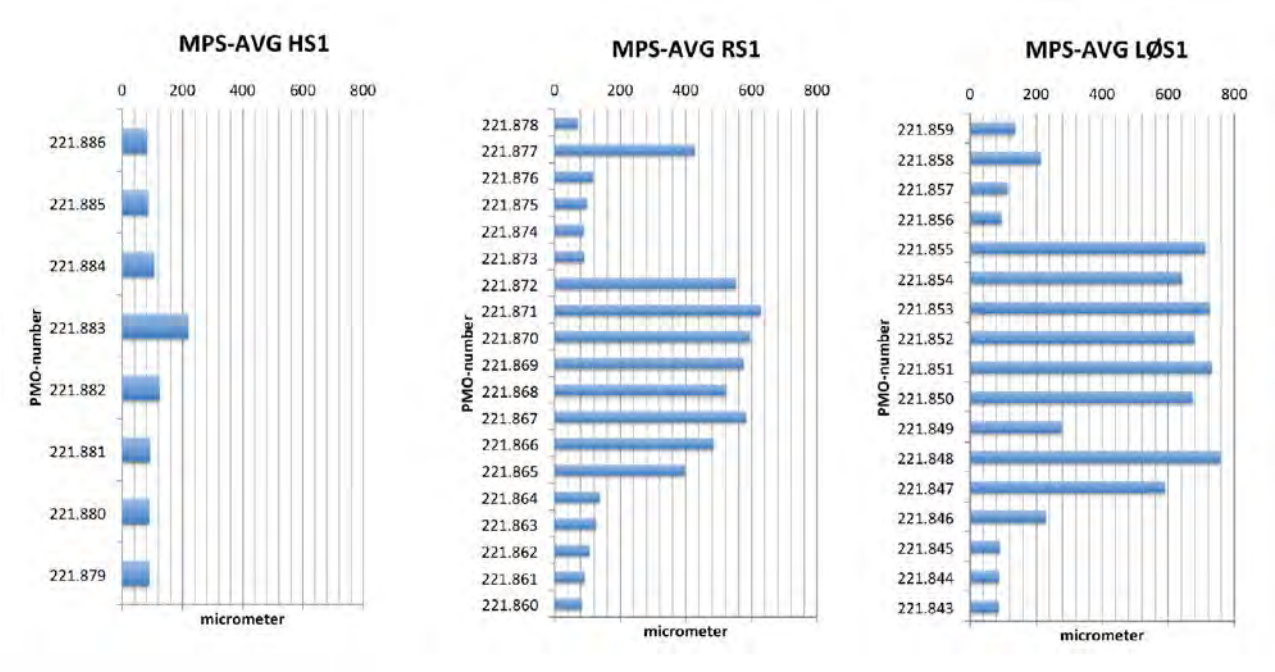

Figure 6.25: Results from MPS-analysis, showing the sections in correct order from west to east.

For the roundness of the grains, a more generalized classification was made. All grains smaller than 0.3 mm are sub-angular to sub-rounded with low sphericity, while all grains larger than 0.3 mm are well-rounded with high sphericity. See example in figure 6.26.

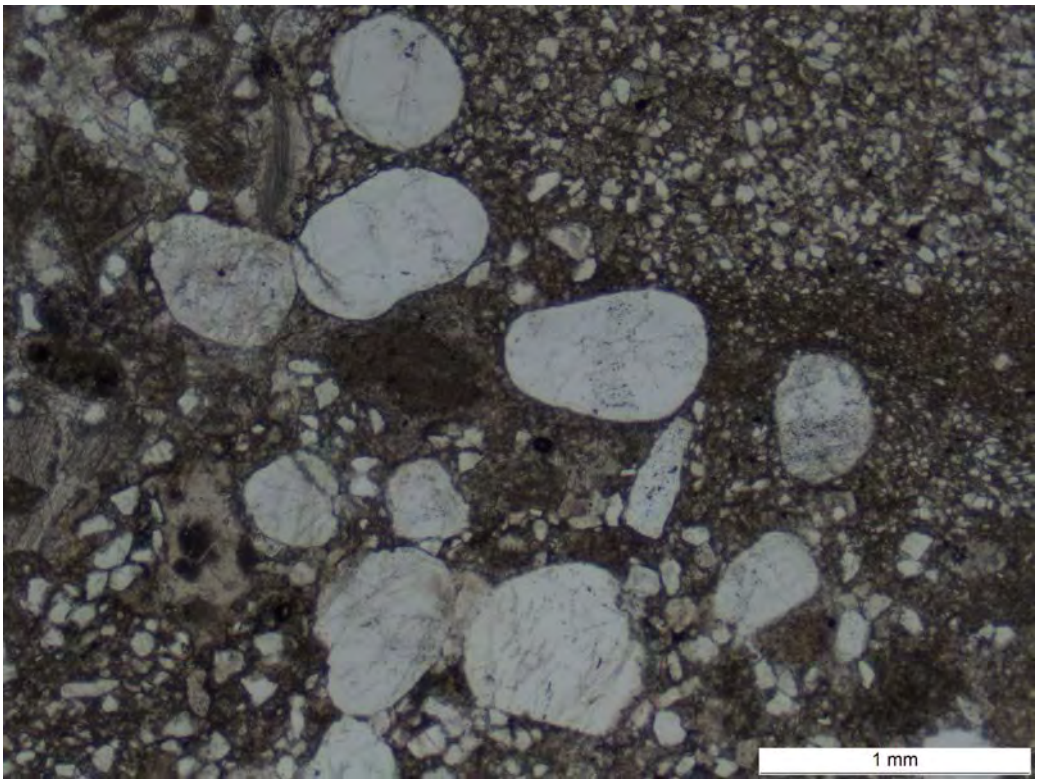

Figure 6.26: Thin-section LØS1-4-221.847 showing the difference between roundness and sphericity related to the size of the grains. Roundness and sphericity generally increase with increasing grain size.

6.6 XRD-bulk results

As pointed out in the Methods chapter, the XRD-bulk analyses were executed on the three samples collected from the brown weathered sandstone (FA-Ia) uppermost in the Husbergøya Formation from the LØS1 section to identify the presence of minerals causing the brownish colour on weathered surfaces.

The results from the XRD-bulk are presented in figure 6.27. The detected minerals are as follows; quartz, albite, microcline, mica, pyrite, chlorite, ankerite, dolomite and calcite. The quartz is clearly the dominating mineral ranging from 36.2 XRD % to 44.1 XRD %. Calcite is also relatively abundant with values ranging from 15.6 XRD % to 21.7 XRD %, chlorite from 1.4 XRD % to 12 XRD %, Microcline from 10.5 to 11 XRD %, ankerite from 7 to 10.5 XRD %, dolomite from 3.1 to 5.8 XRD %.

According to the results, pyrite is only present in one sample with only 0.1 XRD %. However, there are found matching tops for pyrite in the diffractogram from all the samples, but they are overlapped by the peaks of other minerals, and are therefor not recognized by the software used to quantify the different minerals.

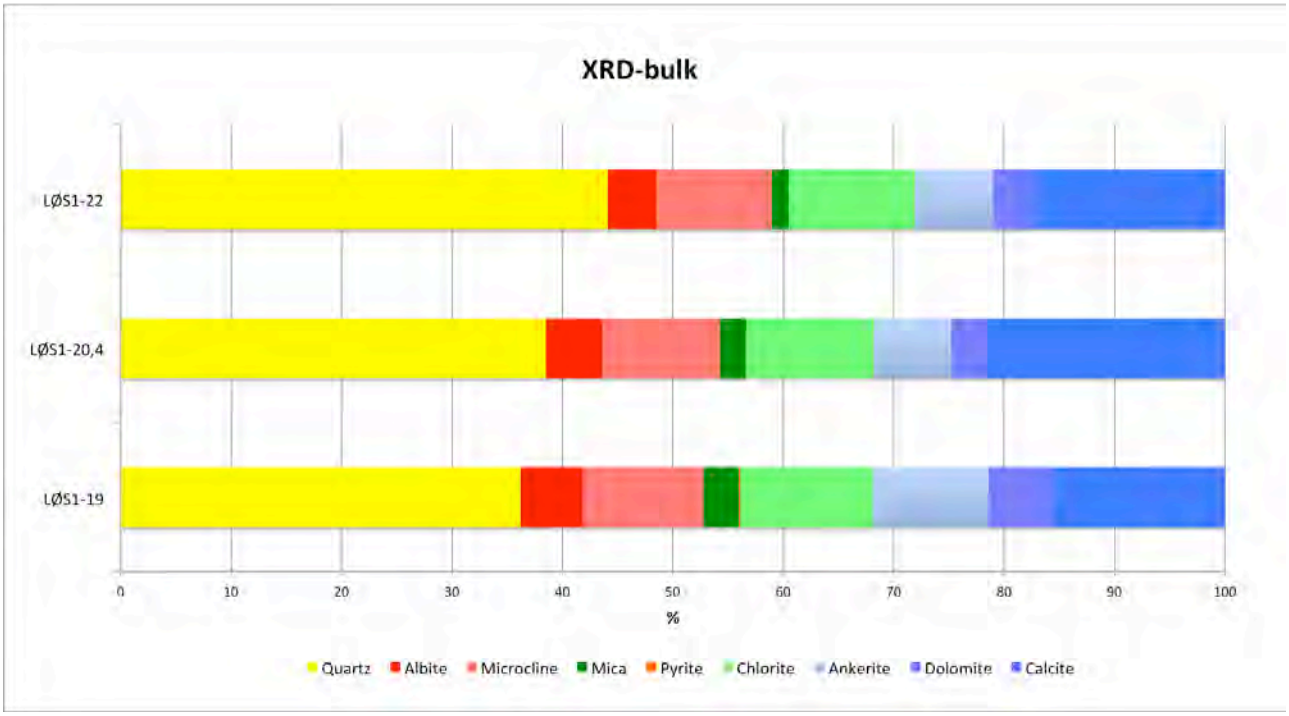

Figure 6.27: Diagramme showing the quantified results from XRD-bulk analysis.

7 Discussion

During the Late Ordovician a gradual change of siliciclastic input into the epicontinental sea took place. In the Langøyene Formation a series of storm deposited siliciclastic layers were deposited with increasing frequency and thickness up in the stratigraphy, along with localized through cross-bedded shoal deposits of quartz and ooid grains. This lower part of the Langøyene Formation was then cut by an erosional surface, the first one of total three erosional surfaces floored by conglomerates, each marking a sub-aerial unconformity (SU). The intervals between these conglomerates vary in thickness and sedimentological features, vertically within one section as well as laterally between the sections. Stratigraphically above the third conglomerate there was a decrease in siliciclastic input and an abrupt change to open marine shale that is represented by the Solvik Formation of Early Silurian age.

The main emphasis of the present chapter is to discuss processes and changes in depositional environment that gave rise to the transition from the Husbergøya Formation to the Langøyene Formation, the stratigraphic package up to the first conglomerate, the formation of the erosional unconformities in the upper part of the Langøyene Formation, the origin of the infill successions above the erosional unconformities, and the boundary between the Langøyene and the Solvik formations (including the Ordovician/Silurian boundary).

This discussion is based on observations done in the field, the logged sections (Appendix C), visual interpretations of thin-sections and other methods, fossil observation, trace fossils and XRD-bulk analysis. The logged sections are constrained within a small area and do not give a full documentation to interpretation and reconstruction of the lateral extent of the depositional systems; previously published literature has therefore been taken into account.

The different studied sections will, as earlier, be referred to “HS1”, “HS2”, “RS1” and “LØS1”.

7.1 Transition across the boundary between the Husbergøya and Langøyene formations

From FA-Ia uppermost in the Husbergøya Formation to the FA-II in the Langøyene Formation an apparent change is observed in the field by the first input of a clean sand layer, which is represented in all three logged sections, and correlated laterally (Figure 7.1). This first input of cleaner sand defines the boundary between the two formations (Brenchley and Newall 1975). The field observations of FA-Ia are the distinct brown weathered colour and some alternating layers of brighter colour with diffuse boundaries. The extensive bioturbation, set to an intensity of 6 in all three sections, has wiped out any sign of lamination. This means that the deposition took place in oxic conditions, and that the organisms had time to thoroughly rework the sediments, and that the rate of deposition was low. The intensity of the bioturbation has been too high to recognize and define any specific ichnofacies. The preserved spines of a bryozoan (Figure 6.16 C) found in facies association FA-Ia, together with the well-preserved stem of a crinoid (Figure 6.19 B), indicate an environment low in energy. Brenchley and Newall (1975) suggested that the high grade of bioturbation could indicate a break in sedimentation. There are, however, not been recorded any omission surfaces in FA-Ia, nor has there been recognized any indication of a hardground that might be expected to have been formed in case of break in sedimentation for a longer time period. In addition, as the beds are intensively and continuously bioturbated from bottom to top, the hypothesis of break in sedimentation is unlikely; there has most likely been a more continuous low rate in sedimentation during the deposition of the FA-Ia beds. The layers of brighter colour with a diffuse boundary could reflect a change in sedimentation or bottom conditions, but these layers have not been studied further (however, see below).

There are some changes within the FA-Ia facies layers, in the top of the Husbergøya Formation. The petrographic studies done on thin-sections from FA-Ia (Chapter 6.5) reveal a vertically change of mineral composition (Figure 6.24 A), maturity (Q/F-ratio) (Figure 6.24 B) and maximum particle size (MPS) (Figure 6.24 C). The mineral composition from facies association FA-Ia in section RS1 (Figure 6.24 A) has a higher content of quartz, and a higher maturity in the middle sample (PMO 221.861) compared to the one below (PMO 221.860) and above (PMO 221.862). It is possible that the middle thin-section (PMO 221.861) was taken from one of the light-coloured layers mentioned above, and that these layers could have been deposited as distal storm deposits, which would explain the higher content of quartz, and the change in colour observed in field.

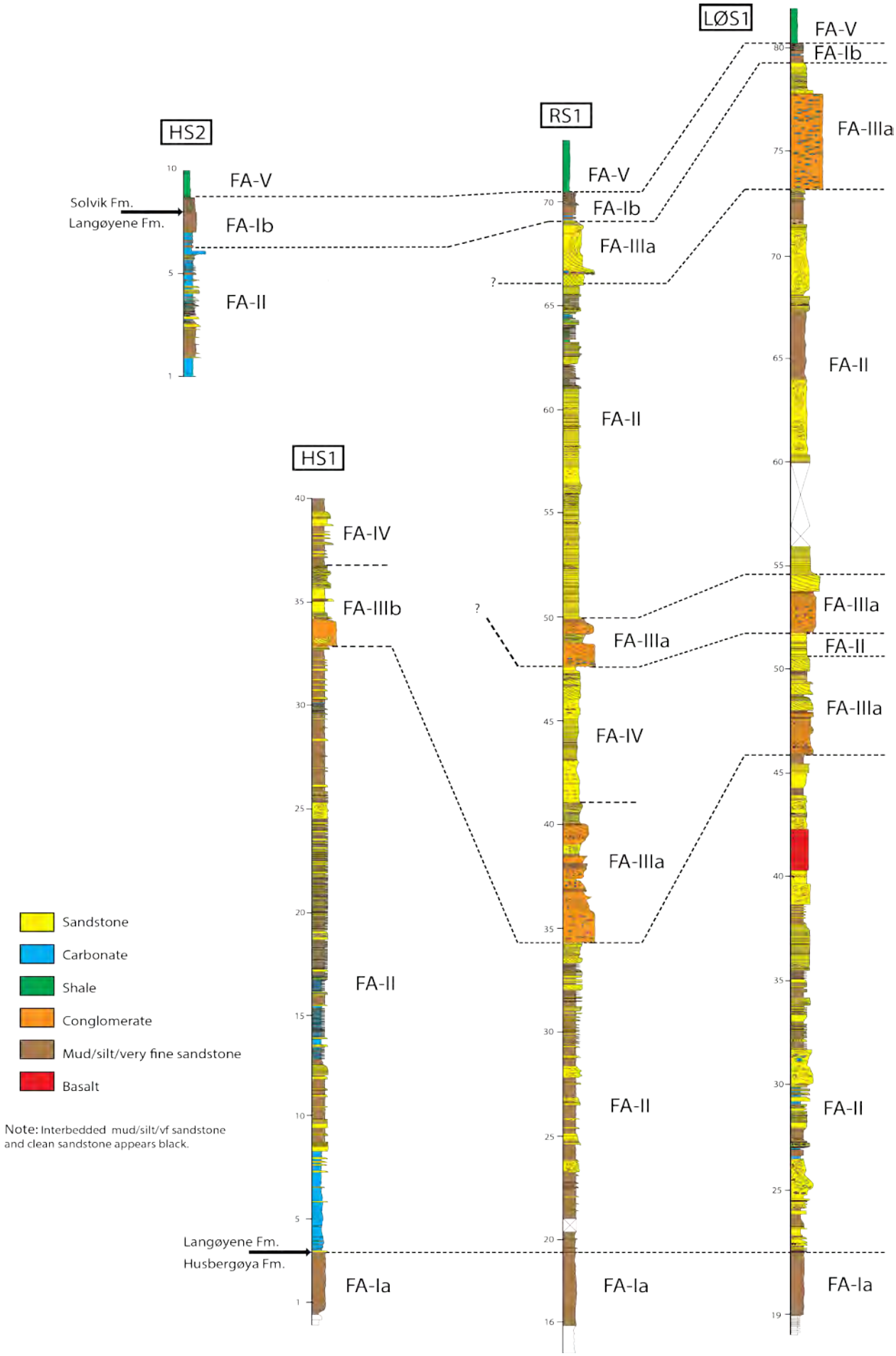

Figure 7.1: Stacked logs with correlated facies associations from the studied sections at Hovedøya, Rambergøya and Langøyene. In Appendix H, a larger figure in A3 format is found.

The maximum particle size increases gradually in the three samples (PMO 221.860, 221.861, 221.862) collected from FA-Ia in RS1, see Figure 6.24 C. The increase of maximum particle size could be related to a fall in relative sea level, resulting in a forced regression moving the shoreline and its processes basinward. This interpretation corresponds with the results of Kjærsgaard (2014) regarding the uppermost section of the Husbergøya Formation. Nielsen (2004) suggested that the condensed, shale-dominated intercalations in the Late Ordovician sedimentary unit of the Oslo area are evidence of three sea level rises, known as the Spannslokket, Husbergøya and the Langøyene drowning events. Whereas the clastic input increased during the lowstand. The upper part of Husbergøya and Langøyene formations are also correlated to the British late Rawtheyan and Hirnantian (Nielsen 2004 and references therein). The sandstone bed, overlying the oolitic sandstone in the upper part of the Langøyene Formation was cut by channels (Nielsen 2004), indicating a lowering of the sea level, but this is discussed later in this chapter.

The results from the XRD-bulk analysis have shown that considerable amounts of ankerite and dolomite are present in the three samples from FA-Ia collected from section LØS1. Oxidation of Fe^{2+} in these carbonate minerals to Fe^{3+} oxides during weathering is believed to be the reason for the brownish colour on weathered surfaces. Morrow (1982) and other authors referred therein suggested that cations such as those of iron and lithium could have a catalytic effect on precipitation of dolomite; with the ankerite also present in the rocks, this indicates that the presence of Fe^{2+} would contribute to an early dolomitization with formation of ferruginous dolomite. Permeable hinders, i.e. hardgrounds could have acted as inhibitors for precipitation of dolomite (Chow and Longstaffe 1995), whereas extensive bioturbation of the bed could have promoted the dolomitization due to homogenization of the sediment and thereby increased fluid flow.

The absence of any lamination or reworking of the sediments indicates that the beds were deposited and became bioturbated below mean fairweather wave base, and also possibly below mean storm wave base, as there are not recorded any alteration of high- and low-energy characteristics of the deposits, which would be the case in a an offshore transition zone, described in Chapter 3.1.2. The basin floor during deposition of FA-Ia is believed to have been relatively even, which is most common in open marine settings in epicontinental shallow seas with low energy (Johnson and Baldwin 1998). The lateral extent of the brown weathered sandstone can be traced westward into the Langåra Formation (Owen et al. 1990), thus

supporting the idea of an even basin floor. The thickness variation of FA-Ia is relatively low, but the lower boundary of the brown weathered sandstone is not sharp enough to give an exact figure, however, it can be estimated to be mostly between 3 to 4 meters thick.

7.2 Development of the Langøyene Formation up to the first erosional unconformity

As described above, the first clean sand-layer defines the boundary between the Husbergøya- and Langøyene formations and can be traced laterally between the logged sections (Figure 7.1). The succession next above the formation boundary is defined as facies association FA-II and described in Chapter 6.1.2, with the facies F6, interpreted as storm deposits, repeated periodically with increasing intensity and thickness upwards in the stratigraphy. Other facies such as the structureless calcareous siltstone (F4), brown weathered sandstone (F1), slumped layers (F5) up to several meters thick and a high grade of bioturbation are also included in FA-II.

Facies association FA-II varies laterally between the logged sections. The HS1 starts with a dominance of structureless calcareous siltstone interbedded with thin layers of shale, before it gets more interbedded with sand-layers (Figure 7.1). Such carbonate deposits would indicate a break in the siliciclastic input to the basin where it was deposited, as carbonate producing organisms must have flourished, or their carbonate products dominated, in the environment during events of very low siliciclastic input. After about 9 meters up in the logged section, the structureless calcareous siltstone is replaced by the brown weathered bioturbated sandstone, up to half a meter thick between the sandstone layers, which relates to the logged sections of FA-II in RS1 and LØS1 (Figure 7.1). The limestone beds present in the lowermost part of facies association FA-II, vary strongly in thickness in Oslo and Asker Region. In Bunnefjorden around 3 – 5 beds of this limestone are observed, but in Asker and parts of Bærum as much as 12 – 15 beds are observed (pers. comm. Dr. Philos. J. Fredrik Bockelie, December 2014).

The absence of the dominating interval of the structureless calcareous sandstone in RS1 and LØS1, but present in HS1, suggests that the area in which the sediments of HS1 were deposited, was located in a more carbonate rich region of the epicontinental sea, making carbonate producing organisms the dominant source of the sediment deposited in the basin.

The only siliciclastic influence would be the most intense storm events carrying suspended sand far out from the source. The first clean sand bed, which marks the boundary between the Husbergøya and Langøyene formations, indicates that there has been a change in setting from open marine, located below storm wave base, represented by the brown weathered sandstone, to an open marine setting influenced by storm events located between the fair weather and storm wave base in facies association FA-II.

The first layers of sand in section HS1 lack any type of lamination, but this does not imply that it was not influenced by any waves. More probably the energy could be so high that it would be deposited as a structureless bed of sand, or that benthic organisms would have removed all signs of lamination by bioturbation. However, laminated sand beds become more common upwards in the stratigraphy of FA-II in all three sections, with more complete "Dott – Bourgeois tempestite sequences" (see Figure 6.7; Figure 6.6 in Chapter 6.1).

Soft sediment deformed layers occur at several levels in the sections RS1 and LØS1, but the facies is recorded only at one place in section HS1. Higher thickness and frequency of the deformed layers in section LØS1 could be a result of the availability of siliciclastic sediments in the local depositional area. The reason for the formation of soft sediment deformed layers in the first FA-II unit is somewhat unclear. The three principal ways the stability of sand is reduced are described in Chapter 6.1.1 within the description of facies F5 (soft sediment deformed layers). As the slope of the basin probably had an extremely low gradient, the slumped layers cannot be explained solely by the indication that it was deposited on a low-gradient slope, but their origin may be a combination of several factors.

Most of the deformed layers have a protruding folded and reoriented lamination (see Figure 6.5 A), which probably means that the deformed layers were semi-consolidated, which requires a more sudden shock to get deformed than if they were not consolidated. Looking at the stacked logs (Figure 7.1), there seems to be some kind of periodicity between the deformed layers, and the two first deformed beds in RS1 and LØS1 seem to correlate, thus indicating that they may have formed at the same time. Catastrophic high-energy events, such as earthquakes, could cause liquefaction and could be a good explanation for the origin of the contorted beds. Braithwaite et al. (1995) also suggested the soft sediment deformed layers to be a result of seismic activity. There have also been done studies regarding seismically

induced soft sediment deformation, linked to distance from epicentre and magnitude of earthquakes (Allen 1986).

All the observed fossils are restricted to a marine environment with normal salinities and within a shallow water depth, supporting the results from other observations during the fieldwork. The observed *Chondrites* burrow in section LØS1 (Figure 6.21 B), indicate an environment below the normal wave base, but is still found in storm influenced marine settings. The large trace fossil *Parataenidium* (Figure 6.21 C) is not restricted to any specific facies, however, as the one found relates closely to the *P. monoliformis* it can tell us that it might have been positioned above fair weather wave base. But this is unlikely, since there is no observed lamination in the bed it was found.

Palaeo current orientation, obtained from the measurements of asymmetrical ripples exposed at 29.25 and 32.25 meters in RS1 (Table 6.4 in Chapter 6.2), implies a direction of sediment transport to be 48° northeast. This would implicate that the sediment source was located somewhere in the southwest. This corresponds with Brenchley et al. (1979) hypothesis that the lower Langøyene sandstone beds were deposited by ebb-currents inflected by the Coriolis force and forced in a northeast direction. This hypothesis has however, been re-evaluated by Braithwaite et al. (1995), who suggested that it is most unlikely that the sands have been transported from the west, as the area has very little sand present. As the sand layers are considered to be storm deposits in a relatively large and shallow epicontinental sea, the sediments found in the studied area could have been reworked, transported and been re-deposited numerous times by geostrophical currents, with a transport direction not related to the location of the original sediment source. Studies done in the Oslo Region, Hadeland and Ringerike (Owen et al. 1990; Braithwaite et al. 1995; Whitaker 1977) might not be enough to give a laterally understanding of the origin of the sediments, as it might extend several kilometres outside the studied area.

Results from a MPS - analysis done on a storm deposited bed above the second conglomerate in RS1 (PMO 221.873), show a MPS no larger than what is found in the brown weathered sandstone uppermost in the Husbergøya Formation (PMO 221.860, 221.861, 221.862), see Figure 6.24 C. So, it seems possible that there had been areas on the epicontinental shelf that were more exposed to sorting of the sediments, and that intense storm events have transported cleaner sand from these areas to adjacent more low-energy sites of the epicontinental seas.

Such areas might have been shoals of mixed quartz-ooid bars, steadily migrating and lateral displacement before final burial.

7.3 Channel infill with facies

The abrupt change from a storm influenced depositional environment to the first occurrence of a SU, located at 33 meters in section HS1, 34.3 meters in section RS1 and 46 meters in section LØS1 marks a severe drop in relative sea level. There are observed in total three large SUs floored by conglomerates in RS1 and LØS1, but only one in HS1. The conglomerates in sections RS1 and LØS1 are defined as *pebble conglomerate* and are described in facies F10 in Chapter 6.1.1. The conglomerate in HS1 has been defined as a *boulder conglomerate*, because of its large boulders located in the base of a channel, and is described in facies F11 in Chapter 6.1.1. The lowermost SU and its overlying conglomerate is interpreted to represent the lower boundary of an incised valley system. This will be discussed further below.

When the relative sea level dropped in this low-gradient epicontinental sea, it would expose wide areas to subaerial erosion and expand the catchments area drastically with only a few meters fall in sea level. As soon as the epicontinental sea became shallow and the carbonate rich marine sediments were exposed to meteoric water, they might be consolidated and lithified during a short period of time by interstitial precipitation of calcite from carbonate saturated water. On the exposed sea bottom, creeks and streams would through time be channelized by natural lows in the earlier seafloor and cause erosion and development of incised valleys. Because of the early lithification of carbonate-rich deposits, the incised valley system would probably have been bordered by steep rims and margins with a canyon-like appearance.

The infill of the incised valley system started with deposition of a matrix-supported conglomerate with brown weathered clasts, which resembles the beds of the underlying brown weathered sandstone and scattered corals. The conglomerate matrix seems to be a mixture of quartz grains of various sizes, where the coarsest grains are those that Brenchley and Newall (1975) referred to as “millet-seeds”, bioclasts in various sizes and some occasional carbonate ooids (Figure 7.2). The well-rounded “millet-seeds” (Figure 6.23) and the carbonate ooids are very similar to those present in the trough cross-bedded mixed carbonate-siliciclastic bars or mounds in the Langøyene Formation beneath the boundary of

the incised valley system. The conglomerates are interpreted to have been formed in high-energy river stream, likely during violent flood events.

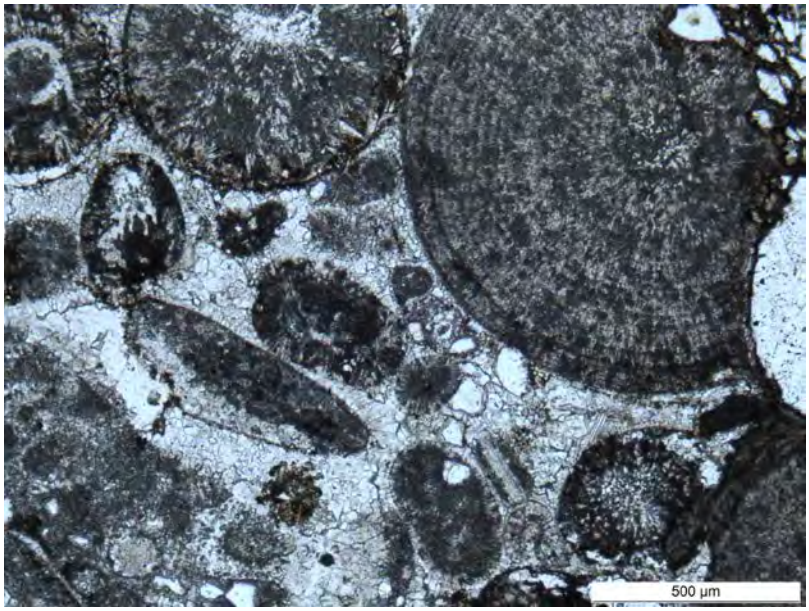

Figure 7.2: Ooids in thin-section PMO 221.854, from the top of the second conglomerate in LØS1.

Upwards in the stratigraphy, within the conglomerate facies, fewer pebble-sized clasts are present, and the quartz grains, bioclasts and ooids are observed in large scale cross bedding. The uppermost unit in facies association FA-IIIa, with the cut and fill structures, low angled cross stratification and asymmetrical ripples (Chaper 6.1.1), reflect a decline in energy of the deposited sediments. Several erosional surfaces are observed within the conglomerate facies, this could be a result from avulsion of the river channel within the incised valley. The clasts of the conglomerate can also be interpreted to reflect a kind of cyclicity of the flow, by their repeated occurrence through the conglomerate unit. Such an apparent cyclicity could be related to the above mentioned avulsion of the river course, or it could be related to a change in seasonal waterflow, like i.e. monsoon seasons which is highly likely, as the location for the studied area was around 30° south of palaeo-equator (Li et al. 2008), thus assuming that the equatorial climate was similar as today.

The infill unit between the first and second conglomerate, defined as facies association FA-IV in RS1 and FA-II in LØS1, has a different vertical thickness between the sections and a different composition of facies. FA-IV in RS1, which is also recorded in HS1, has a more homogeneous sand composition, and the recorded structures reflect an environment higher in energy compared to FA-II. Another important observation is that there has been no recorded evidence in respect of marine influence, such as fossils or bioturbation. This could indicate that the environment had a high input of fresh water, making it brackish or even lacustrine.

This means that the sea level most likely have risen again, developing an estuary in the marine realm, and continuing to rise until facies association FA-II and FA-IV in sections LØS1 and RS1, respectively, in the upper part of the infill successions are cut by a new SU.

The second SU is located at 51.9 meters in LØS1 and 47.6 meters in RS1. This conglomerate is different in respect of lithology in the two sections, the one in section RS1 consists of well rounded, imbricated clasts of laminated sandstone and structureless calcareous siltstones, which differs from the conglomerate in LØS1 that have large scale cross bedding of quartz grains, bioclasts and ooids with scattered coral fragments. In section LØS1, the conglomerate gradually turns over to large scale cross bedding without any coral fragments before the facies association FA-II takes over the infill succession. As described in Chapter 6.1.2, the conglomerate in section RS1 gradually turns upwards into large scale cross bedding, followed by a thin unit with cut and fill and low angled cross stratification, before a new conglomerate bed, with smaller, well rounded clasts of laminated sandstone and structureless calcareous siltstone. This conglomerate bed also passes into low angle cross stratification, before the facies association FA-II takes over the infill succession above this second SU and its basal conglomerate unit. The reason for the difference in lithology between the two conglomerates in LØS1 and RS1, respectively, could be that they have different sources for the deposited sediments, in combination with differences in the current flow conditions. The laminated pebble-clasts in the conglomerate in section RS1 have a similarity to the storm deposited beds of sand and calcareous silt found in facies association FA-II below, and their roundness indicates a certain distance of transport. However, the conglomerate clasts in LØS1 are most likely derived from a more carbonate rich source area.

The succeeding facies association FA-II, which marks a new rise in relative sea level, is also different laterally between sections RS1 and LØS1. In LØS1 soft sediment deformed layers can be several meters thick, whilst in RS1 there are not recorded any soft sediment deformed layers. This can be related to uneven sediment distribution within the incised valley and/or sediment pileups as the sea level rise and the marine realm migrate landwards within the estuary, making sediment deposits unstable due to increasing pore pressure.

The third SU and its conglomerate are located uppermost in the logged section in RS1 and LØS1, stratigraphically above facies association FA-II, representing the last recorded SU in the studied sections. In RS1 it starts with a tabular cross bedded sandstone followed by an

erosional surface floored by a 10 centimetres thick pebble conglomerate succeeded by large scale cross bedded sandstone. This is correlated to match the SU found in the uppermost pebble conglomerate in LØS1, which has the same lithology as the one found in RS1, but is recorded to be over 10 meters thick.

The conglomerates in the two sections are composed of the same imbricated clasts of laminated sandstone, structureless calcareous siltstone and scattered corals. A couple of meters with a partly soft sediment deformed sandstone bed is found on top of the large cross bedded sandstone in RS1 which is capped by parallel laminated sandstone. In LØS1, the conglomerate abruptly shifts to a more homogeneous sand with asymmetrical ripples and low angular cross stratification, before the sandstone gets parallel lamination. The unit above both the conglomerates indicates a decrease in energy.

The uppermost conglomerate recorded in RS1 and LØS1 is considered to have been deposited in a fluvial channel as regard the section RS1, whereas the 10 m thick conglomerate in section LØS1 may have been formed as a bay head delta, as seen from the internal inclined stratification and lateral facies changes.

The one and only SU recorded in section HS1 has a boulder conglomerate at the base, with the boulders consisting of coarse grained quartz, ooids and carbonate matrix (Figure 6.9 D), which is the same lithology as found further north from the logged section (Figure 6.10 B). Above the conglomerate, facies such as cut-and-fill structures and low angle cross-stratification are recorded, before a unit of facies association FA-IV with no bioturbation, or fossils are observed. The FA-IV unit continues up to 40 meters. Section HS2 is believed to be on the rim of the cut down channel, and is therefore interpreted not to be stratigraphically above the other logged section. If the HS2 had been logged further north, the unit seen in Figure 6.10 B would probably have been recorded, but due to tectonic disturbance in the area between, this was not recorded, nor made clear.

Brenchley and Newall (1980) believed that these channels in upper part of the Langøyene Formation were tidal, whereas Braithwaite et al. (1995) thought this was unlikely, as there are no peritidal deposits present. Braithwaite et al. (1995) further argued that large clasts suggest a high energy catastrophic event with imbricated clasts showing a unidirectional

transportation; in Hadeland clasts in this stratigraphic interval imply a proximity to a carbonate source area with no siliciclastic influence.

However, there is unlikely that the channels were created by a single catastrophic event. Lithified seafloor sediments, as demonstrated by all lithoclasts in the conglomerates, would have needed longer time than a sudden catastrophic event to create an incised valley system. One must take into account that tidal influence in such a large, shallow epicontinental sea most likely was marginal, as the friction between the shallow water-mass and the seafloor probably would be too high for any tidal influence. This would explain why there are no tidal deposits present in the strata, and also making Brenchley and Newall (1980) hypothesis that tidal currents created the incised valleys, not very plausible.

The results from point counting (Figure 6.24 A, Chapter 6.5.1) from thin-sections in facies association FA-IIIa in the lowermost conglomerate unit show an increase in quartz and decrease in calcite from the base of the conglomerate (PMO 221.863) to the middle of the conglomerate (PMO 221.864), with a decrease in quartz and increase of calcite in the top of the conglomerate. The second conglomerate follows the same trend. This coincides well with an increase of energy from the base towards a maximum, and then followed by a decrease in energy toward the top. The conglomerate facies is also easily recognised in the MPS results (Figure 6.24 C) as the grain size increases drastically from the erosional surface (PMO 221.864) to the base (PMO 221.865), and a small decline again at the top (PMO 221.869).

Palaeocurrent measurements (Table 6.4 in Chapter 6.2) within facies association FA-IV at 41.25 meters and 42.50 meters show a transport direction of 58° to northeast, which is the same as the measurements done in FA-II. However, measurements of imbricated clasts in section LØS1 at the third conglomerate (Table 6.6 in Chapter 6.2) show a transport direction varying between 214° and 232° southeast, which is the opposite of what the asymmetrical ripples show, indicating that the sediment source of the conglomerate are most likely derived from the northern sector.

Braithwaite et al. (1995) used SEM examination on the “millet-seeds” to find evidence for frosted surface, which is characteristic for wind-transported sand, but without any luck. The grains have during burial and digenesis been exposed to chemical weathering, erasing any evidence of the frosted surface. Figure 6.23 B in Chapter 6.5.1, a monocrystalline “millet-

seed" quartz grain shows an irregular, corroded surface, most likely due to chemical dissolution.

It is difficult to predict an estimate of how deep incision has taken place in the Langøyene Formation by the present data set. However, studies done by Johan Fredrik Bockelie on Bjerkøya in Asker suggest that the down cutting can be up to 85 meters (pers. comm. Dr. Philos. J. Fredrik Bockelie December 2014), which indicates a severe drop in relative sea level during a relatively short period of time. The boundary between Langøyene and Solvik formations, exposed further northeast of the logged section on Hovedøya (Figure 6.10 B in Chapter 6.1.2), shows evidence of a karstic surface (see arrows) suggesting it have been subaerially exposed. This unconformity could probably be correlated to one of the two uppermost SUs found in RS1 and LØS1. The through cross-stratified quartz and oolithic sandstone with a karstic surface, is also most likely the source for the coarse-grained quartz, ooids and carbonate matrix found in the conglomerate facies. As three episodes of relative sea level falls are recorded, the erosion from each fall and rise in sea level would also be of significance.

7.4 The Ordovician/Silurian transition

Facies association FA-Ib marks the end of FA-IIIa with the appearance of brown weathered sandstone, structureless calcareous siltstone and nodular limestone, indicating once again an open marine setting, without any noticeable storm influence. The FA-Ib beds can be correlated between the logged sections LØS1, RS1 and HS1 (Figure 7.1). The succeeding facies association FA-V is composed of heavily bioturbated shale and is the uppermost logged unit, belonging to the Solvik Formation. Worsley et al. (1983) defined the base of the Solvik Formation to include the nodular limestone. The Ordovician-Silurian boundary is unresolved in the Oslo region due to one or more sedimentary gaps near the transition between the Langøyene and Solvik formations. In the Asker area the boundary is considered to "be positioned in the lowest part of the Solvik Formation" (Baarli 2014: p. 30).

The brown weathered sandstone has the same composition and grade of bioturbation as the one found in FA-Ia, but is interbedded first by structureless calcareous siltstone, which gradually becomes more nodular, as seen in Figure 6.10 A, C and D. These beds have a high

fossil content, see Figure 6.3 A and C. The results from pointcounting (Figure 6.24 A) of thin-section 221.876, taken from a nodule, also show a low amount of quartz present, with a low MPS value (Figure 6.24 C). The fact that the layers seems to go from more continuous to discontinuous beds, and at the top over to nodules, could suggest a decreasing rate in sedimentation. As the sea level continuous to rise, forcing the marine realm landwards, the sediment input decreases. At the time when the continuous structureless calcareous siltstone beds were formed, the rate of sedimentation still was relatively high, and the interbedded brown weathered sandstone buried them. However, as the rate of sedimentation decreases, the carbonate beds may have been exposed to the seawater for a longer time, and the beds may have been partly dissolved, all the way to form nodules. The structureless calcareous siltstone beds were most likely formed as storm deposits, carried out in suspension from carbonate-rich source areas.

There seems to be an abrupt change from the brown weathered sandstone with interbedded nodules, into facies association FA-V, consisting of the bioturbated shale (Figure 6.2) in the Solvik Formation. This indicates that the sea level continued to rise, and at the time, the only deposits are fine particles carried far out into open marine setting in suspension. The boundary between facies association FA-Ib and FA-V is also correlated laterally between all three sections (Figure 7.1).

7.5 Impact of the Late Ordovician glaciation of Gondwanaland

The observations made during this study suggest that at least three episodes of lowering of the relative sea level happened during the deposition of the Langøyene Formation, all within the age of Hirnantian, which suggests an extremely rapid change in relative sea level. Brenchley and Newall (1980) linked this regressive phase during deposition of the Langøyene Formation to glacio-eustatic changes, related to the glaciation of Gondwanaland during the Late Ordovician.

In the Anti-Atlas fold belt in Morocco a thick Palaeozoic succession is exposed, holding evidence from the glaciation of the continent, which was part of the North Gondwana cratonic platform (Loi et al. 2010 and references therein).

The Late Ordovician Gondwana glaciation is unusual because it happened during a time when the Earths CO_2 levels were particularly high. However, there has been done some work (Poussart et al. 1999; Crawley and Baum 1991; Crowley et al. 1993) using different models to show that a glaciation of the southern hemisphere is possible due to high CO_2 levels. Hermann et al. (2004), based on an ocean general circulation model using pCO_2 values, suggested a complex interaction of prerequisite factors to explain the onset of the Hirnantian glaciation with the associated drop in sea level, including southward drift of Gondwana, causing the southward ocean heat transport to be reduced, together with a drop in pCO_2, resulting in reduced greenhouse effect and concomitant drop in the global temperature.

Fieldwork done on the Palaeozoic succession in the Anti-Atlas fold belt by Loi et al. (2010), Le Heron et al. (2007), and in Libya, Morocco, South Africa and wireline logs and core from Ahnet basin, Algeria by Sutcliffe et al. (2000), shows evidence for at least two major glacioeustatic sea level variations within the Hirnantian. However, field studies done in Turkey by Monod et al. (2003), suggest three glacial events during the Hirnantian stage, which corresponds with the results from this study as well, with evidence for three lowering in the relative sea level, all with an interval with marine influence in-between. James (2013) has found evidence of two separate sea level low-stands in the Welsh Basin (UK), which as well has been related to the glaciation of Gondwana. There is also evidence supporting a hypothesis that the glaciation of Gondwana started as early as the base of Katian, and did not fully disappear before the Lower Silurian (Loi et al. 2010 and references therein). Studies done on diversities in faunas during the Late Ordovician on the Yangtze Platform (Xu 1983), indicates a rapid melting of the ice sheet, which support the hypothesis of a rapid fluctuation in the sea level.

This glaciation would support the hypothesis of the formation of an incised valley system formed by a rather rapid glacio-eustatic drop in sea level, changing into an estuarie when the ice-sheet on Gondwana melted, with three cutbacks before the final flooding happened in the Early Silurian, see illustration in Figure 7.3. Braithwaite et al. (1995) coupled the mechanism of glacioeustacy with tectonic uplift caused by the initiation for formation of the Caledonian nappes to the northwest.

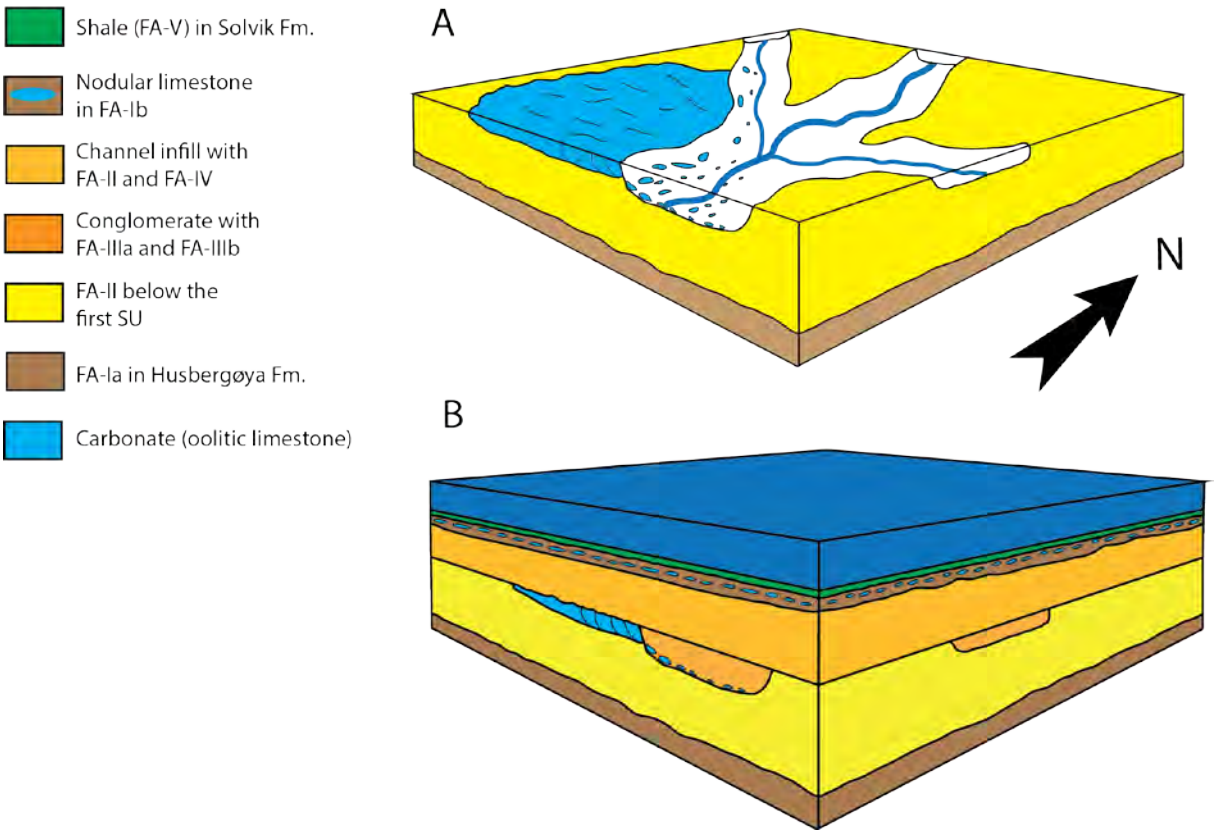

Figure 7.3: Reconstruction of the depositional environment during the development of the first SU in the Langøyene Formation (A), and during the deposition of facies association FA-V in the Solvik Formation.

However, for the first, erosion caused by a glacioeustatic sea level drop would have taken place at a much higher rate than a tectonic uplift as for example that of a foreland bulge of a thick continental crust in front of eastward moving nappes. Secondly, the Caledonian nappes were during the time of deposition of the Langøyene Formation most likely too far away in the western part of Baltica to have any major and localized tectonic influence in the Oslo Region. A tectonic uplift might also have created a high relief on the continent, thus accelerating the erosion of the hinterland and also making the shelf less sensitive regarding sea level changes, which in this case is not very plausible, as the sediments seems to have had a great sensitivity to the sea level fluctuations.

At the Lake Mjøsa, there is a hiatus in the Upper Ordovician. Recent studies (Bergström et al. 2010; 2011 and references therein) on conodont biostratigraphy and $\delta^{13}C$ chemostratigraphy indicate that above the Mjøsa Formation, a more than100 m thick unit, there is a stratigraphic gap that comprises the middle and upper Katian, Hirnantian and Rhuddanian stages. The Mjøsa limestone is terminated by a karstic surface filled by quartzite of middle Llandovery

age. The emergence of the shallow-marine Møsa limestone and the subsequent stratigraphic break could be the result of a foreland bulge related to the onset of south-eastward moving Caledonian nappes. The Hirnantian deep erosion further south in the Oslo Region might thus have been superimposed onto the southernmost part of such a bulge. Bergström et al. (2011) concluded that most of the Oslo Region sea level changes (in Late Ordovician) are of local rather than eustatic may be except for the Katian highstand suggested by Nielsen (2004). An overall discussion of sea level changes in the Late Ordovician is beyond the scope of this study and will not be discussed further here. Though, the erosional unconformities described in this thesis (Figure 7.1) must imply a marked fall in relative sea level.

Braithwaite et al. (1995) also argued for the increasing influence of siliciclastic material in the Langøyene Formation to be related to a faulted graben system. However, if the Laurentian and Baltican plates were converging, thus forming a compressional regime, this would have made the development of a graben system in the Late Ordovician unlikely. There has not been found any evidence of faulting, i.e. scree deposits derived from the rims of the faulted blocks, supporting this hypothesis.

8 Conclusion

- The Langøyene Formation succeeds the Husbergøya Formation and was deposited in a storm-influenced, shallow epicontinental sea. The sedimentary succession is generally upward coarsening, revealing increasing energy and decreasing water depth of the depositional environment. The Langøyene Formation is in the middle part cut by a major subaerial unconformity (SU), separating the Langøyene succession in a lower and upper part.
- The boundary between the Husbergøya Formation and overlying Langøyene Formation represents a transition from sea level highstand with water depths generally below storm wave to an upward shallowing sea close to or above storm wave base. The brown colour of the strongly bioturbated and dirty fine-grained Husbergøya sandstones is due to oxidised ferruginous dolomite or/and ankerite.
- Mudstone, shale and thin limestone layers in the lower part of the Langøyene Formation were formed during open-marine oxygenated conditions with high bioturbation activity in mudstone facies beneath storm wave base. Clean sand layers showing a unidirectional transport direction were transported by wind-driven currents from a shoreface area, or by reworking of clean sand from shoals within the epicontinental sea.
- Three major subaerial erosional unconformities (SU) in the Langøyene Formation were formed by eustatic lowering of the sea level, most likely caused by the Gondwana glaciation in Hirnantian time. The SU surfaces and their infill successions represent the upper part of the Langøyene Formation.
- The first glacioeustatic drop in sea level gave rise to an incised valley, or several linked valleys in a valley system during lowstand, with southerly-directed fluvial to bay-head delta transport and deposition. During highstand the incised valley turned into an estuary and was filled by marine sandy deposits, mostly by the influence of storm-generated currents.
- The lowermost SU represents the maximum regressive surface with deepest incision, at least 35 meters in the study area, during glacial maximum for the late Ordovician glaciation in Gondwana. The next two erosional unconformities and subsequent sediment infill successions reflect two additional events of sea level low stands during the glacial Hirnantian stage.

- The karst surface of oolithic calcareous sandstone at the southeastern shore in Hovedøya, just beneath the Ordovician-Silurian boundary and the Silurian Solvik Formation, may represent a subaerially exposed interfluvial area within the incised valley system.
- Three sequences bounded by erosional unconformities have been identified also in other regions with Hirnantian successions. Possible correlation needs to be shown by further studies.

9 References

Ahokas, J. M., Nystuen, J. P. & Martinius, A. W. 2014a: Depositional dynamics and sequence development in a tidally influenced marginal marine basin: Early Jurassic Neill Klinter Group, Jameson Land Basin, East Greenland. *Int. Assoc. Sedimentol. Spec. Publ. 46*, 291 – 338.

Ahokas, J. M., Nystuen, J. P. & Martinius, A. W. 2014b: Stratigraphic signatures of punctuated rise in relative sea-level in an estuary-dominated heterolithic succession: Incised valley fills of the Toarcian Ostraelv Formation, Neill Klinter Group (Jameson Land, East Greenland). *Marine and Petroleum Geology 50*, 103 – 129.

Allen, J. R. L. & Banks, N. L. 1972: An Interpretation and Analysis of Recumbent - Folded Deformed Cross-Bedding. *Sedimentology 19(3-4)*, 257-283.

Allen, J. R. L. 1986: Earthquake magnitude-frequency, epicentral distance, and soft - sediment deformation in sedimentary basins. *Sedimentary geology 46(1)*, 67-75.

Baarli, B.G. 2014: The early Rhuddanian survival interval in the Lower Silurian of the Oslo Region: A third pulse of the end-Ordovician extinction. *Palaeogeography, Palaeoclimatology, Palaeoecology 395*, 29–41.

Benton, M. J. & Harper, D. A. T. 2009: The basal metozoans: sponges and corals; Trace fossils. In: Introduction to Paleobiology and the Fossil Record. *Wiley – Blackwell*. Ch. 11, 19, pp. 260 – 296, 509 – 532.

Bergström, S.M., Schmitz, B., Young, S.A. & Bruton, D.L. 2010: The $\delta^{13}C$ chemostratigraphy of the Upper Ordovician Mjøsa Formation at Furuberget near Hamar, southeastern Norway: Baltic, Trans-Atlantic, and Chines relations. *Norwegian Journal of Geology 90*, 65-78.

Bergström, S.M., Schmitz, B., Young, S.A. & Bruton, D.L. 2011: Lower Katian (Upper Ordovician) $\delta^{13}C$ chemostratigraphy, global correlation and sea-level changes in Baltoscandia. *GFF 133*, 1-17.

Bjørlykke, K. 1973: Origin of limestone nodules in the Lower Palaeozoic of the Oslo Region. *Norsk Geologisk Tidsskrift 53*, 419 – 431.

Bjørlykke, K. 1974: Depositional history and geochemical composition of Lower Palaeozoic epicontinental sediments from the Oslo Region. *Norges Geologiske Undersøkelse 305,* 81 pp.

Bockelie, J. F. 1982: The Ordovician of Oslo-Asker. In: Bruton, D. L. & Williams, S. H. (Eds.), Field Excursion Guide. IV International Symposium on the Ordovician System. *Paleontological Contribution from the University of Oslo (279),* 106 – 121.

Bockelie, J. F. 1984: The *Diploporita* of the Oslo Region, Norway. *Palaeontology 27 (1),* 1 - 68.

Bockelie, J. F. & Nystuen, J. P. 1985: The southeastern part of the Scandinavian Caledonides. In: Gee, D. G. & Sturt, B. A. (Eds). The Caledonide orogen–Scandinavia and related areas; Part 1. *John Wiley and Sons*, 69 – 88.

Boyd, R., Dalrympe, R.. & Zaitlin, B.A. 1992: Classification of clastic coastal depositional environments. *Sedimentary geology 80(3),* 139-150.

Braithwaite, C.J.R., Owen, A.W. & Heath R.A. 1995: Sedimentological changes across the Ordovician Silurian boundary in Hadeland and their implications for regional patterns of deposition in the Oslo Region. *Norsk Geologisk Tidsskrift 75*, 199-218.

Brenchley, P. J. & Cocks, L. R. M. 1982: Ecological associations in a regressive sequence: the latest Ordovician of the Oslo-Asker district, Norway. *Palaeontology 25(4),* 783-815.

Brenchley, P. J. & Newall, G. 1975: The stratigraphy of the upper Ordovician stage 5 in the Oslo-Asker District, Norway. *Norsk Geologisk Tidsskrift 55*, 243-275.

Brenchley, P. J. & Newall, G. 1977: The significance of contorted bedding in upper Ordovician sediments of the Oslo region, Norway. *Journal of Sedimentary Research 47(2)*, 819-833.

Brenchley, P. J. & Newall, G. 1980: A facies analysis of Upper Ordovician regressive sequences in the Oslo Region of Norway – a record of glacio-eustatic changes. *Palaeogeography, Palaeoclimatology, Palaeoecology 31*, 1-38.

Brenchley, P. J., Newall, G. & Stanistreet, I. G. 1979: A storm surge origin for sandstone beds in an epicontinental platform sequence, Ordovician, Norway. *Sedimentary Geology 22*, 185-217.

Bruton, D. L., Gabrielsen, R. H. & Larsen, B. T. 2010: The Caledonides of the Oslo Region, Norway - stratigraphy and structural elements. *Norwegian Journal of Geology 90*, 93-121.

Brøgger, W. C. 1882: Die silurischen Etagen 2 und 3 im Kristianiagebiet und auf Eker etc. *Univ. progr., Kristiania 1882*, 376 pp.

Buckman, J. O. 2001: Parataenidium, a new taenidium - like ichnogenus from the carboniferous of Ireland. *Ichnos: An International Journal of Plant & Animal 8(2)*, 83-97.

Calner, M., Ahlberg, P., Lehnert, O. & Erlström, M. 2013: The Lower Palaeozoic of southern Sweden and the Oslo Region, Norway. Field Guide for the 3rd Annual Meeting of the IGCP project 591. *Sveriges geologiska undersökning Rapporter och meddelanden 133,* 96 pp.

Chow, N. & Longstaffe, F. J. 1995: Dolomites of the Middle Devonian Elm Point Formation, southern Manitoba: intrinsic controls on early dolomitization. *Bulletin of Canadian Petroleum Geology 43(2)*, 214-225.

Collinson, J. D. 1996: Alluvial sediments In: Reading, H. G. (Ed.), Sedimentary Environments: Processes, Facies and Stratigraphy. *Blackwell Publishing.* Ch. 3, pp. 37 – 82.

Crowley, T. J. & Baum, S. K. 1991: Towards reconciliation of Late Ordovician (440 Ma) glaciation with very high CO_2 levels. *Journal of Geophysical Research 96*, 22,597 – 22,610.

Crowley, T. J., Baum, S. K. & Kim, K. Y. 1993: General circulation model sensitivity, experiments with pole-centered supercontinents. *Journal of Geophysical Research 98*, 8793 – 8800.

Dalrymple, M., Prosser, J. & Williams, B. 1998: A dynamic systems approach to the regional controls on deposition and architecture of alluvial sequences, illustrated in the Statfjord Formation (United Kingdom, Northern North Sea). *Special Publication 59,* 65 – 81.

DeCelles, P. G. & Giles, P.A. 1996: Foreland basin systems. *Basin Research 8(2),* 105-123.

Dott, R. H. & Bourgeois, J. 1982: Hummocky stratification: significance of its variable bedding sequences. *Geological Society of America Bulletin 93(8),* 663-680.

Doyle, P. 1996: Molluscs: Bivalves and Gastropods; Brachiopods; Echinoderms; Trilobites; Bryozoans, Understanding Fossils – An Introduction to Invertebrate Palaentology. *Wiley*. Ch. 8, 10, 11, 12, 15. 136 – 158, 182 – 200, 201 – 219, 220 – 237.

Ethridge, F. G., Wood, L.J. & Schumm, S.A. 1998: Cyclic variables controlling fluvial sequence development: problems and perspectives. *Society for Sedimentary Geology. Special Publication No. 59*, 17 – 29.

Fisher, D. W. 1962: Small conoidal shells of uncertain affinities. In: Moore, R. C. (Ed) Treatise on Invertebrate Paleontology. *Univ. Kansas Press & Geologic Society of America*, 130 – 143.

Fossen, H., Pedersen, R.-B., Bergh, S. & Andresen, A. 2008: Creation of a mountain chain, The building up of the Caledonides; about 500 – 405 Ma. In: Ramberg, I. B., Bryhni, I., Nøttvedt, A., Rangnes, K. (Eds.), The Making of a Land – Geology of Norway. *Norwegian Geological Association.* Ch. 6, pp. 178 – 231.

Gabrielsen, R., Nystuen, J. P., Jarsve, E. M. & Lundmark, M. 2014: The Sub-Cambrian Peneplain in southern Norway: Its geological significances for post-Caledonian faulting, uplift and denudation. In: Jarsve, E. M., Mesozoic and Cenozoic basin development and sediment infill in the North Sea region - shifting depocenters associated with regional structural development. PhD Thesis, *Faculty of Mathematics and Natural Science, Departement of Geosciences, University of Oslo, Norway, Paper 5*, 39 pp + figures.

Gary, M. & McAfee, R. 1973: Glossary of geology. *Washington, DC. American Geological Institute.*

Glørstad – Clark, E., Birkeland, E. P., Nystuen, J. P., Faleide, J. I. & Midtkandal, I. 2011: Triassic platform-margin deltas in the western Barents Sea. *Marine and Petroleum Geology 28*, 1294 – 1314.

Hansen, J., Nielsen, J.K. & Hanken, N.M. 2009: The relationships between Late Ordovician sea-level changes and faunal turnover in western Baltica: Geochemical evidence of oxic and

dysoxic bottom-water conditions. *Palaeogeography, Palaeoclimatology, Palaeoecology 271(3)*, 268-278.

Heckel, P. H. 1972: Recognition of ancient shallow marine environments. *The Society of Economic Paleontologists and Mineralogists, Recognition of Ancient Sedimentary Environments (SP16)*, 226 - 286.

Henningsmoen, G. 1974: A comment. Origin of limestone nodules in the Lower Palaeozoic of the Oslo Region. *Norsk Geologisk Tidsskrift 54*, 401-412.

Hermann, A. D., Patzkowsky, M. E. & Pollard, D. 2004: The impact of paleogeography, pCO_2, poleward ocean heat transport and sea level change on global cooling during the Late Ordovician. *Palaeogeography, Palaeoclimatology, Palaeoecology 206,* 59 – 74.

Hubbert, M. K. & Rubey, W. W. 1959: Role of fluid pressure in mechanics of overthrust faulting I. Mechanics of fluid-filled porous solids and its application to overthrust faulting. *Geological Society of America Bulletin 70(2),* 115-166.

Jaanusson, V. 1984: Ordovician benthic macrofaunal associations. In: Bruton, D. L. (Ed.), aspects of the Ordovician System. *Universitetsforlaget*, pp. 127 – 140.

James, D. M. D. 2013: Assessment of Hirnantian synglacial eustacy and palaeogeography in a tectonically active setting: the Welsh Basin (UK). *Geological Magazine 151*, 447 – 471.

Johnson, H.D. & Baldwin, C.T. 1996: Shallow clastic seas. In: Reading, H.G. (Ed.), Sedimentary Environments: Processes, Facies and Stratigraphy. *Blackwell Publishing.* Ch. 7, pp. 232-280.

Kiær, J. A. 1897: Den repraesentative undersøgelsesmethode. I Kommission hos Jacob Dybwad.

Kiær, J. A. 1902: Etage 5 i Asker ved Kristiania (English summary). *Norges Geologiske Undersøkelse 34(1),* 1-112.

Kiær, J. A. 1908: Das Obersilur im Kristianiagebeite: eine stratigraphisch-faunistische Untersuchung. *Christiania: I kommisjon hos Jacob Dybwad*.

Kjærsgaard, M. 2014: Mixed siliciclastic-carbonate sedimentation in the Late Ordovician shallow marine epicontinental sea, Oslo Region. Unpubl. MSc. Thesis. *Digitale Utgivelser ved UiO,* pp. 209.

Larsen, B. T. & Olaussen S. 2005: The Oslo Region: A Study in Classical Palaeozoic Geology, Stabekk, Oslo. *Geological society of Norway*, 88 pp.

Le Heron, D. P., Ghienne, J.-F., El Houicha, M., Khoukhi, Y., Rubino, J.-L. 2007: Maximum extent of ice sheets in Morocco during the Late Ordovician glaciation. *Palaeogeography, Palaeoclimatology, Palaeoecology 245,* 200 – 226.

Li, Z.-X., Bogdanova, S. V., Collins, A. S., Davidson, A., De Waele, B., Ernst, R. E., Fitzsimons, I. C. W., Fuck, R. A., Gladkochub, D. P. & Jacobs, J. 2008: Assembly,

configuration, and break-up history of Rodinia: a synthesis. *Precambrian research 160(1)*, 179-210.

Loi, A., Ghienne, J. F., Dabard, M.-P., Paris, F., Botquelen, A., Christ, N., Elaouad-Debbaj, Z., Gorini, A., Vidal, M. & Videt, B. 2010: The Late Ordovician glacio-eustatic record from a high-latitude storm-dominated shelf succession: The Bou Ingarf section (Anti-Atlas, Southern Morocco). *Palaeogeography, Palaeoclimatology, Palaeoecology 296(3)*, 332-358.

Midtkandal, I. & Nystuen, J. P. 2009: Depositional architecture of a low - gradient ramp shelf in an epicontinental sea: the lower Cretaceous of Svalbard. *Basin Research 21(5)*, 655-675.

Monod, O., Kozlu, H., Ghienne, J.-F., Dean, W. T., Günay, Y., Le Hérisse, A., Paris, F. & Robardet, M. 2003: Late Ordovician glaciation in southern Turkey. *Terra Nova 15*, 249 – 257.

Morrow, D. W. 1982: Diagenesis 1. Dolomite-Part 1: The chemistry of dolomitization and dolomite precipitation. *Geoscience Canada 9(1),* 5 - 13.

Möller, N.K. & Kvingan, K. 1988: The genesis of nodular lime- stones in the Ordovician and Silurian of the Oslo Region (Norway). *Sedimentology* 35, 405-420.

Myers, K. J. & Milton, N. J. 1996: Concepts and Principles. In: Emery, D. & Myers, K. J. (Eds.), Sequence Stratigraphy. *Blackwell Publishing.* Ch. 2, pp. 11 – 44.

Myrow, P. M. & Southard, J. B. 1996: Tempestite deposition. *Journal of Sedimentary Research 66(5)*, 875 - 887.

Nichols, G. 2009: Terrigenous Clastic Sediments: Gravel, Sand and Mud; Post-depositional structures and diagenesis. In: Sedimentology and Stratigraphy. *Wiley – Blackwell*. Ch. 2, 18, pp. 5 – 27, 274 – 296.

Nielsen, A. T. 2004: Ordovician sea level changes: a Baltoscandian perspective In: Webby, B. D., Paris, F., Droser, M. L. & Percival, I. G. (Eds.), The Great Ordovician Biodiversification Event. *Columbia University Press, New York.* Ch. 10, pp. 84-93.

Nielsen, A. T. & Schovsbro, N. H. 2011: The Lower Cambrian of Scandinavia, depositional environment, sequence stratigraphy and palaeostratigraphy. *Earth-Science Reviews, 107,* 207-310.

Nystuen, J. P. 1987: Synthesis of the tectonic and sedimentological evolution of the late Proterozoic – early Cambrian Hedmark Basin, the Caledonian Thrust Belt, southern Norway. *Norsk Geologisk Tidsskrift 67*, 395 – 418.

Owen, A.W., Bruton, D.L., Bockelie, J.F. & Bockelie, T.G. 1990: The Ordovician successions of the Oslo Region, Norway. *Norges Geologiske Undersøkelse, Special Publication No. 4*, 1-54 + chart.

Posamentier, H. W., Jervey, M. T. & Vail, P. R. 1988a: Eustatic controls on clastic deposition I - Conceptual Framework. *Special Publications 42,* 109 – 124.

Posamentier, H. W. & Vail, P. R. 1988b: Eustatic controls on clastic deposition II - Sequence and Systems tract models. *Special Publications 42*, 125 – 154.

Poussart, P. F., Weaver, A. J. & Barnes, C. R. 1999: Late Ordovician glaciation under high atmospheric CO_2: A coupled model analysis. *Paleoceanography 14(4),* 542 – 558.

Powers, M. C. 1953: A new roundness scale for sedimentary particles. *Journal of Sedimentary Research 23(2)*, 117 – 119.

Reading, H. G. & Collinson, J. D. 1996: Clastic coasts, In: Reading, H.G. (Ed.), Sedimentary Environments: Processes, Facies and Stratigraphy. *Blackwell Publishing.* Ch. 6, pp. 154-231.

Reading, H.G. & Levell, B. K. 1996: Controls on the sedimentary rock record, In: Reading, H.G. (Ed), Sedimentary Environments: Processes, Facies and Stratigraphy. *Blackwell Publishing.* Ch. 2, pp. 5 - 36.

Richards, R. P. 1974: Ecology of the Cornulitidae. *Journal of Paleontology 48(3)*, 514-523.

Ross, J. R. P. 1984: Palaeoecology of Ordovician Bryozoa, In: Bruton, D. L. (Ed.), Aspects of the Ordovician System. *Universitetsforlaget*, 141 – 148.

Seilacher, A. & Meischner, D. 1965: Fazies-Analyse im Paläozoikum des Oslo-Gebietes. *Geologische Rundschau 54(2)*, 596 – 619.

Skjeseth, S. 1963: Contributions to the geology of the Mjøsa Districts and the classical Sparagmite area in Southern Norway: Sammendrag. *NGU 220,* 126 pp.

Spjeldnæs, N. 1957: The Silurian/Ordovician border in the Oslo district. *Norsk Geologisk Tidsskrift 37*, 355 - 371.

Spjeldnæs, N. 1961: Ordovician climatic zones. *Norsk Geologisk Tidsskrift 41(1),* 45-77.

Stow, D. A. V. 2005: Principal Characteristics of Sedimentary Rocks, Sedimentary Rocks in the Field – A Color Guide. *Academic Press*. Ch. 3, pp. 28 – 125.

Sutcliffe, O. E., Dowdeswell, J. W., Whittington, R. J., Theron, J. N. & Craig, J. 2000: Calibrating the Late Ordovician glaciation and mass extinction by the eccentricity cycles of Earth´s orbit. *The Geological Society of America 28*, 967 – 970.

Talbot, M. R. & Allen, P. A. 1996: Lakes. In: Reading, H.G. (Ed.), Sedimentary Environments: Processes, Facies and Stratigraphy. *Blackwell Publishing.* Ch. 4, pp. 83 - 124.

Vidal, G. & Nystuen, J.P. 1990: Micropaleontology, depositional environment, and biostratigraphy of the upper Proterozoic Hedmark Group, southern Norway. *American Journal of Science 290,* 170-211.

Vinn, O. 2013: Cornulitid tubeworms from the Ordovician of eastern Baltic. *Carnets de Geologie-Notebooks on Geology.*

Vinn, O. & Mutvei, H. 2004: Cornulitids, problematic Ordovician calcitic tubicolous fossils. 8th Meeting on the Working Group on the Ordovician Geology of Baltoscandia May 13–18, 2004, Tallinn and Tartu, Estonia Organising Comittee. In: Hints, O. & Ainsaar, L. (Eds.), Conference Materials, Abstracts and Field Guidebook, Tartu University Press, p. 102.

Wentworth, C. K. 1922: A scale of grade and class terms for clastic sediments. *The Journal of Geology,* 377-392.

Whitaker, J. H. M. 1977: A guide to the Geology around Steinsfjord, Ringerike, Oslo, Norway. *Universitetsforlaget, University of Oslo,* 175 pp.

Worsley, D. (Ed.) 1982: IUGS Subcommission on Silurian Stratigraphy. Field Meeting, Oslo Region 1982. *Paleontological Contribution from the University of Oslo* 278, 175 pp.

Worsley, D., Aarhus, N., Bassett, M.G., Howe, M.P.A., Mørk, A. & Olaussen, S. 1983: The Silurian succession of the Oslo Region. *Norges Geologiske Undersøkelse Bulletin 384*, 57 pp.

Worsley, D. & Nakrem, H. A. 2008: The Lower Palaezoic, Cambrian, Ordovician and Silurian – The Sea Teems With Life 542 – 416 Million Years. In: Ramberg, I. B., Bryhni, I., Nøttvedt, A. & Rangnes, K. (Eds.), The Making of a Land – Geology of Norway. *Norwegian Geological Association.* Ch. 5, pp. 148 – 177.

Xu, C. 1983: Influence of the Late Ordovician glaciation on basin configuration of the Yangtze Platform in China. *Lethaia 17(1),* 51 – 59.

Zaitlin, B. A., Dalrympe, R.W. & Boyd, R. 1994: The stratigraphic organization of incised-valley systems associated with relative sea-level change. In: Dalrymple, R. W., Boyd, R. & Zaitlin, B. A. (Eds.), Incised – Valley Systems: Origin and Sedimentary Sequences. *Society for Sedimentary Geology, Special Publications No. 51,* 45 – 60.

http://www2.nau.edu/rcb7/

http://kart.finn.no/

Appendix A

Legend

Lithology:

- Mud/silt/very fine sandstone
- Sandstone
- Conglomerate
- Carbonate
- Shale
- Basalt

Fossils:

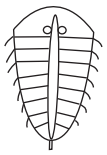
Trilobite

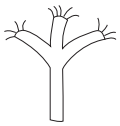
Bryozoans


Brachiopods


Cornulites


Blastoids


Corals


Crinoids


Gastropods

Sedimentary structures:

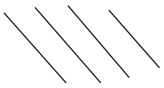
Tabular cross bedding


Cross bedding


Paralell Lamineted

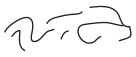
Slumping structures

Water escape structures


Low angle cross stratification


Cut and fill


Hummocky cross stratification

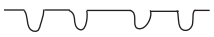
Load cast

Erosion


Symmetrical ripples


Climbing ripples


Assymetrical ripples


Carbonate clasts


Nodular limestone


Clasts w/lamination


Vertical burrows


Grade of bioturbation

Appendix B

Slab scans, Hovedøya

HS2-48,75m

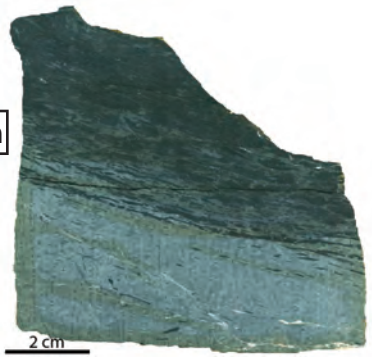

HS2-48m

HS2-47,9m

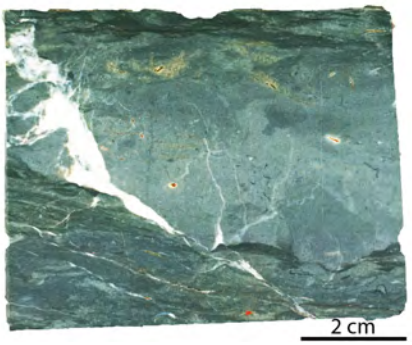

HS2-47,5m

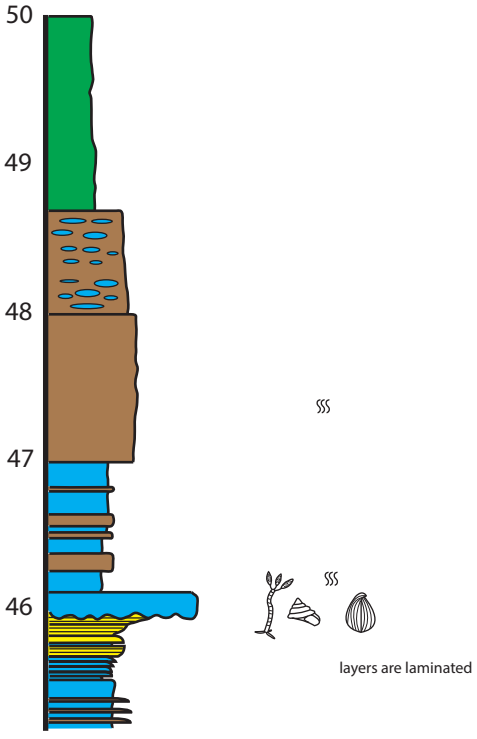

HS2-46,9m

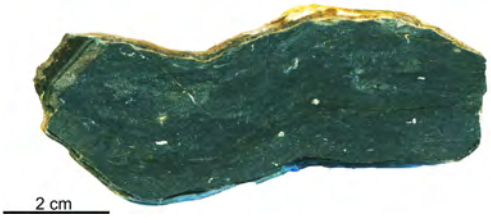

HS2-46m

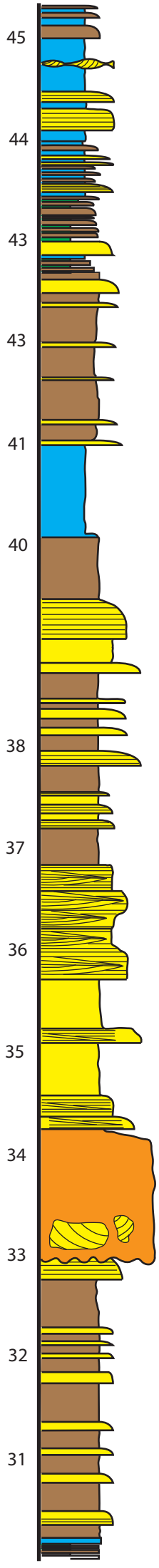

Fine sand layers are laminated

Some layers are discontinous, looks like nodules.

HS1-35m

HS1-30,5m

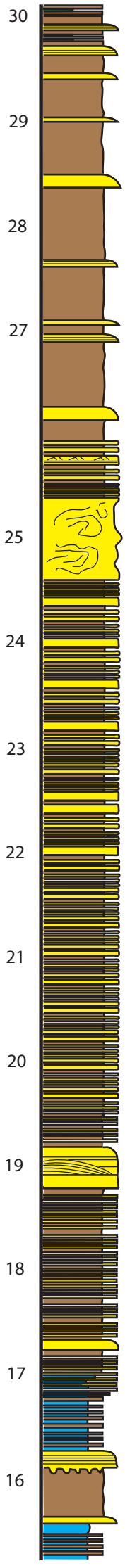

HS1-19,43m

HS1-19m

Some of the FS layers has some lamination in bottom.

Small scale hcs

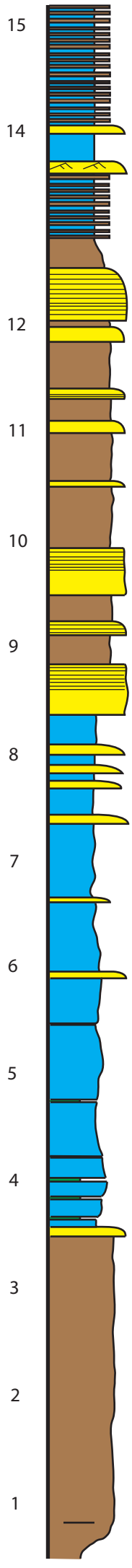

Brown clasts. Rip up clasts?

HS1-3,30m

HS1-2m

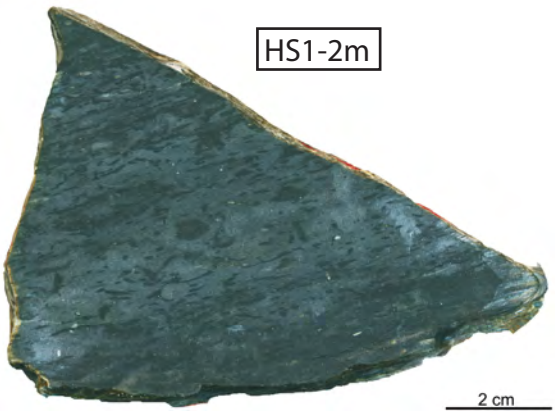

HS1-1m

Slab scans, Rambergøya

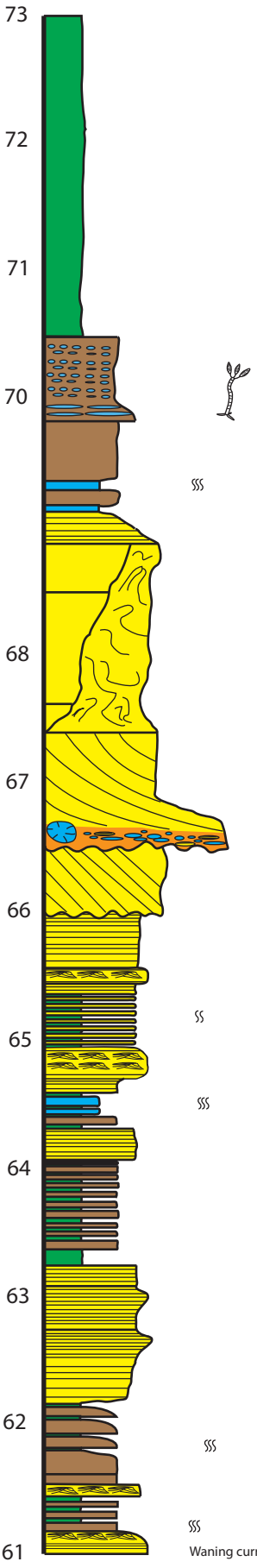

RS1-71,25m

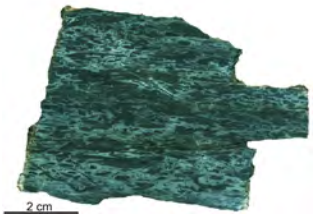

RS1-69,9m

RS1-69,8m

RS1- 69m

RS1-65,5m

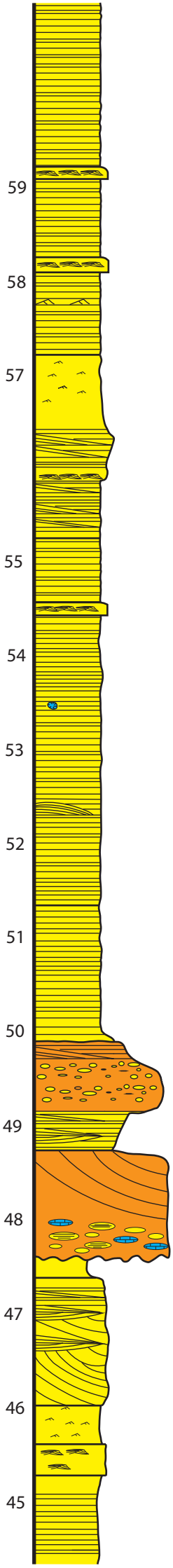

CR: 56 NE

CR: 56 NE
wavelength 3cm
Symmetrical ripples: trend 70v
Asymmetrical ripples: NE

wavelength 14cm

RS1-49,50m

RS1-47,6m

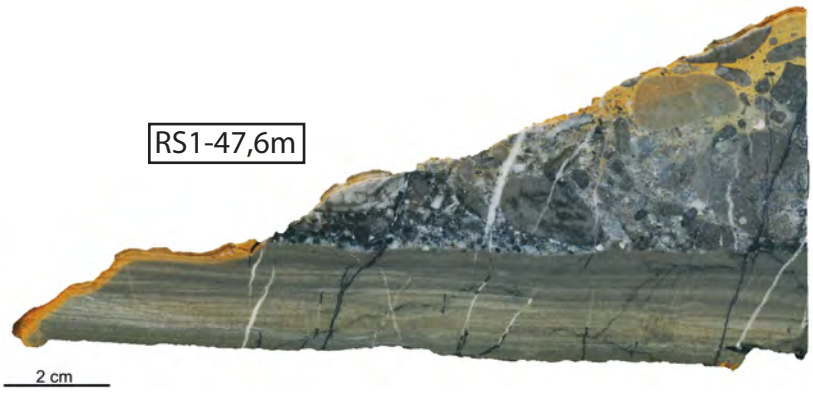

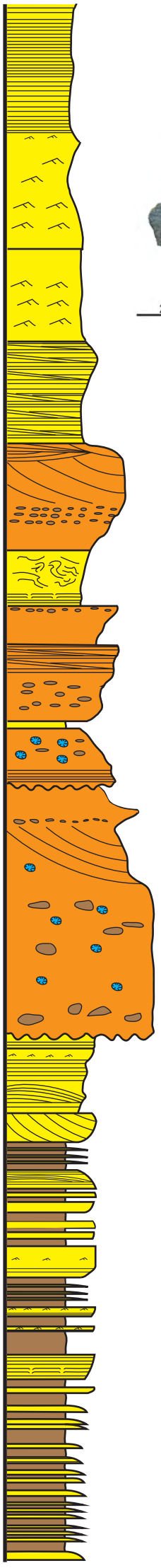

RS1-37,30m

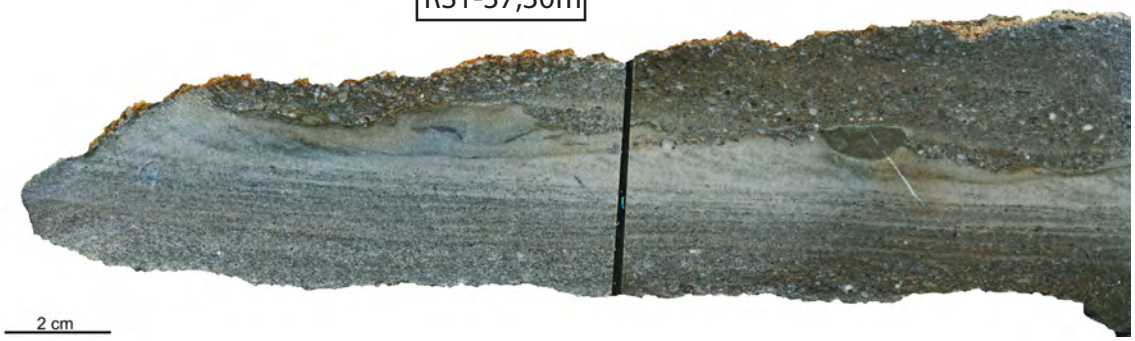

RS1-35,5m

Cut and fill

RS1-34,30m

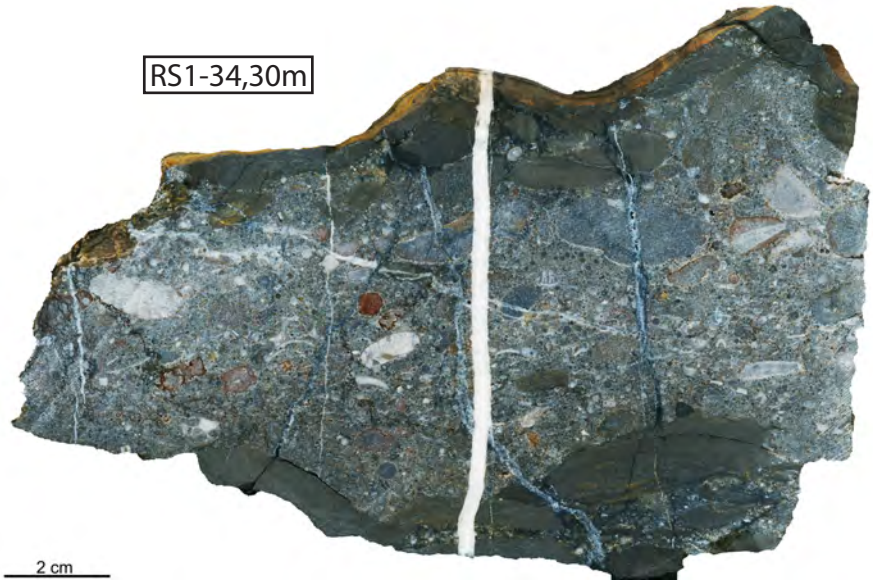

RS1-34,25m

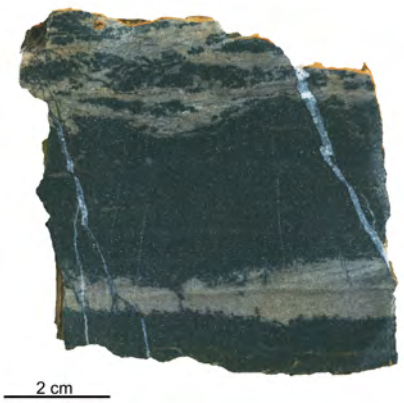

Asymmetrical ripples: 48 NE

Ripples in bottom of fine sandbedding.

Asymmetrical ripples: 48 NE

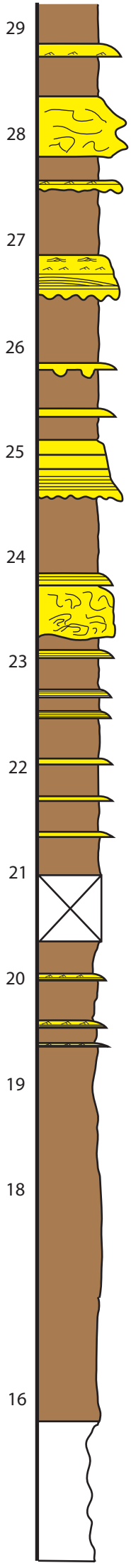

Symmetrical ripples: 230 trend
18 plunge

Amalgamated

Vertical burrows

Overturned ripples in top

Husberg/Langøyene fm.

The base of the brown weathered sandstone is diffuse.

RS1-18,75m

RS1-17m

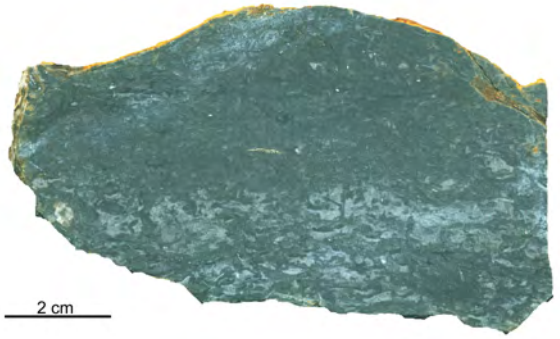

RS1-16,20m

Slab scans, Langøyene

LØS1-81m

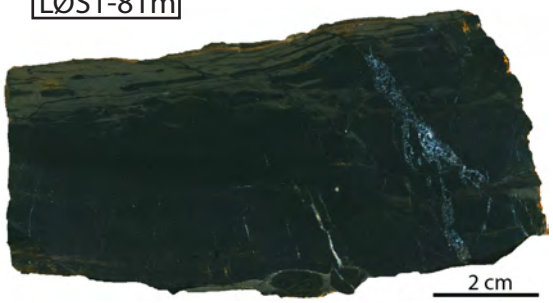

LØS1-79,9m

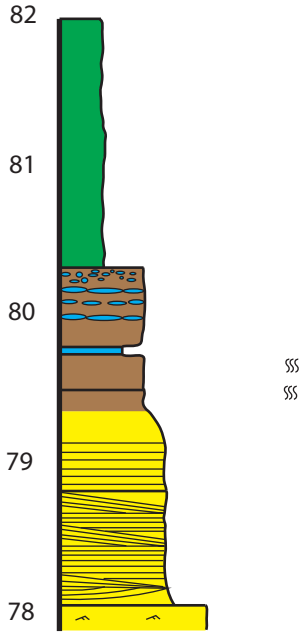

LØS1-79,8m

LØS1-79,5m

LØS1-77,9m

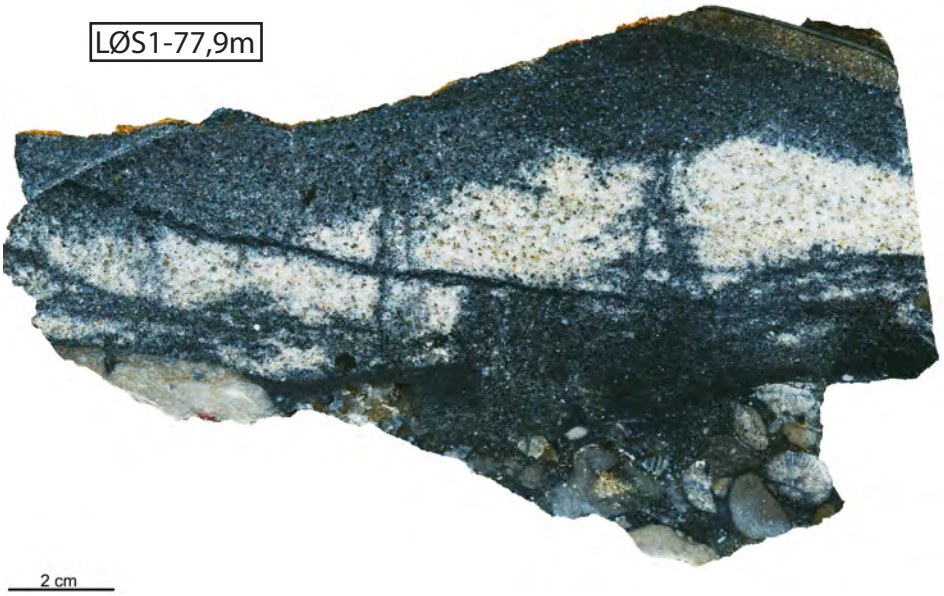

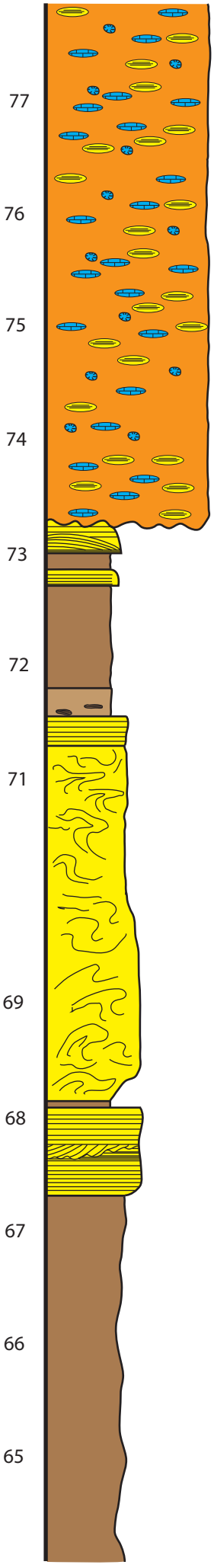

Light brown Sandstone: w/lam. clasts.

LØS1-74,7m

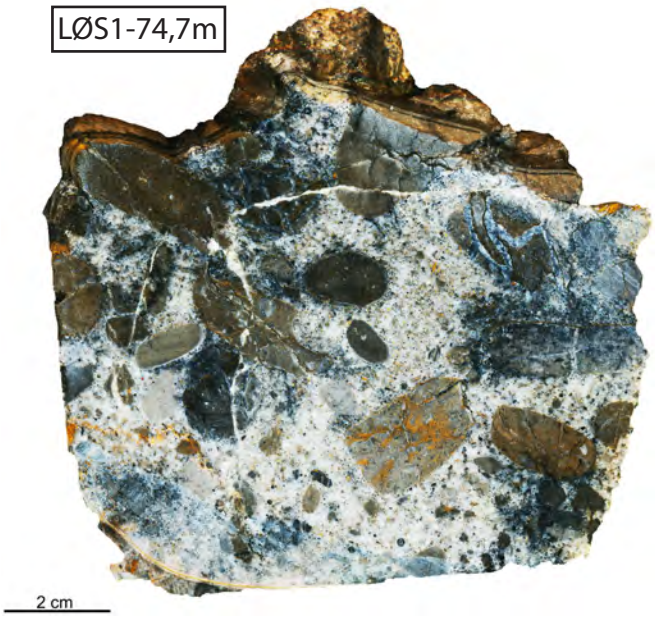

LØS1-73,3m

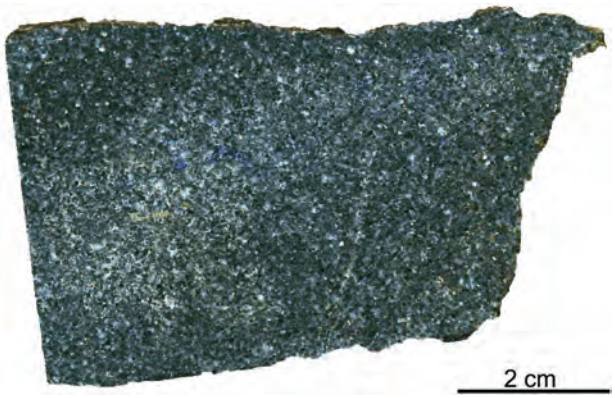

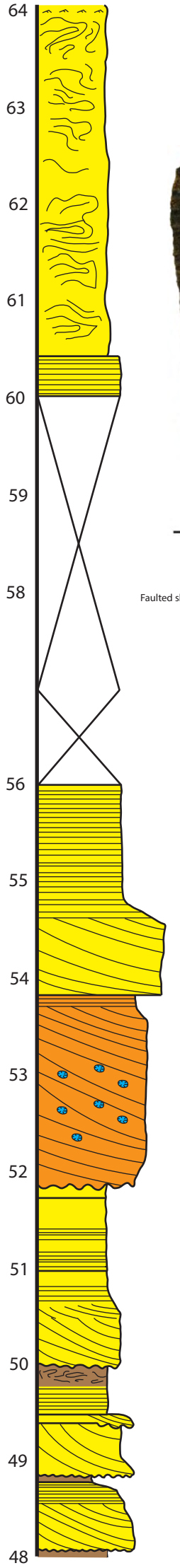

LØS1-55,9m

Faulted sliding plane of 4,20m

LØS1-53m

LØS1-51,9m

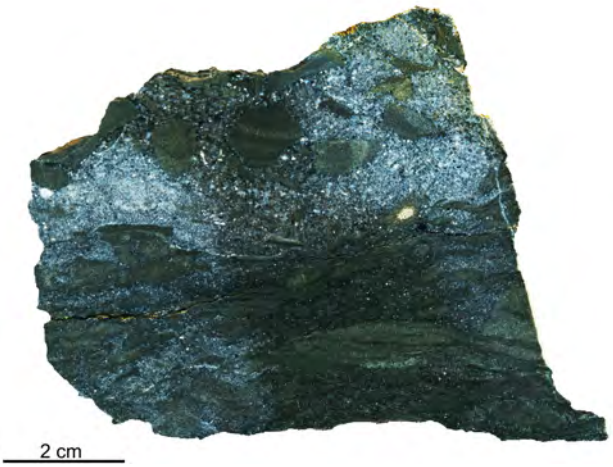

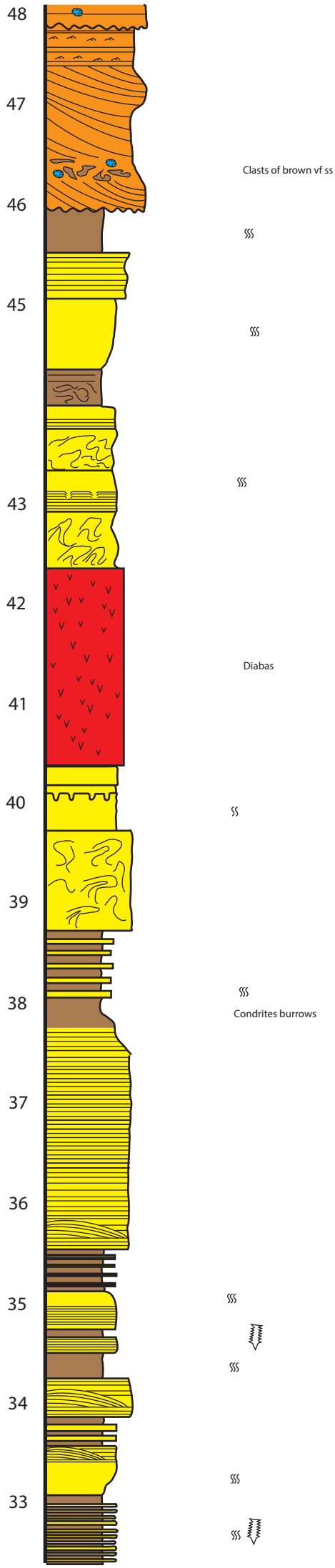
48
47
46
45
43
42
41
40
39
38
37
36
35
34
33
Clasts of brown vf ss
Diabas
Condrites burrows

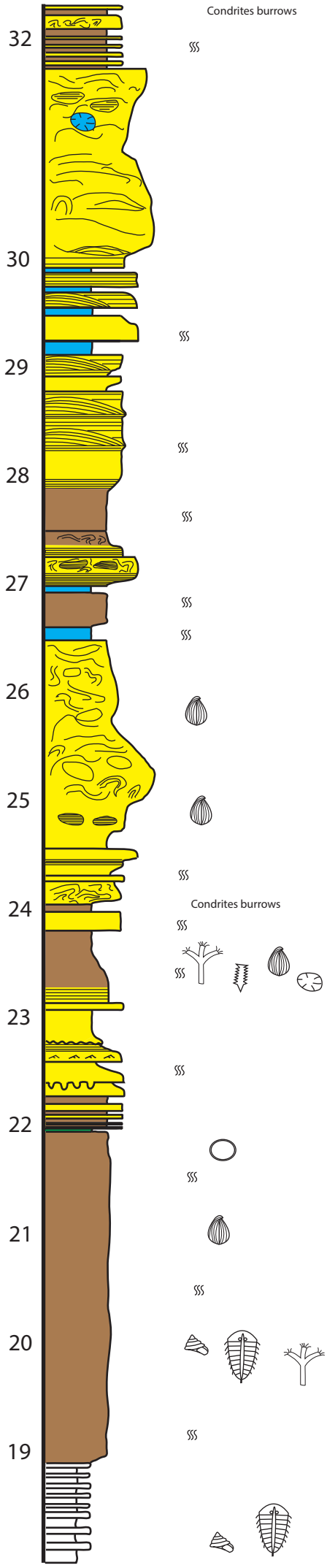

LØS1-22m

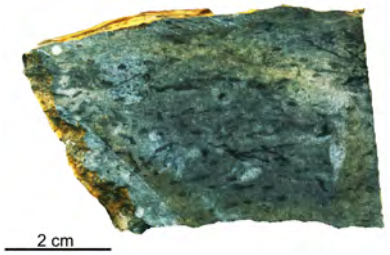

LØS1-20,4m

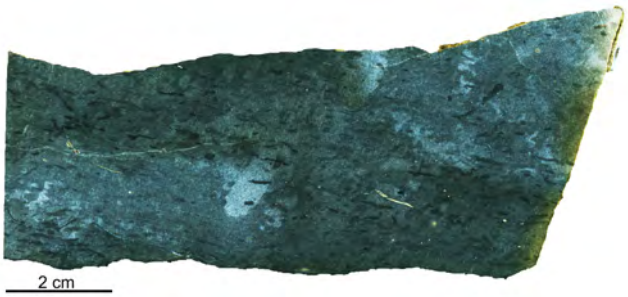

LØS1-19m

Appendix C

LOCALITY Hovedøya Section 1 SHEET 8 OF 8 DATE: 12/07.14 SCALE: 1:25

m | LITH | mm (Φ) 0.0625 (4) | 0.125 (3) | 0.25 (2) | 0.5 (1) | 1 (0) | 2 (-1) | 4 (-2) | 16 (-4) | 64 (-6) | CLAY | SILT | SAND: VF F M C VC | G | PEB.

GEOLOGIST: Martin Sandbakken
FORMATION: Langøyene/ Solvik
AGE: Upper Ordovician/ Lower Silurian

50
49
48
47
46

HS1-48,75m

HS1-48m

HS1-47,9m

HS1-47,5m

HS1-46,9m

HS1-46m

layers are laminated

CLAY SILT VF F M C VC G PEB.

LOCALITY Hovedøya Section 1 SHEET 7 OF 8 DATE: 12/07.14 SCALE: 1:25

m | LITH | mm / ϕ | 0.0625 (4) | 0.125 (3) | 0.25 (2) | 0.5 (1) | 1 (0) | 2 (-1) | 4 (-2) | 16 (-4) | 64 (-6)
CLAY | SILT | SAND: VF F M C VC | G | PEB.

GEOLOGIST: Martin Sandbakken
FORMATION: Langøyene
AGE: Upper Ordovician

45
44
43
43
41
40

Fine sand layers are laminated

CLAY SILT VF F M C VC G PEB.

LOCALITY Hovedøya Section 1 SHEET 6 OF 8 DATE:12/07.14 SCALE: 1:25

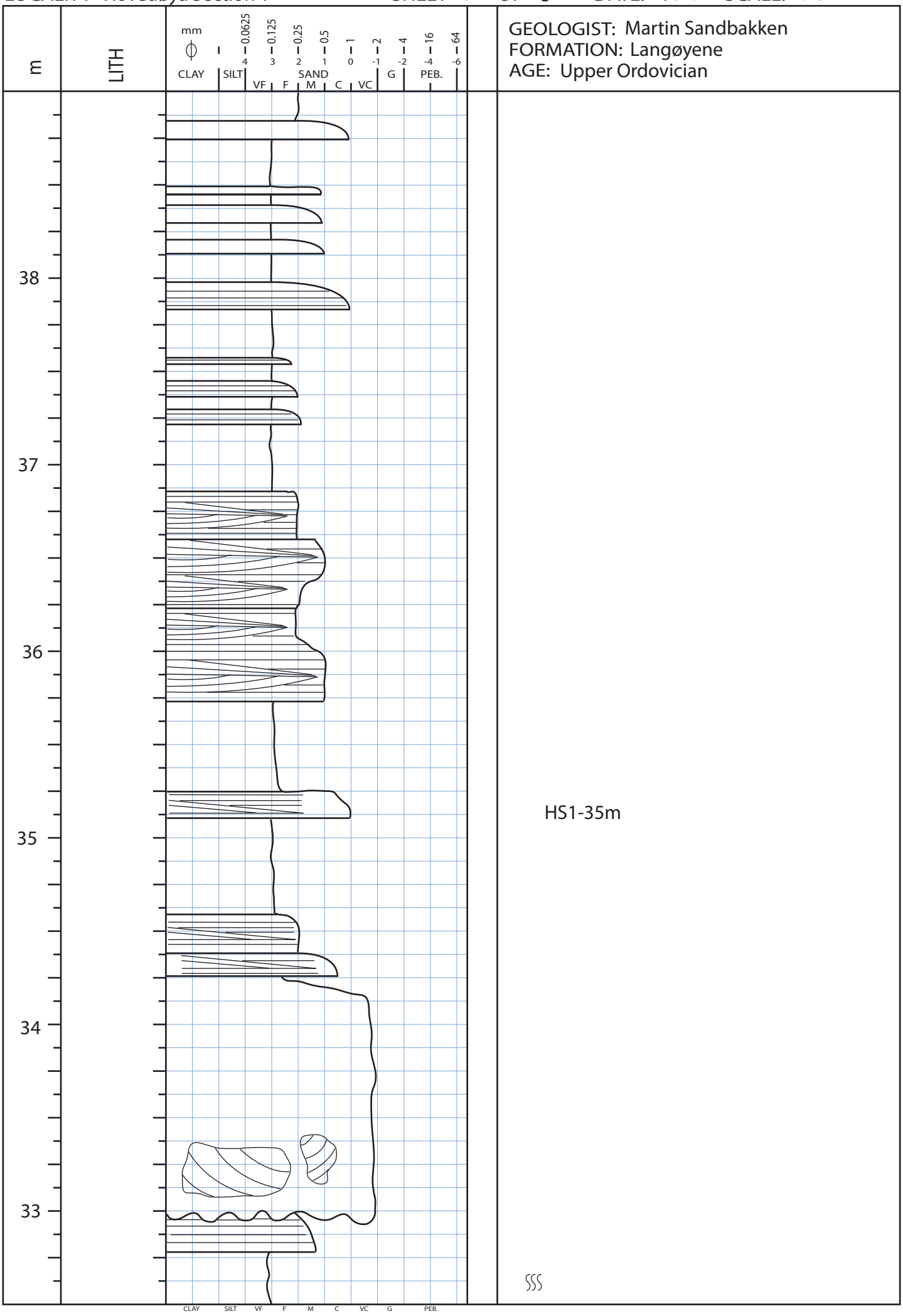

LOCALITY Hovedøya Section 1 SHEET 5 OF 8 DATE: 12/07.14 SCALE: 1:25

m | LITH | mm (φ) 0.0625 (4) 0.125 (3) 0.25 (2) 0.5 (1) 1 (0) 2 (-1) 4 (-2) 16 (-4) 64 (-6) | CLAY SILT VF F M C VC G PEB. SAND

GEOLOGIST: Martin Sandbakken
FORMATION: Langøyene
AGE: Upper Ordovician

32
31
30
29
28
27

Some layers are discontinous, looks like nodules.

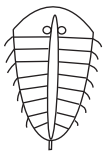

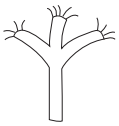

HS1-30,5m

SSS

SSS

CLAY SILT VF F M C VC G PEB.

LOCALITY Hovedøya Section 1 SHEET 4 OF 8 DATE: 02/07.14 SCALE: 1:25

GEOLOGIST: Martin Sandbakken
FORMATION: Langøyene
AGE: Upper Ordovician

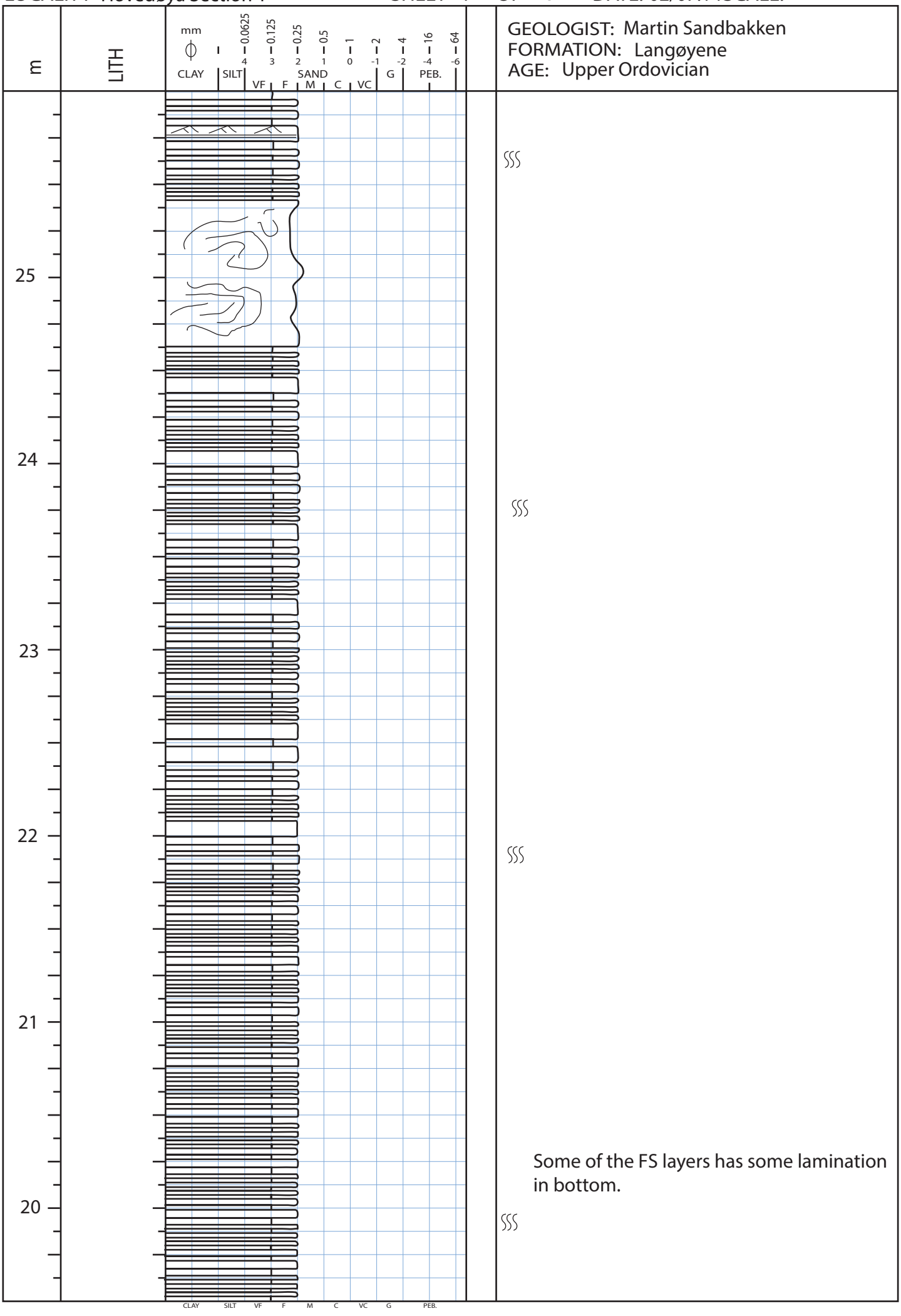

Some of the FS layers has some lamination in bottom.

LOCALITY Hovedøya Section 1 SHEET 3 OF 8 DATE: 02/07.14 SCALE: 1:25

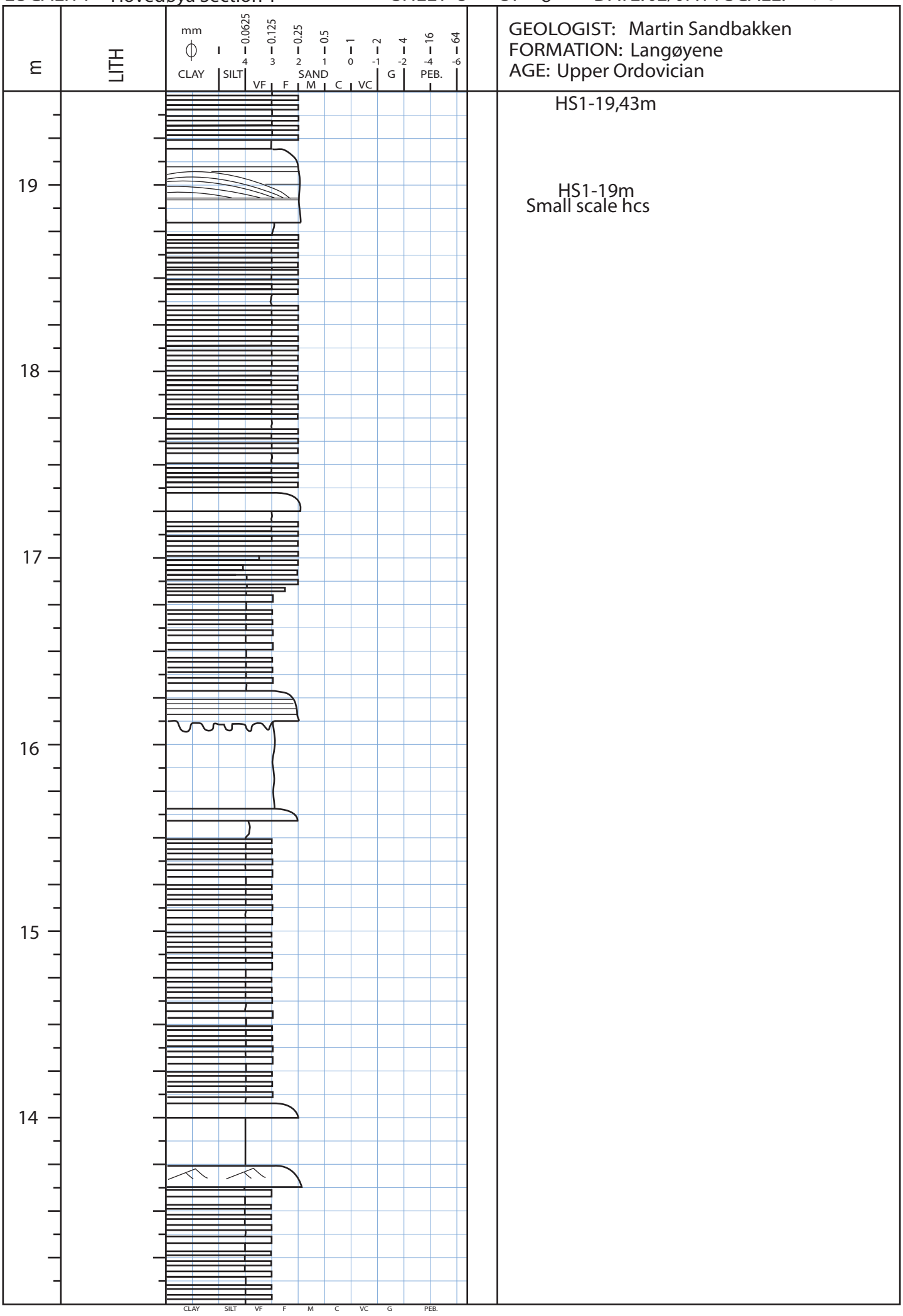

LOCALITY Hovedøya Section 1 SHEET 2 OF 8 DATE: 02/07.14SCALE: 1:25

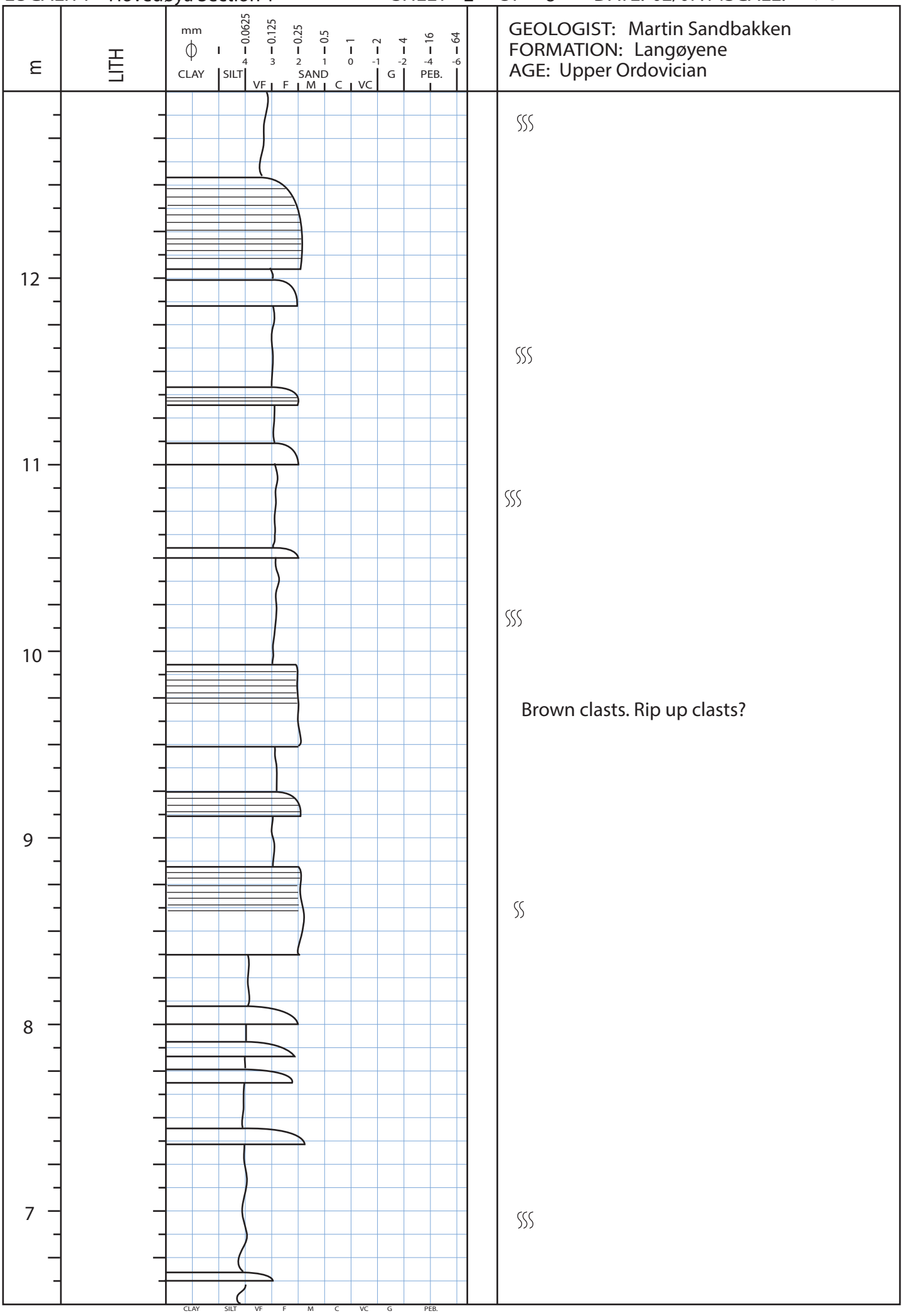

LOCALITY Hovedøya Section 1 SHEET 1 OF 8 DATE: 02/07.14SCALE: 1:25

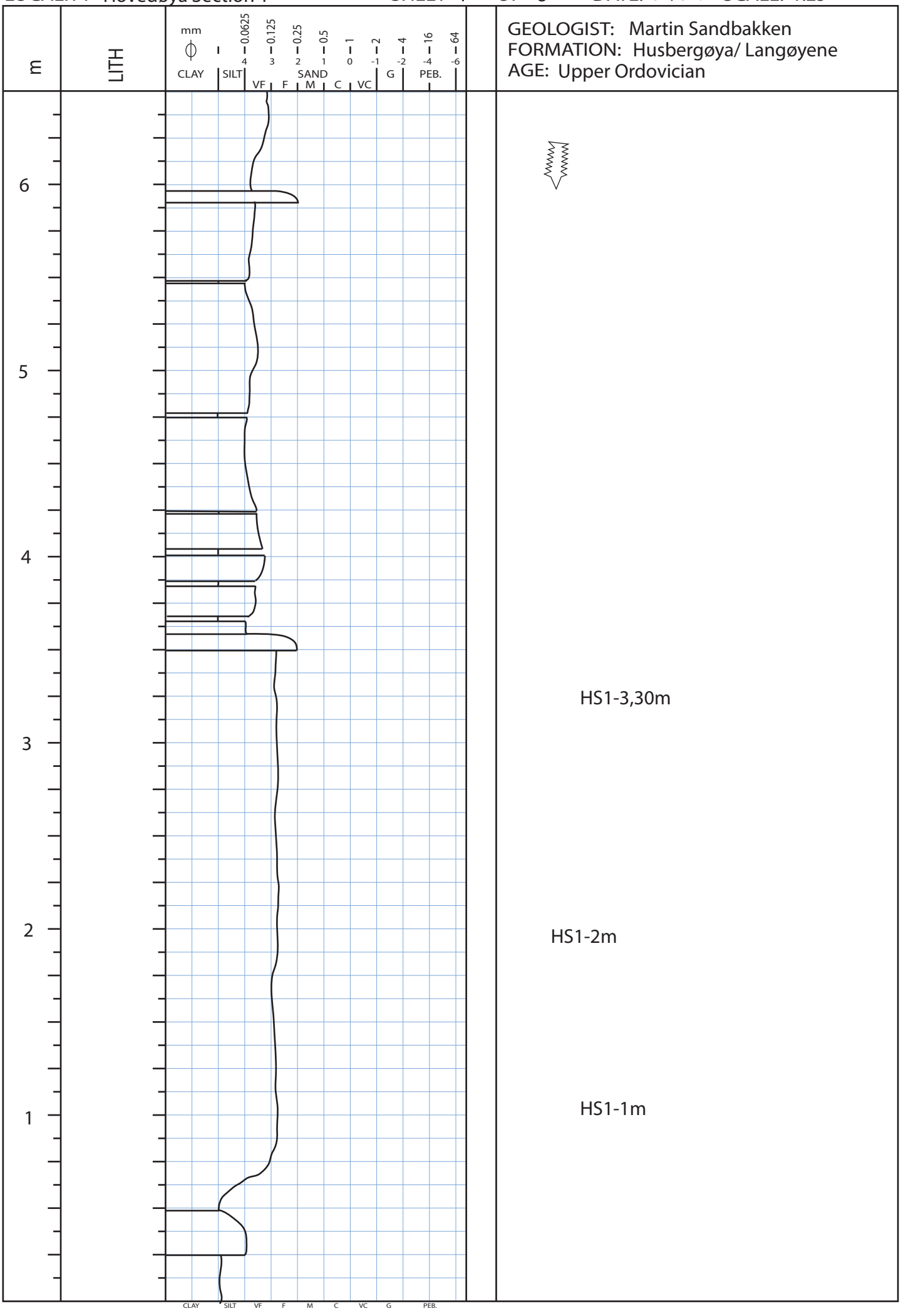

LOCALITY Rambergøya Section 1 SHEET 8 OF 8 DATE:17/06.14 SCALE: 1:25

GEOLOGIST: Martin Sandbakken
FORMATION: Langøyene/Solvik
AGE: Upper Ordovician/ Lower Silurian

m

LITH

mm
0.0625 0.125 0.25 0.5 1 2 4 16 64
4 3 2 1 0 -1 -2 -4 -6
CLAY SILT VF F M C VC G PEB.
SAND

73
72
71
70

RS1-71,25m

RS1-69,9m

RS1-69,8m

CLAY SILT VF F M C VC G PEB.

LOCALITY Rambergøya Section 1 SHEET 7 OF 8 DATE: 17/06.14 SCALE: 1:25

m | LITH | mm ϕ | 0.0625 4 | 0.125 3 | 0.25 2 | 0.5 1 | 1 0 | 2 -1 | 4 -2 | 16 -4 | 64 -6 | CLAY | SILT | VF | F | M | C | VC | G | PEB. | SAND

GEOLOGIST: Martin Sandbakken
FORMATION: Langøyene
AGE: Upper Ordovician

RS1- 69m

68

67

honeycomb coral facing down

66

RS1-65,5m

65

64

63

CLAY SILT VF F M C VC G PEB.

LOCALITY Rambergøya Section 1 SHEET 6 OF 8 DATE: 17/06.14 SCALE: 1:25

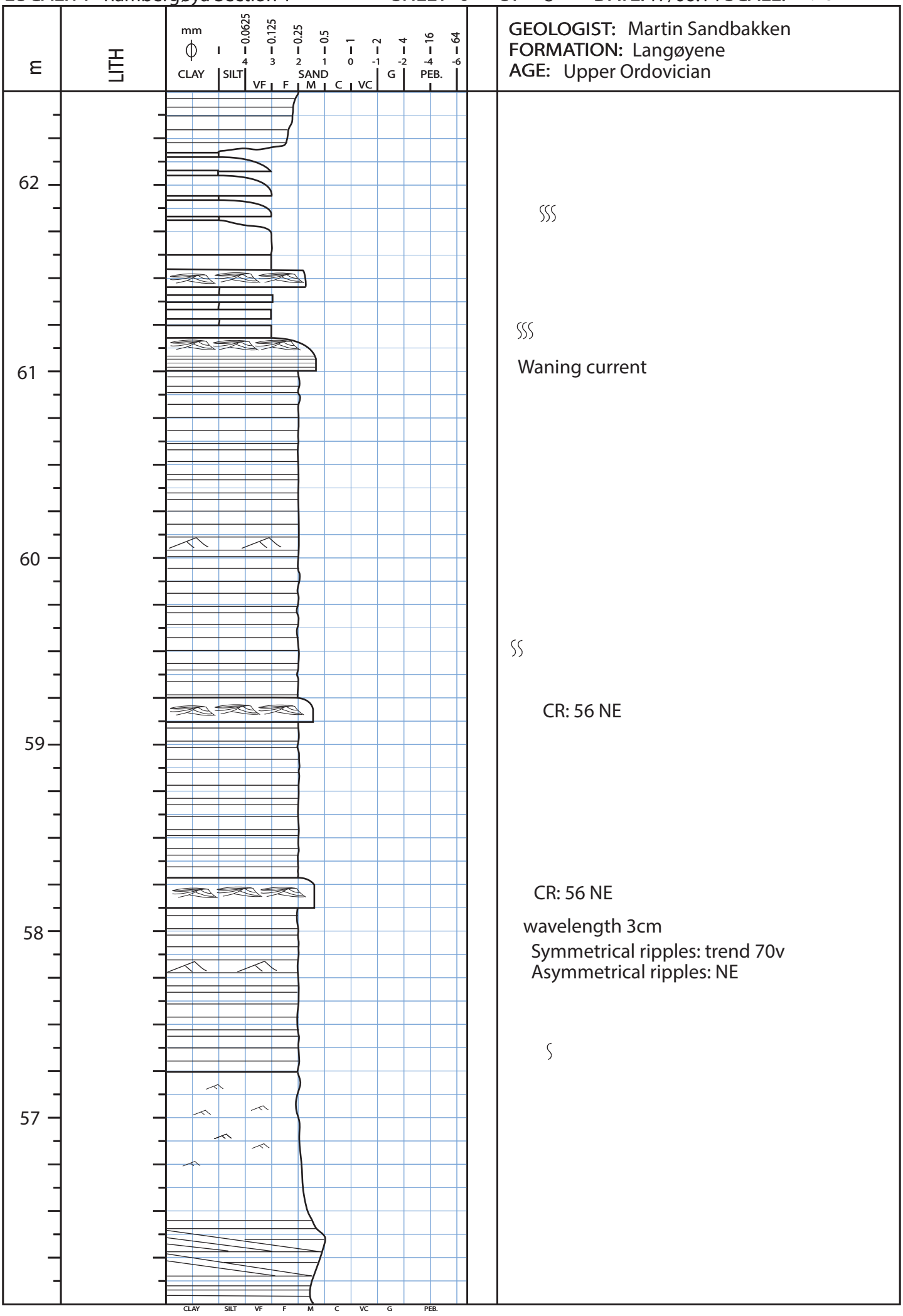

LOCALITY Rambergøya Section 1 SHEET 5 OF 8 DATE:17/06.14 SCALE: 1:25

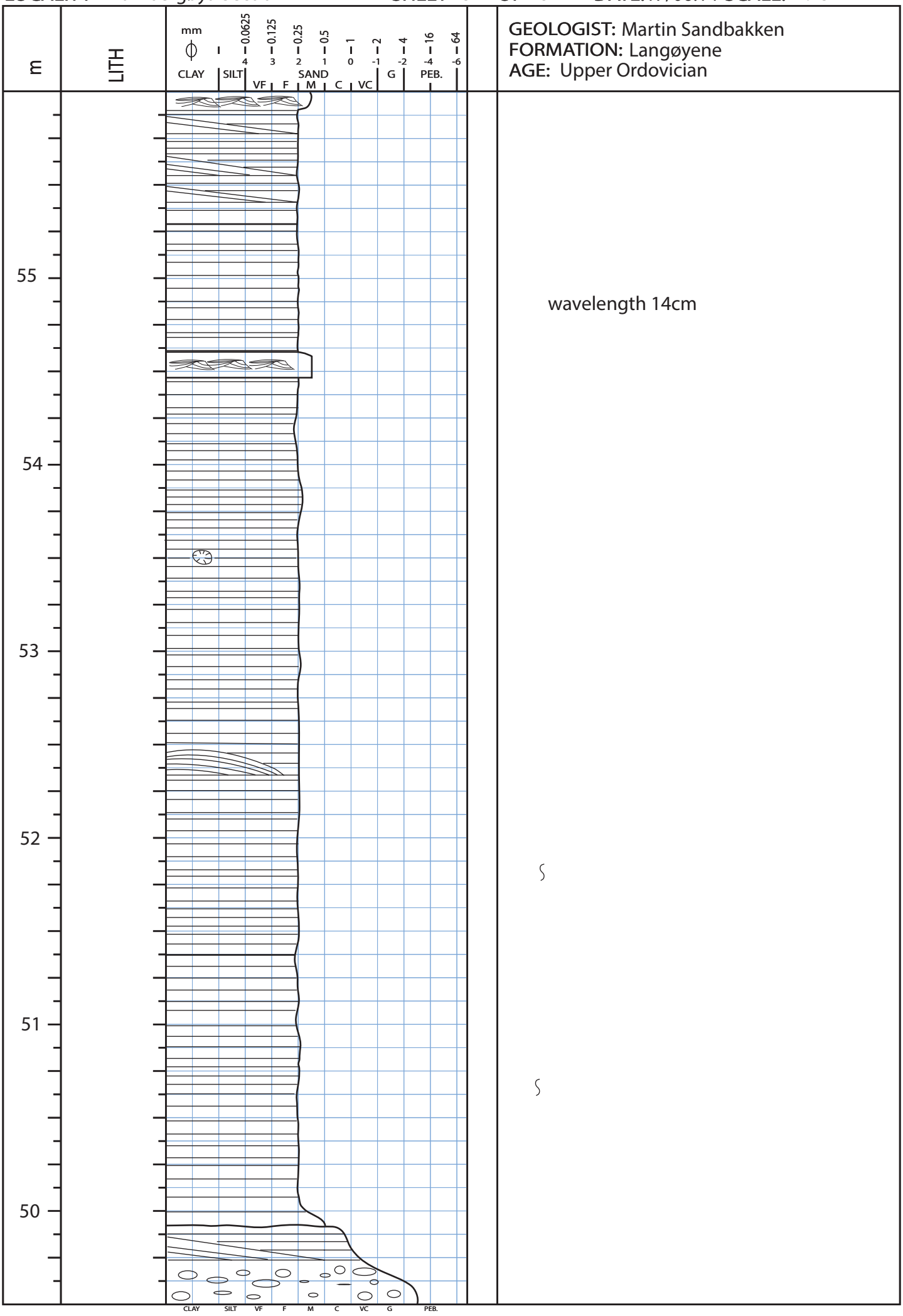

GEOLOGIST: Martin Sandbakken
FORMATION: Langøyene
AGE: Upper Ordovician

wavelength 14cm

LOCALITY Rambergøya Section 1 SHEET 4 OF 8 DATE:17/06.14 SCALE: 1:25

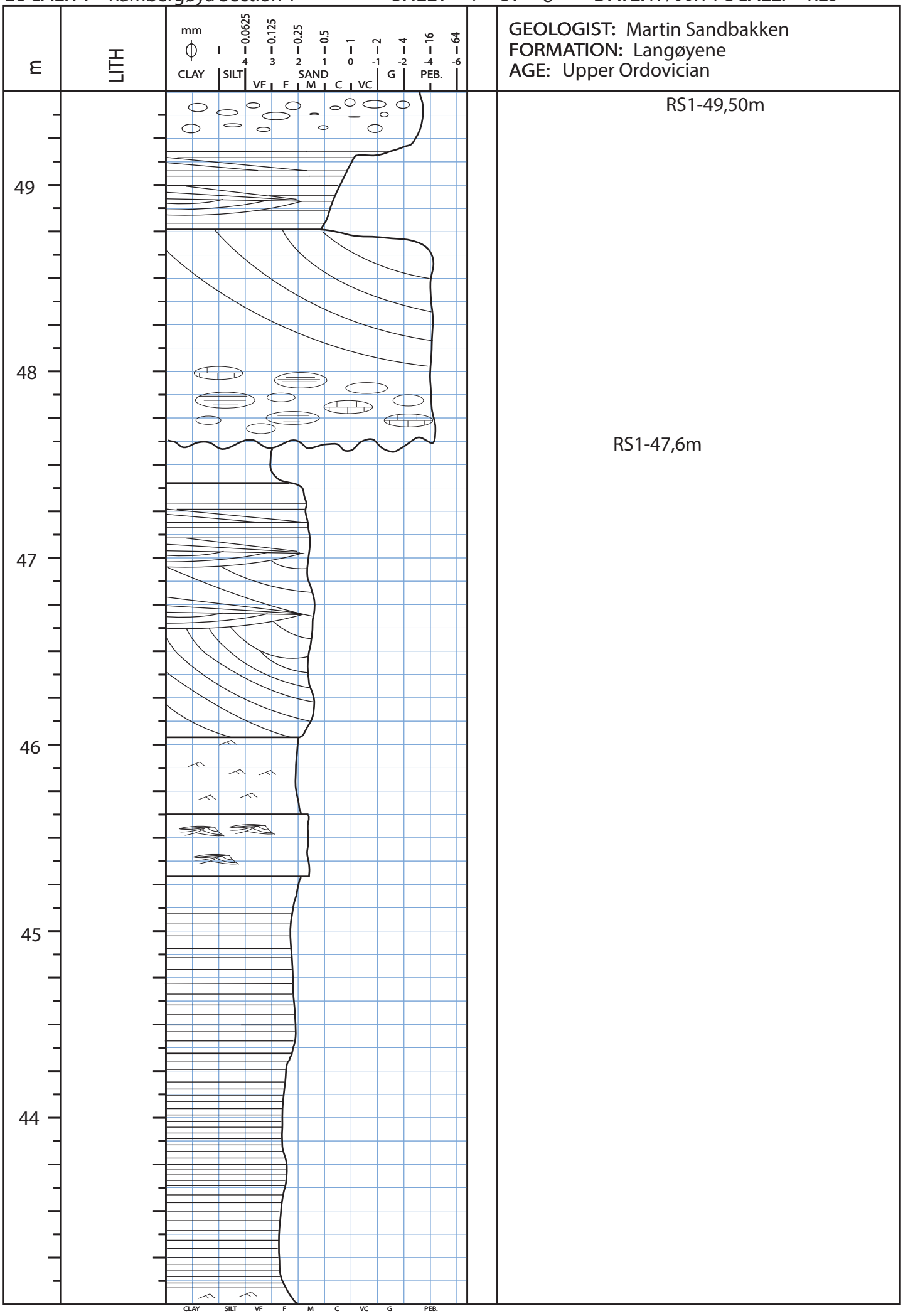

LOCALITY Rambergøya Section 1 SHEET 3 OF 8 DATE: 21/05.14 SCALE: 1:25

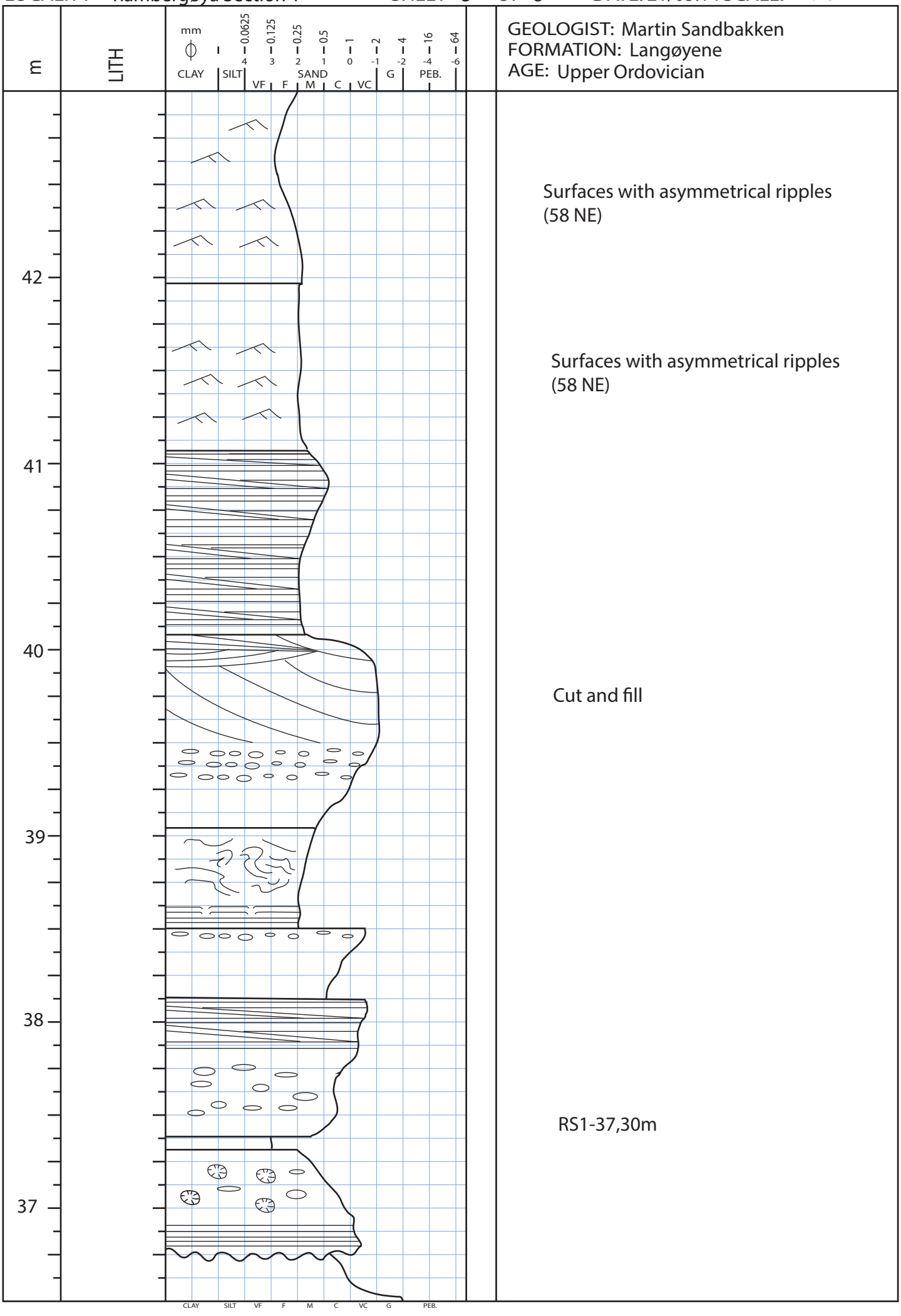

GEOLOGIST: Martin Sandbakken
FORMATION: Langøyene
AGE: Upper Ordovician

LOCALITY Ramberøya Section 1 SHEET 2 OF 8 DATE: 21/08.14 SCALE: 1:25

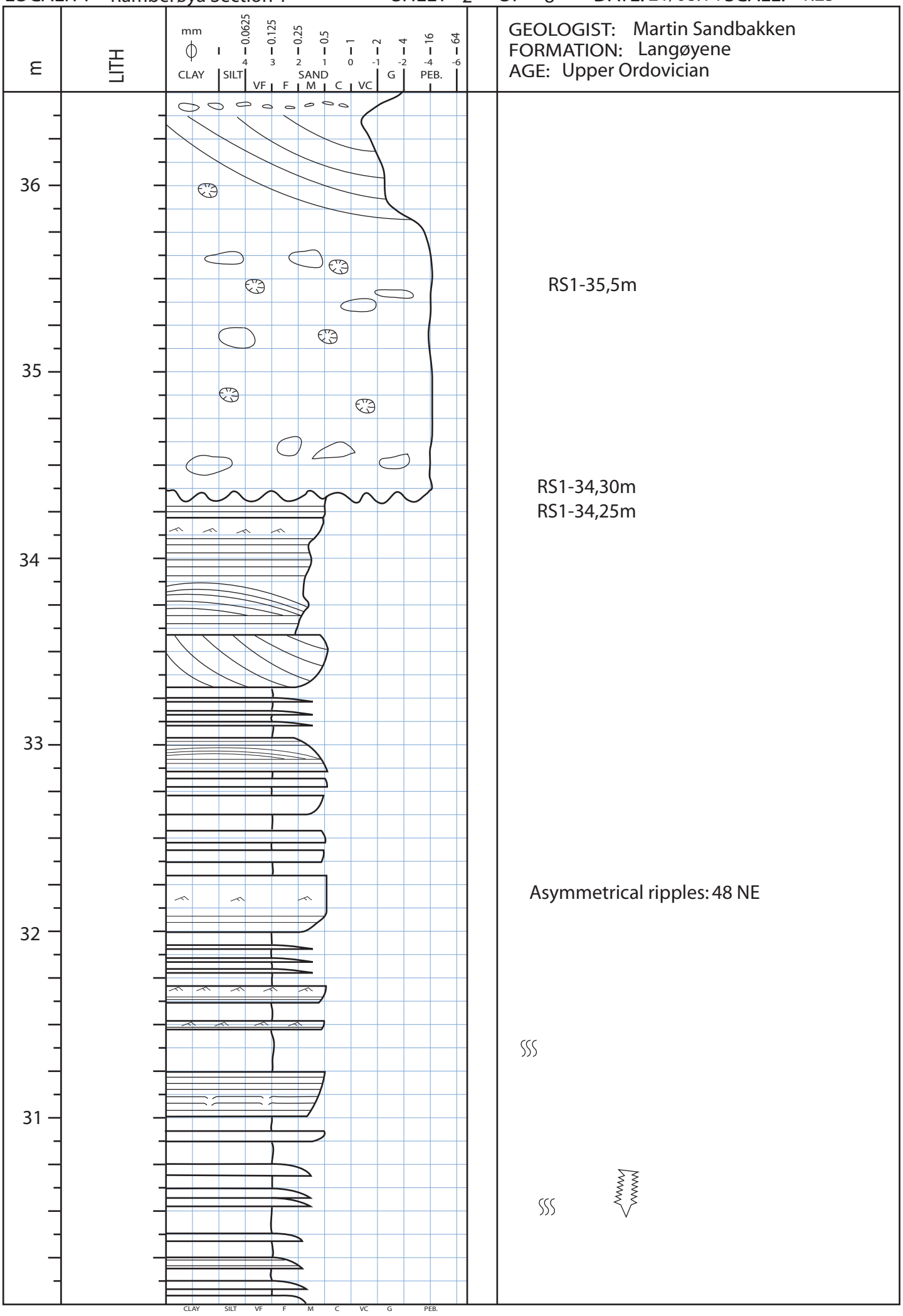

LOCALITY Rambergøya Section 1 SHEET 1 OF 8 DATE: 21/05.14 SCALE: 1:25

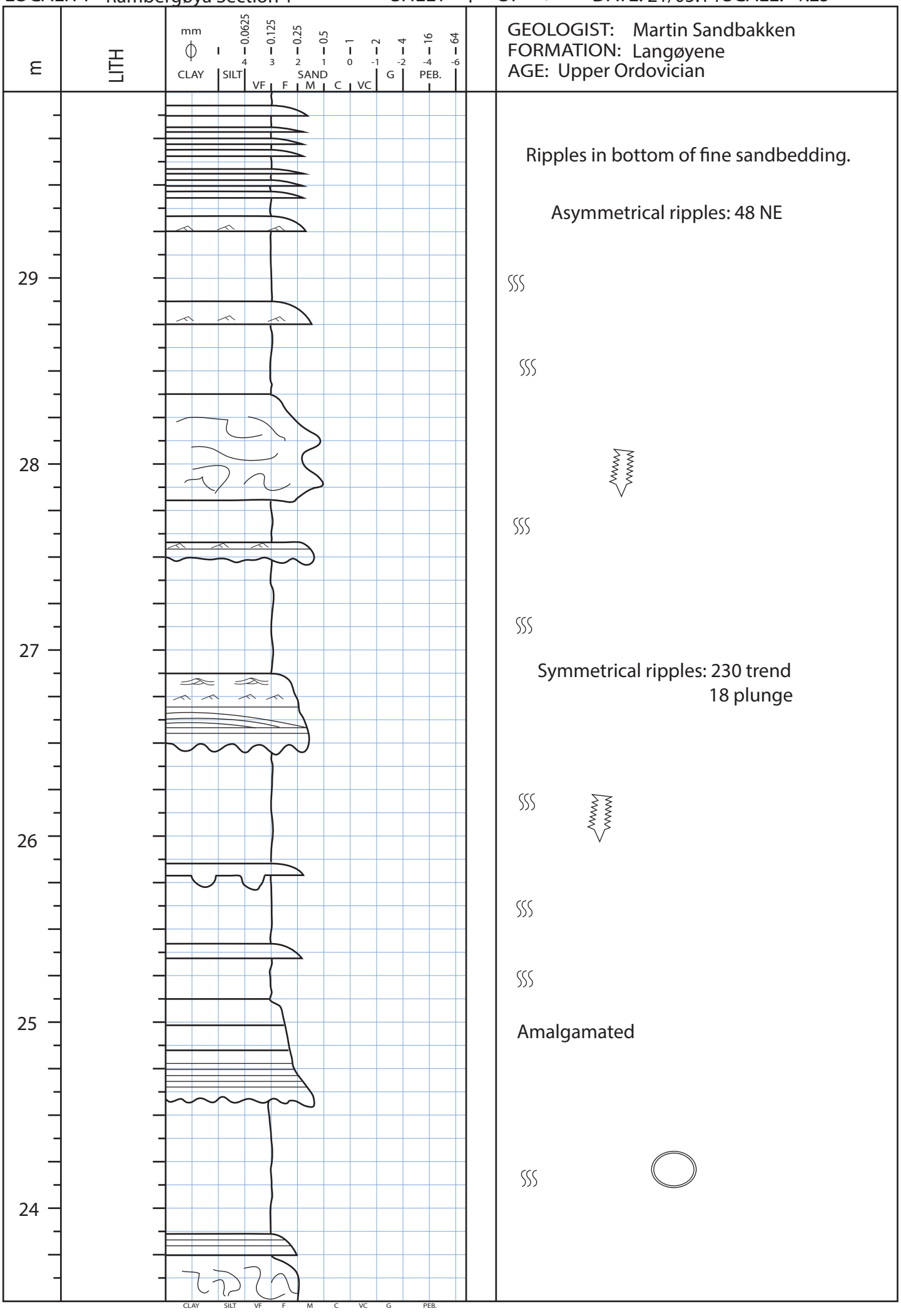

LOCALITY Rambergøya Section 1 SHEET -2 OF 8 DATE:18/06.14 SCALE: 1:25

m | LITH | mm (Φ): 0.0625 (4) | 0.125 (3) | 0.25 (2) | 0.5 (1) | 1 (0) | 2 (-1) | 4 (-2) | 16 (-4) | 64 (-6) | CLAY | SILT | SAND: VF F M C VC | G | PEB.

GEOLOGIST: Martin Sandbakken
FORMATION: Husbergøya/Langøyene
AGE: Upper Ordovician

16

RS1-17M

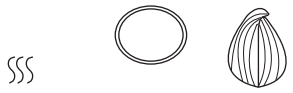

RS1-16,20m

The base of the brown weathered sandstone is diffuse.

CLAY SILT VF F M C VC G PEB.

LOCALITY Rambergøya Section 1 SHEET -1 OF 8 DATE: 18/06.14 SCALE: 1:25

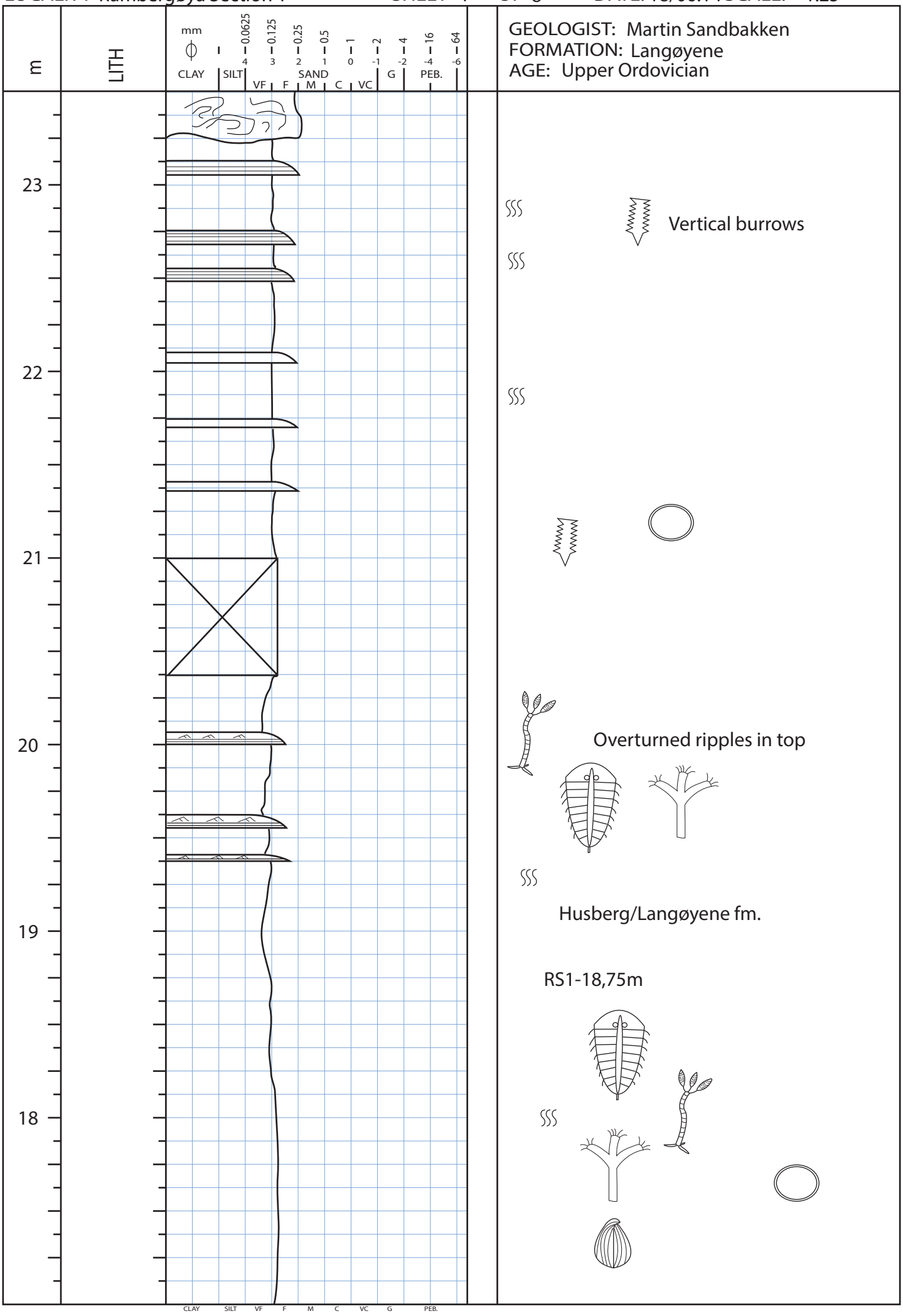

LOCALITY Langøyene Section 1 SHEET 10 OF 10 DATE: 26/06.14 SCALE: 1:25

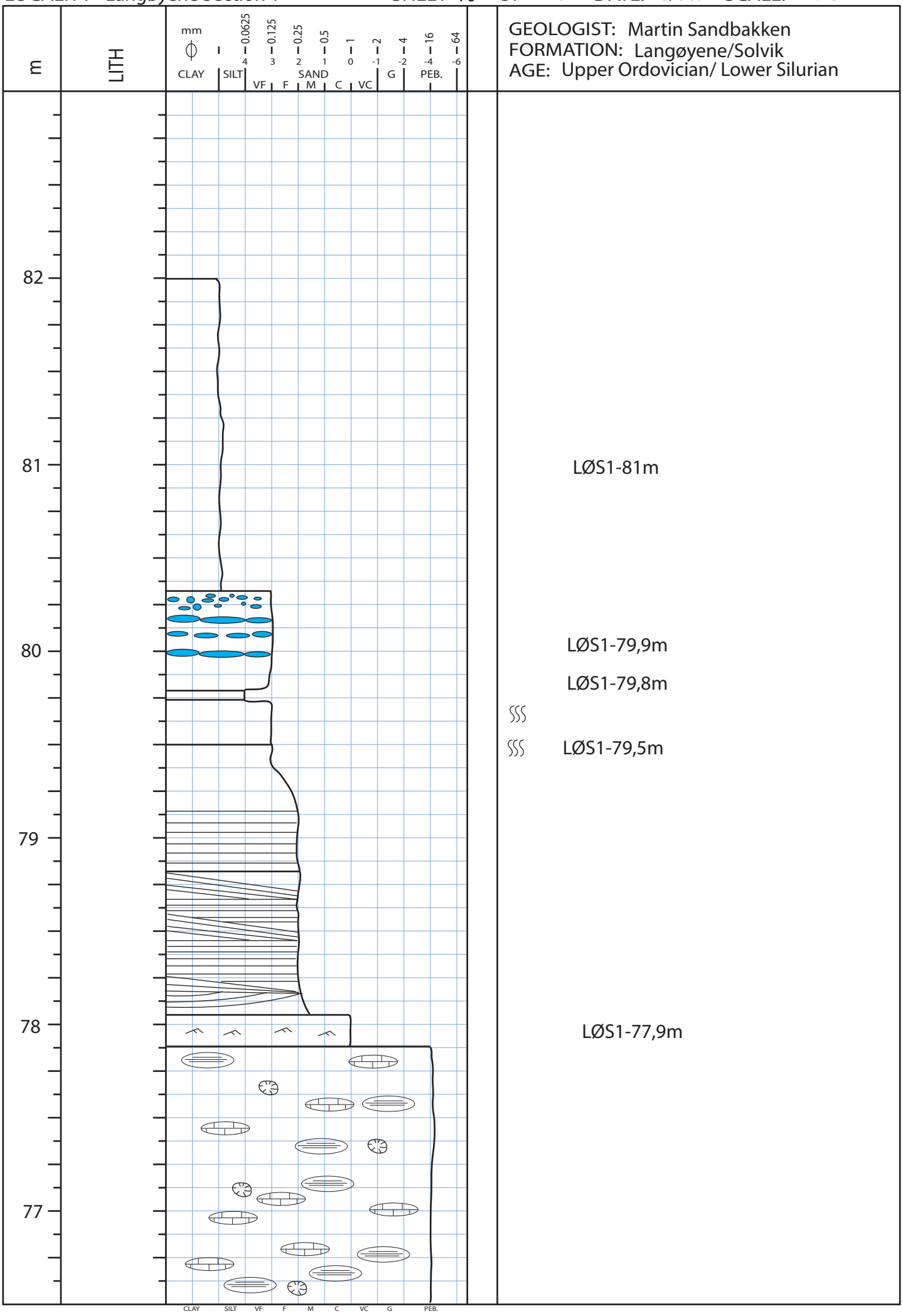

LOCALITY Langøyene Section 1 SHEET 9 OF 10 DATE: 26/06.14 SCALE: 1:25

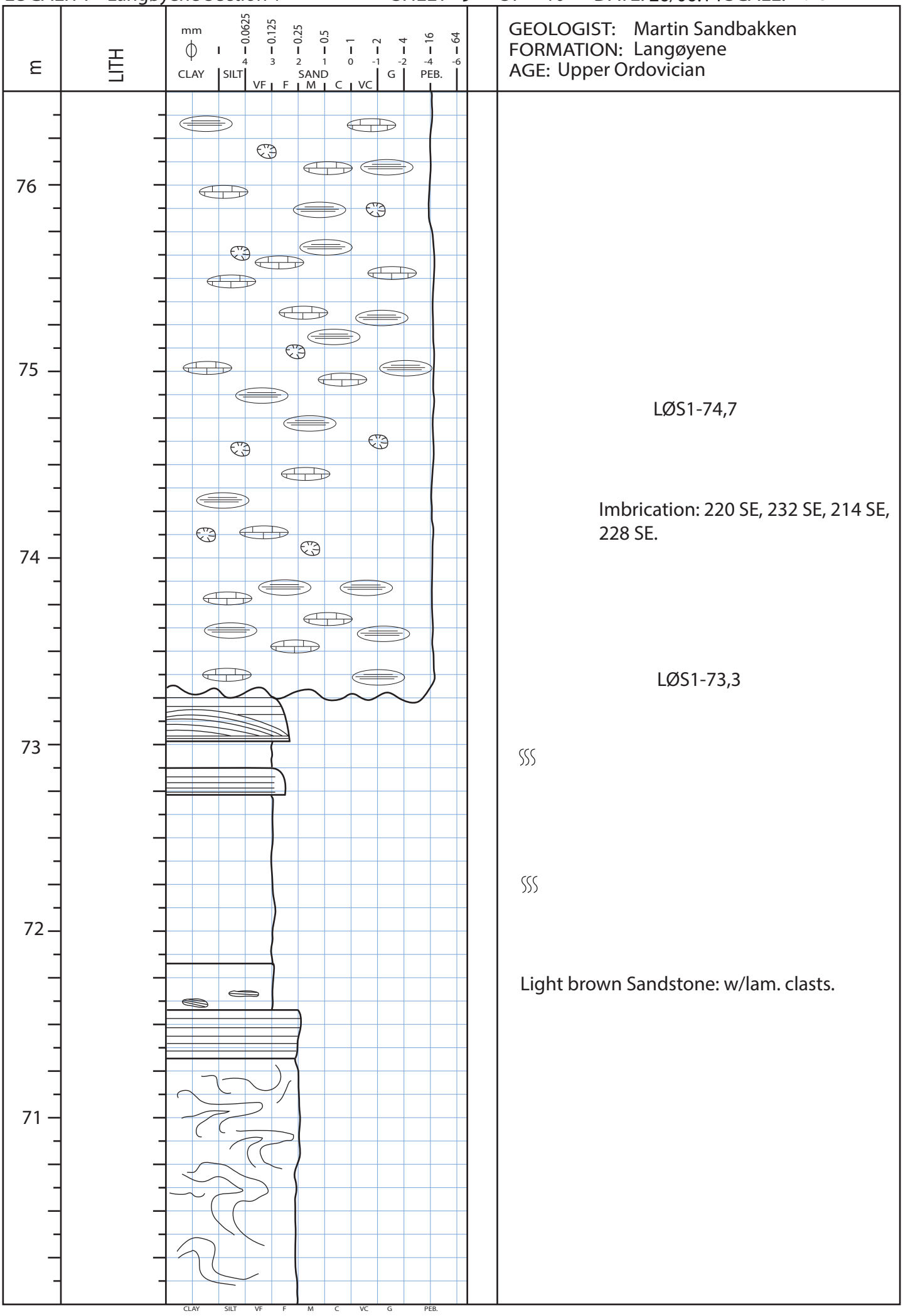

GEOLOGIST: Martin Sandbakken
FORMATION: Langøyene
AGE: Upper Ordovician

LØS1-74,7

Imbrication: 220 SE, 232 SE, 214 SE, 228 SE.

LØS1-73,3

Light brown Sandstone: w/lam. clasts.

LOCALITY Langøyene Section 1 SHEET 8 OF 10 DATE: 26/06.14 SCALE: 1:25

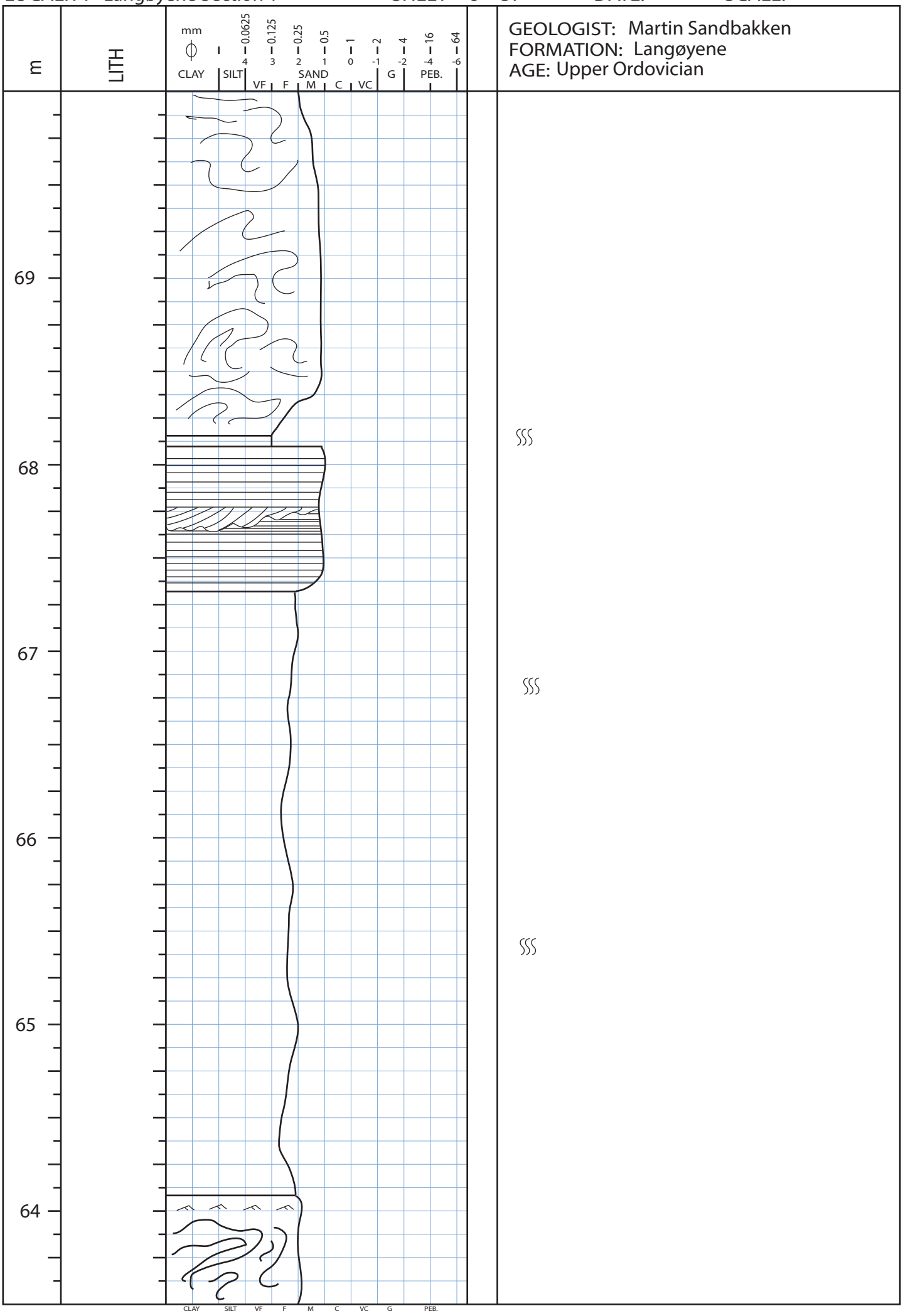

LOCALITY Langøyene Section 1 SHEET 7 OF 10 DATE: 26/06.14 SCALE: 1:25

GEOLOGIST: Martin Sandbakken
FORMATION: Langøyene
AGE: Upper Ordovician

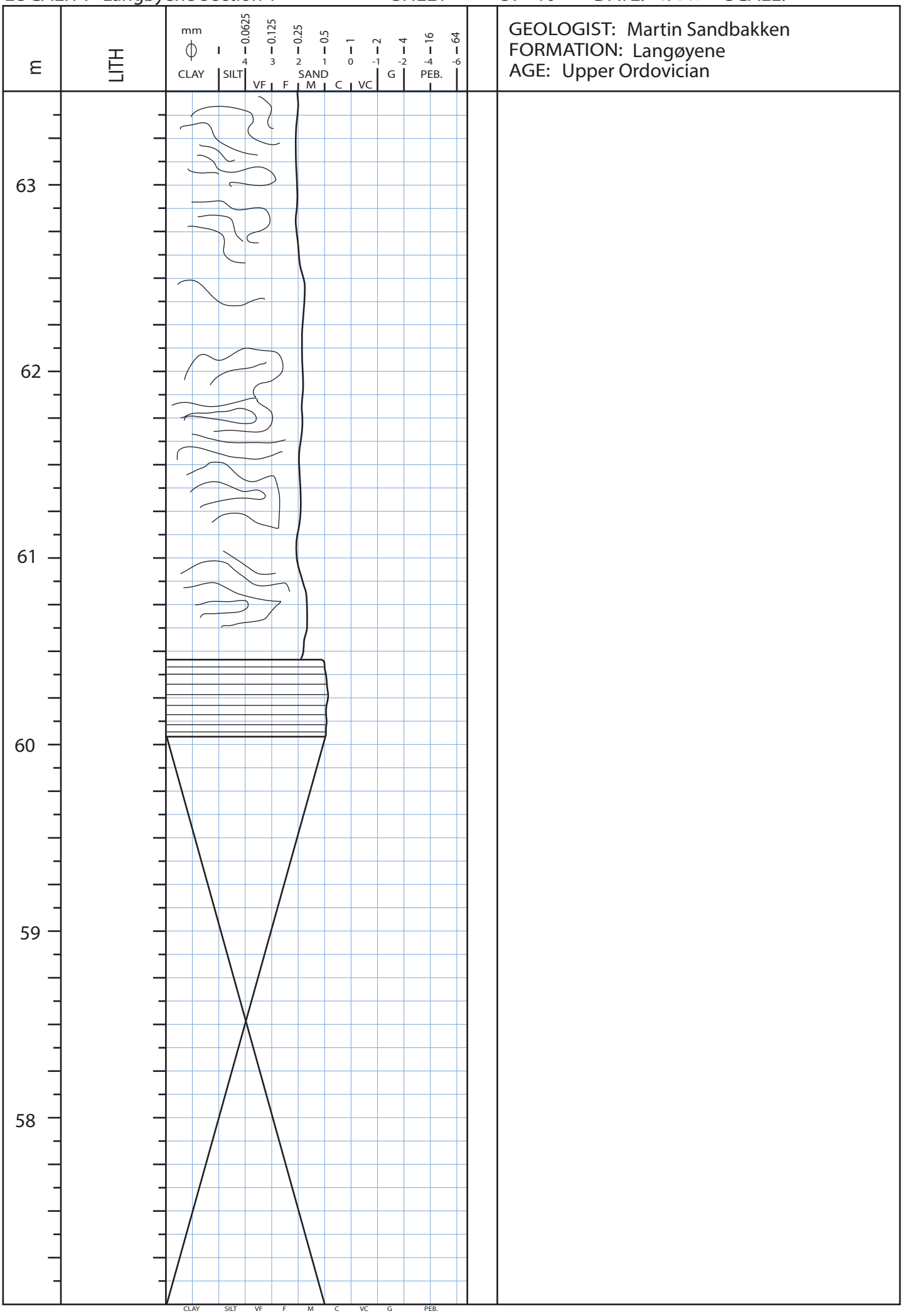

LOCALITY Langøyene Section 1 SHEET 6 OF 10 DATE: 26/06.14 SCALE: 1:25

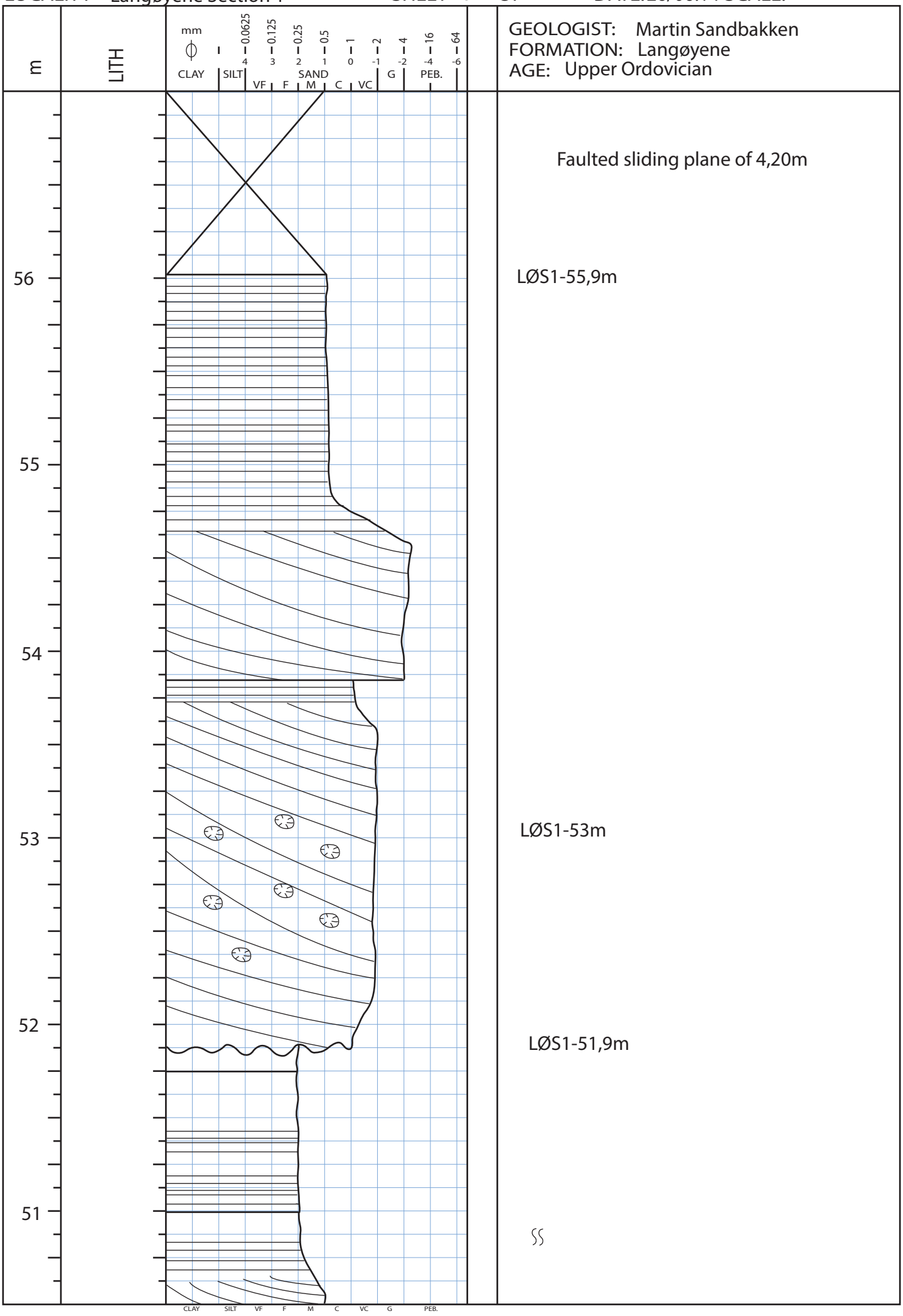

LOCALITY Langøyene Section 1 SHEET 5 OF 10 DATE: 25/06.14 SCALE: 1:25

GEOLOGIST: Martin Sandbakken
FORMATION: Langøyene
AGE: Upper Ordovician

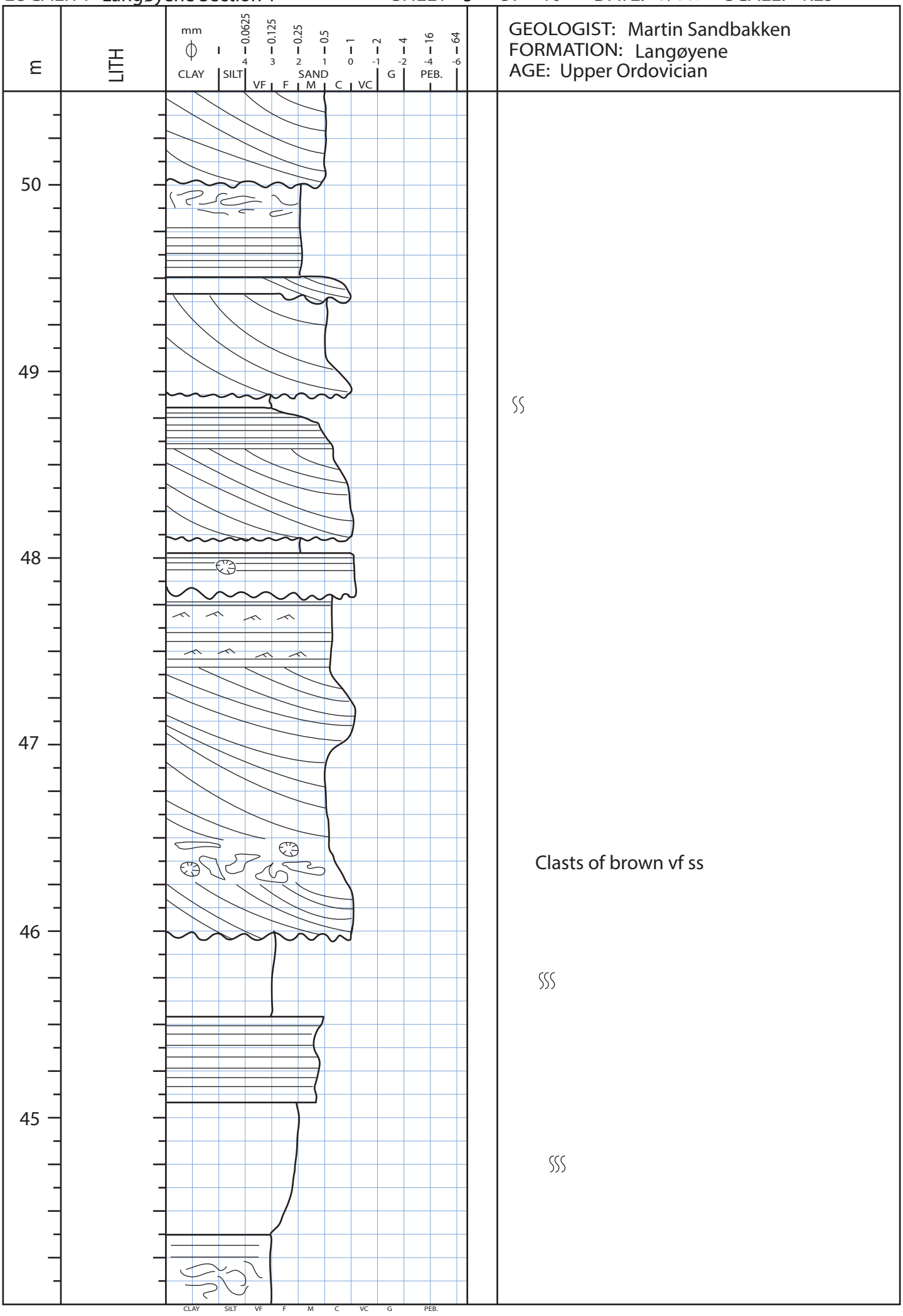

LOCALITY Langøyene Section 1 SHEET 4 OF 10 DATE: 20/06.14 SCALE: 1:25

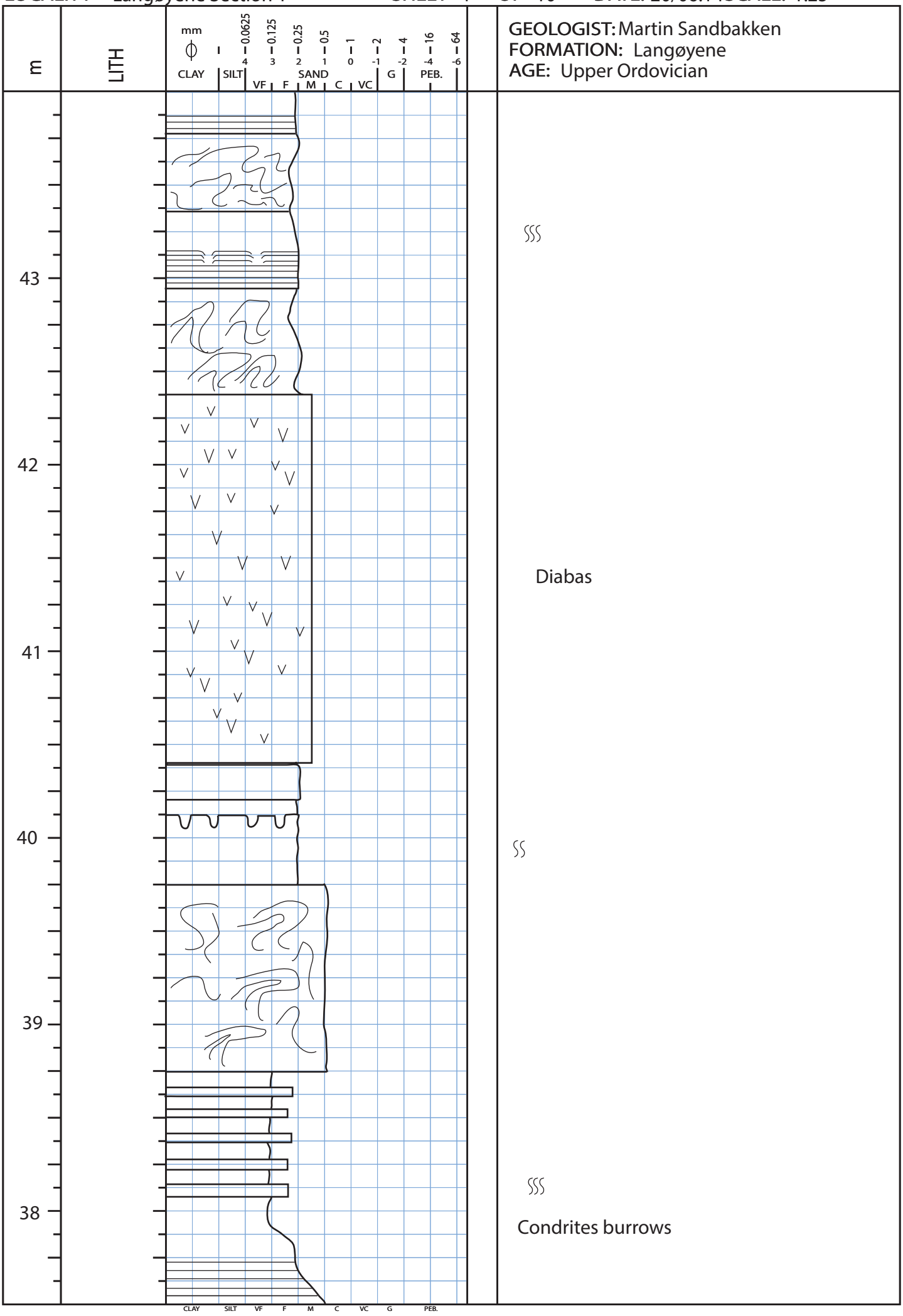

LOCALITY Langøyene Section 1 SHEET 3 OF 10 DATE: 20/06.14 SCALE: 1:25

GEOLOGIST: Martin Sandbakken
FORMATION: Langøyene
AGE: Upper Ordovician

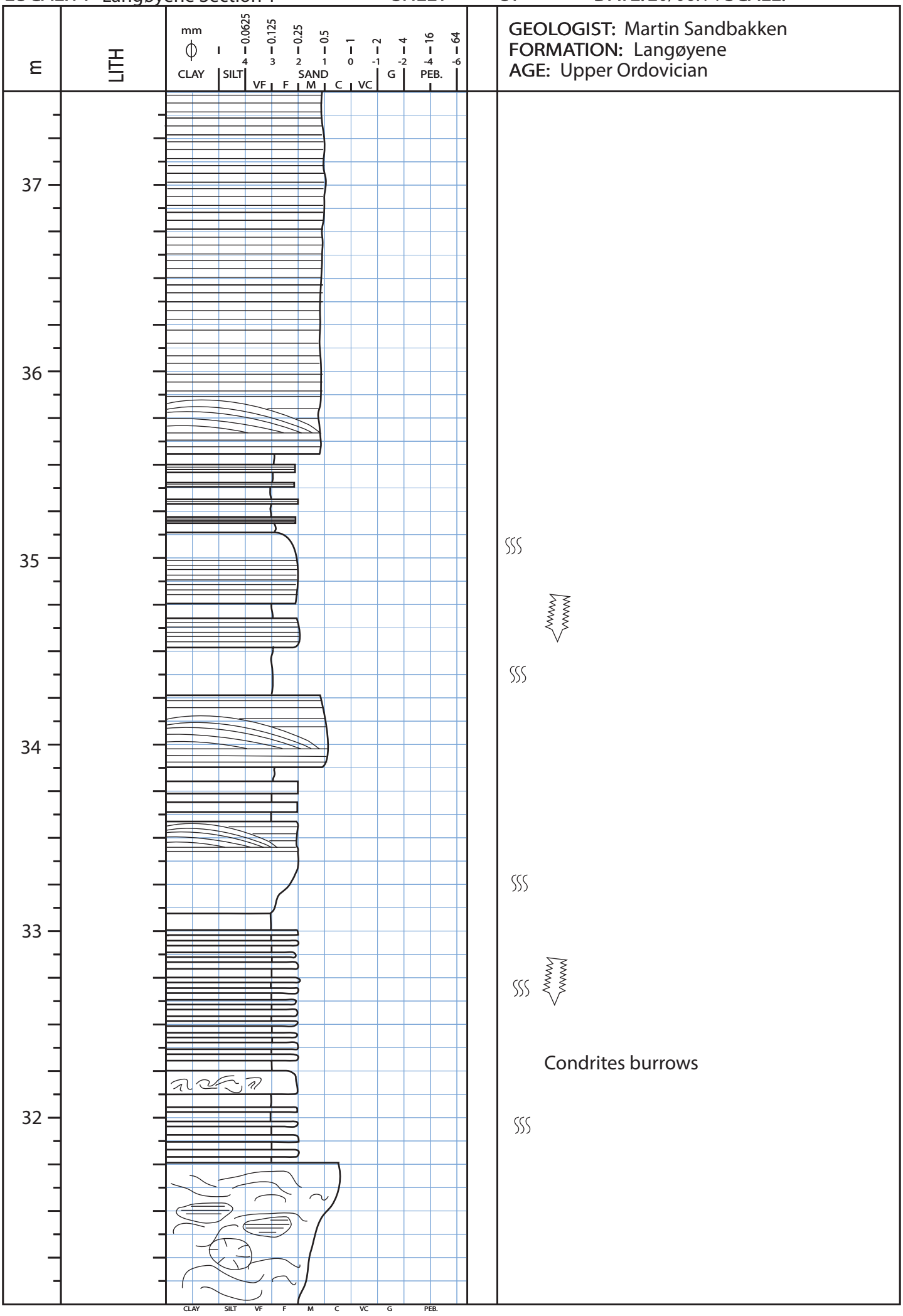

LOCALITY Langøyene Section 1 SHEET 2 OF 10 DATE: 20/06.14 SCALE: 1:25

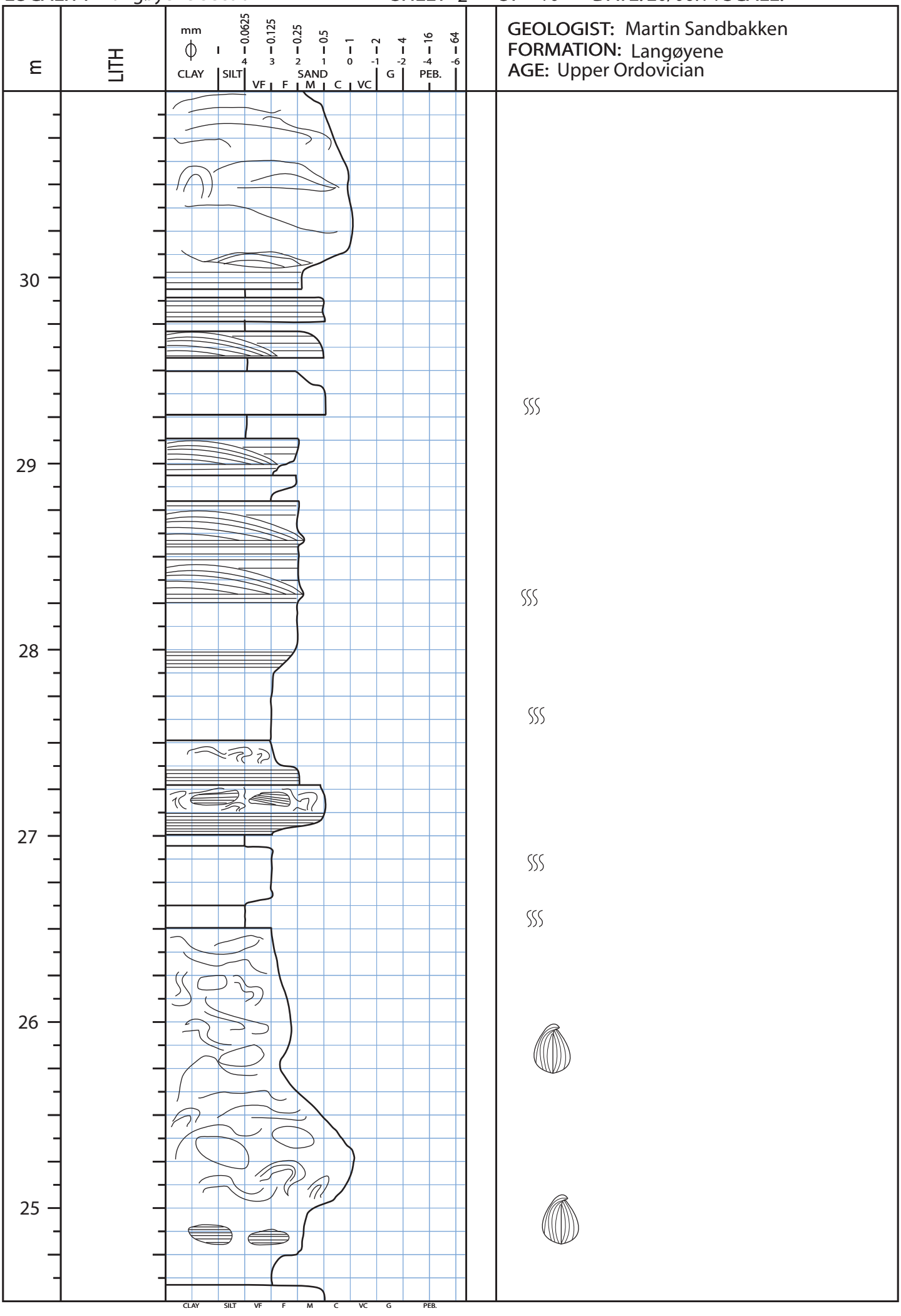

LOCALITY Langøyene Section 1 SHEET 1 OF 10 DATE: 20/06.14 SCALE: 1:25

GEOLOGIST: Martin Sandbakken
FORMATION: Husbergøya/Langøyene
AGE: Upper Ordovician

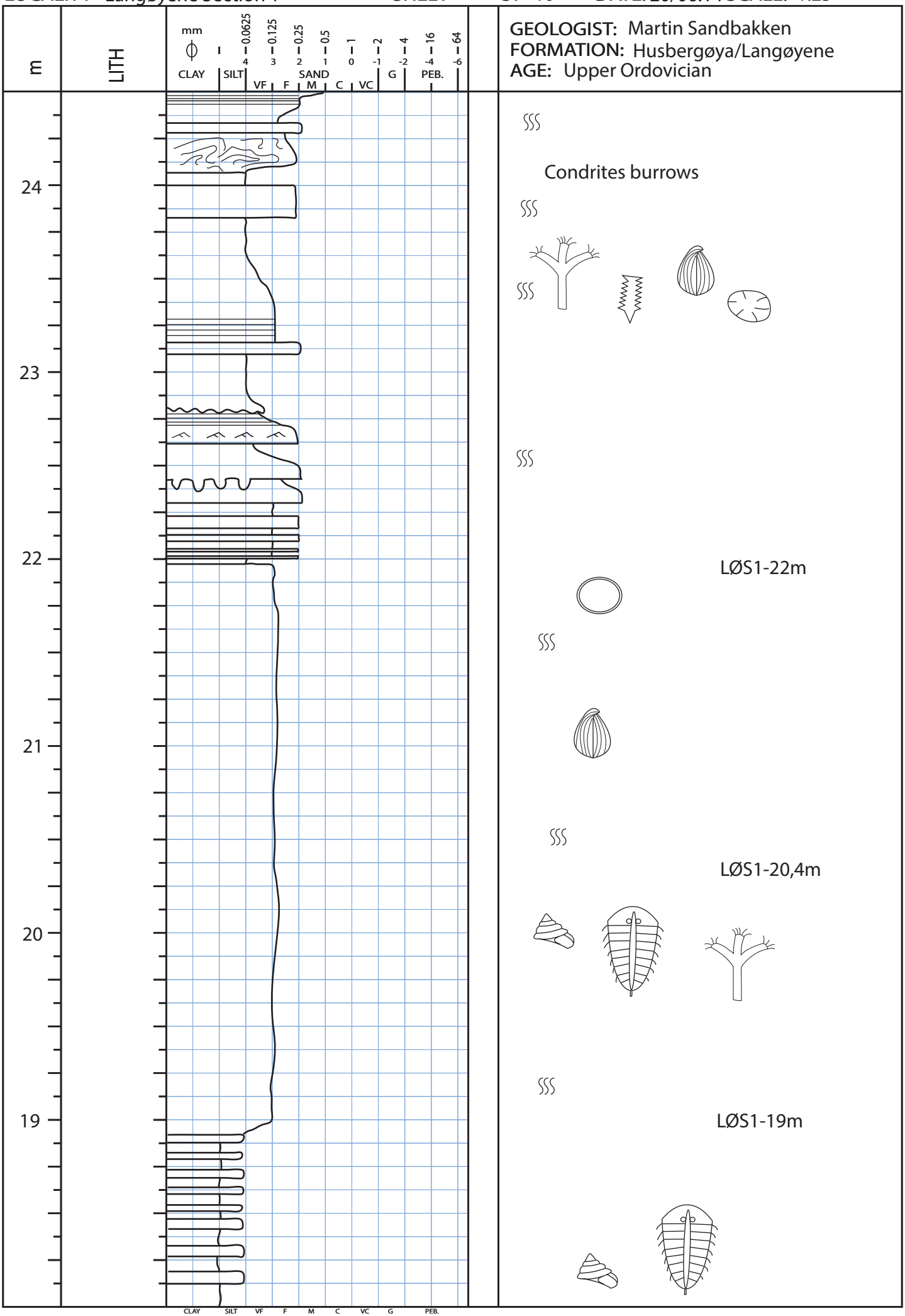

Appendix D

LOCALITY SHEET OF DATE: SCALE:

m	LITH	mm / Φ	0.0625	0.125	0.25	0.5	1	2	4	16	64
			4	3	2	1	0	-1	-2	-4	-6
		CLAY	SILT	VF	F	M	C	VC	G	PEB.	

GEOLOGIST:
FORMATION:
AGE:

CLAY SILT VF F M C VC G PEB.

Appendix E

Sample nr.	Meter	Facies Assosiations	Description	Sample Collector	Slip nr. (PMO)	Thinsection methods	Other methods
HS1-1	1	FA-Ia	Brown bioturbated ss	Martin Sandbakken	221.879	MPS	Slab-scan
HS1-2	2	FA-Ia	Brown bioturbated ss	Martin Sandbakken	221.880	MPS	Slab-scan
HS1-3	3,3	FA-Ia	Brown bioturbated ss	Martin Sandbakken	221.881	MPS	Slab-scan
HS1-4	19	FA-II	Storm deposited layer w/climbing ripples	Martin Sandbakken	221.882	MPS	Slab-scan
HS1-5	19,43	FA-II	Storm deposited layer	Martin Sandbakken	none	none	Slab-scan
HS1-6	30,5	FA-II	Bioturbated sandstone	Martin Sandbakken	none	none	Slab-scan
HS1-7	35	FA-II	Parallell laminated sandstone	Martin Sandbakken	221.883	MPS	Slab-scan
HS2-8	46	FA-II	Coquina bed	Martin Sandbakken	none	none	Slab-scan
HS2-9	46,9	FA-Ib	Base brown bioturb ss	Martin Sandbakken	221.884	MPS	Slab-scan
HS2-10	47,5	FA-Ib	Middle brown bioturb ss	Martin Sandbakken	221.885	MPS	Slab-scan
HS2-11	47,9	FA-Ib	Structureless calcareous siltstone	Martin Sandbakken	none	none	Slab-scan
HS2-12	48	FA-Ib	Top brown bioturb sandstone beneath nodular	Martin Sandbakken	221.886	MPS	Slab-scan
HS2-13	48,75	FA-V	Solvik shale	Martin Sandbakken	none	none	Slab-scan

Sample nr.	Meter	Facies Assosiation	Description	Sample Collector	PMO	Thinsection methods	Other methods
LØS1-1	19	FAIa	Brown bioturbated ss bottom	Martin Sandbakken	221.843	MPS	Slab-scan, XRD-analysis
LØS1-2	20,4	FAIa	Brown bioturbated ss middle	Martin Sandbakken	221.844	MPS	Slab-scan, XRD-analysis
LØS1-3	22	FAIa	Brown bioturbated ss top	Martin Sandbakken	221.845	MPS	Slab-scan, XRD-analysis
LØS1-4	51,9	FAIIIa	Conglomerat 1 bottom	Martin Sandbakken	221.846, 221.847	MPS	Slab-scan
LØS1-5	53	FAIIIa	Conglomerat 1 middle	Martin Sandbakken	221.848	MPS	Slab-scan
LØS1-6	55,9	FAIIIa	Conglomerat 1 top	Martin Sandbakken	221.849	MPS	Slab-scan
LØS1-7	73,3	FAIIIa	Conglomerat 2 bottom	Martin Sandbakken	221.850	MPS	Slab-scan
LØS1-8	74,7	FAIIIa	Conglomerat 2 middle	Martin Sandbakken	221.851, 221.852	MPS	Slab-scan
LØS1-9	77,9	FAIIIa	Conglomerat 2 top	Martin Sandbakken	221.853, 221.854, 2	MPS	Slab-scan
LØS1-10	79,5	FAIa	Brown bioturb ss (XL ichnofacies)	Martin Sandbakken	221.856	MPS	Slab-scan
LØS1-11	79,8	FAIb	Brown bioturb ss	Martin Sandbakken	221.857	MPS	Slab-scan
LØS1-12	79,9	FAIb	Knollekalk	Martin Sandbakken	221.858, 221.859	MPS	Slab-scan
LØS1-13	81	FA-V	Solvik shale	Martin Sandbakken	none	none	Slab-scan

Sample nr.	Meter	Facies assosiations	Description	Sample Collector	Slip nr. (PMO)	Thinsection methods	Other methods
RS1-1	16,2	FAIa	Brown bioturbated ss	Martin Sandbakken	221.860	MPS, Point-counting	Slab-scan
RS1-2	17	FAIa	Brown bioturbated ss	Martin Sandbakken	221.861	MPS, Point-counting	Slab-scan
RS1-3	18,75	FAIa	Brown bioturbated ss	Martin Sandbakken	221.862	MPS, Point-counting	Slab-scan
RS1-4	34,25	FAIIIa	Erosjonsgrense til Conglomerat 1	Martin Sandbakken	221.863, 221.864	MPS, Point-counting	Slab-scan
RS1-5	34,3	FAIIIa	Conglomerat 1 - base	Martin Sandbakken	221.865, 221.866	MPS, Point-counting	Slab-scan
RS1-6	35,5	FAIIIa	Conglomerat 1 - middle	Martin Sandbakken	221.867	MPS, Point-counting	Slab-scan
RS1-7	37,3	FAIIIa	Conglomerat 1 - top	Martin Sandbakken	221.868, 221.869	MPS, Point-counting	Slab-scan
RS1-8	47,6	FAIIIa	Conglomerat 2 - base	Martin Sandbakken	221.870, 221.871	MPS, Point-counting	Slab-scan
RS1-9	49,5	FAIIIa	Conglomerat 2 - middle	Martin Sandbakken	221.872	MPS, Point-counting	Slab-scan
RS1-10	65,5	FAII	Storm deposited layer	Martin Sandbakken	221.873	MPS, Point-counting	Slab-scan
RS1-11	69	FAIa	Brown bioturbated ss base	Martin Sandbakken	221.874	MPS, Point-counting	Slab-scan
RS1-12	69,8	FAIa	Brown bioturb ss middle	Martin Sandbakken	221.875	MPS, Point-counting	Slab-scan
RS1-13	69,9	FAIb	Nodular limestone/brown bioturb ss top	Martin Sandbakken	221.876, 221.877	MPS, Point-counting	Slab-scan
RS1-14	71,25	FA-V	Solvik shale	Martin Sandbakken	221.878	MPS, Point-counting	Slab-scan

Appendix F, H

	Polycrystalline qz	Monocrystalline qz	Metamorph qz	Metarhyoliths	Feldspar	Pyrite	Opaque minerals	Matrix	Calsite	Mica	SUM	AVG. Grain size
221.843												**85,43**
221.844												**86,54**
221.845												**90,63**
221.846												**229,01**
221.847												**590,27**
221.848												**757,32**
221.849												**276,89**
221.850												**674,11**
221.851												**731,68**
221.852												**677,10**
221.853												**725,97**
221.854												**642,44**
221.855												**712,76**
221.856												**95,29**
221.857												**113,25**
221.858												**214,40**
221.859												**137,04**
221.860			57			4	7		332			**400** **82,78**
221.861			129			7	6		233	23	2	**400** **92,24**
221.862			79			7	5		284	25		**400** **106,15**
221.863		38	86	54		10	7		129	76		**400** **126,97**
221.864		17	97	48		11	1		204	22		**400** **136,62**
221.865		2	62	7	1	11	4		133	180		**400** **396,02**
221.866		3	74	6	2	4	1		205	105		**400** **485,26**
221.867		7	51	14	1	3	1		248	75		**400** **584,61**
221.868		5	97	20	5	5	4		182	78		**396** **523,97**
221.869		8	99	58	1	9	5		159	61		**400** **576,37**
221.870		4	83	43	1	9		2	210	48		**400** **594,67**
221.871		19	81	46	7	7	5		184	50	1	**400** **627,72**
221.872		16	89	80	5	10	4	4	110	81	1	**400** **553,10**
221.873			163			6	8	5	80	138		**400** **90,36**
221.874			173			4	11	4	120	88		**400** **88,88**
221.875			126			2	3	3	223	42	1	**400** **98,90**
221.876			31			1		2	361	5		**400** **117,56**
221.877			97			3	1		269	30		**400** **426,91**
221.878			22						375	3		**400** **70,45**
221.879												**90,10**
221.880												**89,71**
221.881												**91,94**
221.882												**124,55**
221.883												**219,10**
221.884												**107,33**
221.885												**86,83**
221.886												**84,06**

Appendix G

	Polycrystalline qz	Monocrystalline qz	Metamorph	Metarhyoliths	Feldspar	Pyrite	Opaque	Matrix	Calcite	Mica	Qurtz	Q/(Q+F)
221.860		14,25			1,00	1,75	-	83,00			14,25	0,93
221.861		32,25			1,75	1,50		58,25	5,75	0,50	32,25	0,95
221.862		19,75			1,75	1,25		71,00	6,25		19,75	0,92
221.863	9,5	21,5	13,5		2,50	1,75		32,25	19,00		44,5	0,95
221.864	4,25	24,25	12		2,75	0,25		51,00	5,50		40,5	0,94
221.865	0,5	15,5	1,75	0,25	2,75	1,00		33,25	45,00		17,75	0,87
221.866	0,75	18,5	1,5	0,50	1,00	0,25		51,25	26,25		20,75	0,95
221.867	1,75	12,75	3,5	0,25	0,75	0,25		62,00	18,75		18	0,96
221.868	1,5	24,75	5	1,25	1,25	1,00		45,75	19,50		31,25	0,96
221.869	2	24,75	14,5	0,25	2,25	1,25		39,75	15,25		41,25	0,95
221.870	1	20,75	10,75	0,25	2,25		0,50	52,50	12,00		32,5	0,94
221.871	4,75	20,25	11,5	1,75	1,75	1,25		46,00	12,50	0,25	36,5	0,95
221.872	4	22,25	20	1,25	2,50	1,00	1,00	27,50	20,25	0,25	46,25	0,95
221.873		40,75			1,50	2,00	1,25	20,00	34,50		40,75	0,96
221.874		43,25			1,00	2,75	1,00	30,00	22,00		43,25	0,98
221.875		31,5			0,50	0,75	0,75	55,75	10,50	0,25	31,5	0,98
221.876		7,75			0,25		0,50	90,25	1,25		7,75	0,97
221.877		24,25			0,75	0,25		67,25	7,50		24,25	0,97
221.878		5,5						93,75	0,75		5,5	1,00

Appendix I (A3 size)

Appendix: I

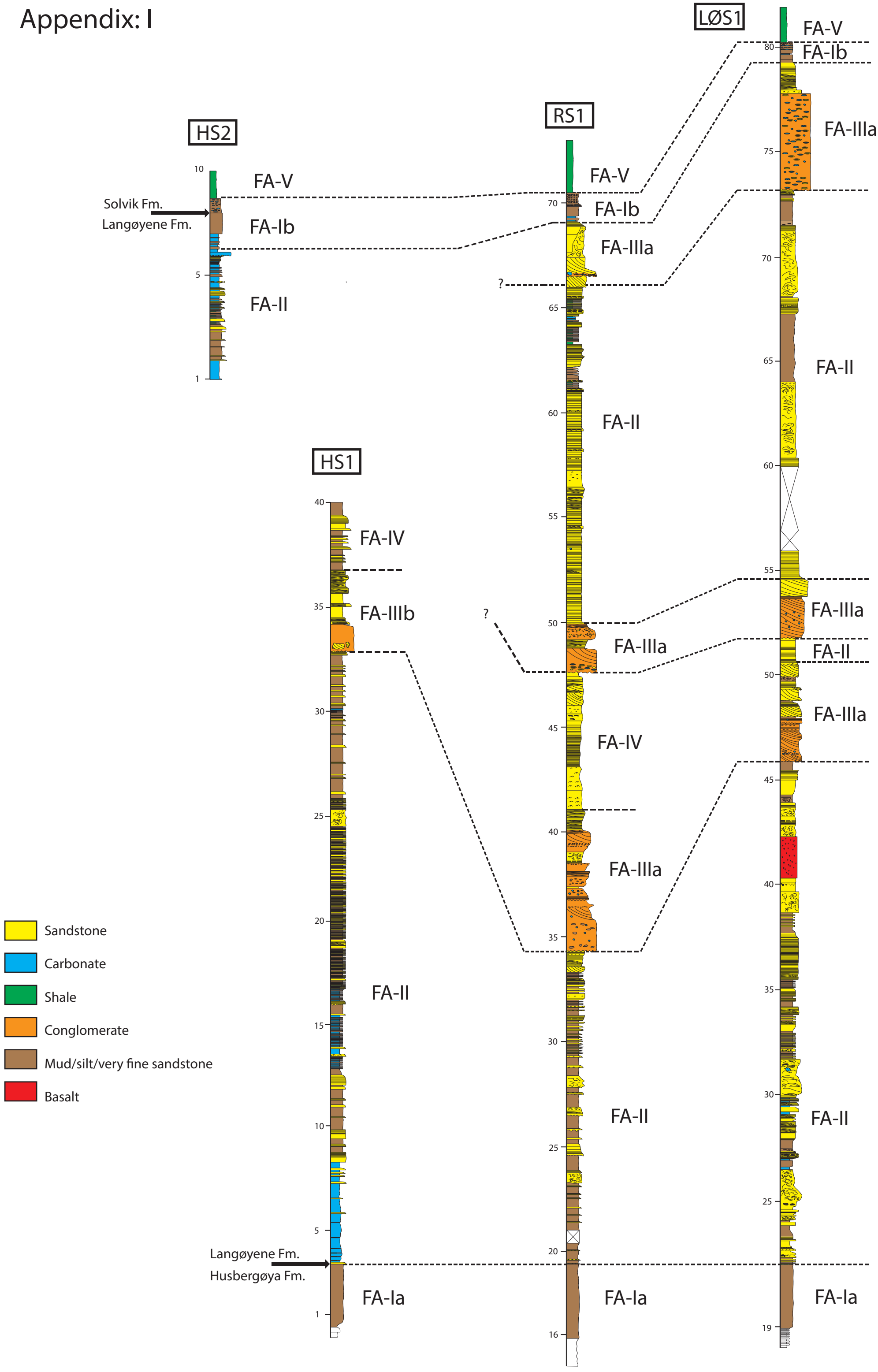
HS2
10
FA-V
Solvik Fm.
Langøyene Fm.
FA-Ib
5
FA-II
1
RS1
FA-V
70
FA-Ib
FA-IIIa
?
65
60
FA-II
LØS1
FA-V
80
FA-Ib
75
FA-IIIa
70
65
FA-II
60
HS1
40
FA-IV
35
FA-IIIb
30
25
20
FA-II
15
10
5
Langøyene Fm.
Husbergøya Fm.
1
FA-Ia
?
55
50
FA-IIIa
45
FA-IV
40
FA-IIIa
35
30
FA-II
25
20
16
FA-Ia
55
FA-IIIa
FA-II
50
FA-IIIa
45
40
35
30
FA-II
25
19
FA-Ia
Sandstone
Carbonate
Shale
Conglomerate
Mud/silt/very fine sandstone
Basalt